UNDERSTANDING CONTROLS ON SPRINGTIME EVAPOTRANSPIRATION FROM JACK PINE (PINUS BANKSIANA) FOREST WITH SEASONALLY FROZEN SOILS

A Thesis Submitted to the College of

Graduate and Postdoctoral Studies

In Partial Fulfillment of the Requirements

For the Degree of Master of Environment and Sustainability

In the School of Environment and Sustainability

University of Saskatchewan

Saskatoon

By

Mahtab Nazarbakhsh

PERMISSION TO USE

In presenting this dissertation in partial fulfillment of the requirements for a Postgraduate degree from the University of Saskatchewan, I agree that the Libraries of this University may make it freely available for inspection. I further agree that permission for copying of this dissertation in any manner, in whole or in part, for scholarly purposes may be granted by the professor or professors who supervised my thesis work or, in their absence, by the Head of the Department or the Dean of the College in which my thesis work was done. It is understood that any copying or publication or use of this dissertation or parts thereof for financial gain shall not be allowed without my written permission. It is also understood that due recognition shall be given to me and to the University of Saskatchewan in any scholarly use which may be made of any material in my dissertation.

DISCLAIMER

Reference in this dissertation to any specific commercial products, process, or service by trade name, trademark, manufacturer, or otherwise, does not constitute or imply its endorsement, recommendation, or favoring by the University of Saskatchewan. The views and opinions of the author expressed herein do not state or reflect those of the University of Saskatchewan, and shall not be used for advertising or product endorsement purposes.

Requests for permission to copy or to make other uses of materials in this dissertation in whole or part should be addressed to:

Executive Director

School of Environment and Sustainability

University of Saskatchewan

Room 323, Kirk Hall

117 Science Place

Saskatoon, Saskatchewan S7N 5C8, Canada

OR

Dean

College of Graduate and Postdoctoral Studies

University of Saskatchewan

116 Thorvaldson Building, 110 Science Place

Saskatoon, Saskatchewan S7N 5C9, Canada

ABSTRACT

The exchanges of water, energy and carbon between the land surface and the atmosphere are tightly coupled, so that errors in simulating evapotranspiration will lead to errors in simulating the water, carbon and energy cycles. This will impair water resource evaluations and numerical weather predictions. Currently, land surface schemes have shown deficiencies in the simulation of evapotranspiration at the southern edge of the boreal forest in Saskatchewan, Canada. The purpose of this research is to improve the understanding of controls on evapotranspiration from forest canopies in regions with seasonally frozen soils, by critically examining field observations and outputs from state–of–the–art models. Simulated evapotranspiration is sensitive to soil and vegetation properties, which are variable in time and space and therefore introduce large uncertainties. Seasonally frozen soils present a particular challenge due to their snowmelt–dominated hydrology and the impact of soil freezing on the soil hydraulic properties and plant root water uptake. This thesis critically assesses the performance of the Canadian Land Surface Scheme (CLASS) and the coupled Canadian Land Surface Scheme and Canadian Terrestrial Ecosystem Model (CLASS–CTEM) for simulating point–scale evapotranspiration at a mature jack pine site located at the southern edge of the boreal forest in Saskatchewan, Canada. Past models applied to this site have consistently over–predicted evapotranspiration, particularly in the period following snowmelt. This research applies sensitivity analysis to explore how evapotranspiration is controlled by soil hydraulic and plant properties (soil water retention and conductivity, root depth/distribution, leaf area index, and the canopy conductance model), with special focus on the spring melt period when transpiration commences.

This investigation found that errors in the soil hydraulic properties, root distribution, or leaf area index could not individually explain the model errors although these properties do all have

important impacts on the water balance. The parameterization of canopy conductance could potentially explain the model errors. Although canopy conductance and leaf area index are dependent, the bias in simulation of evapotranspiration cannot be explained by the errors in leaf area index – given the fact that at this site we have site specific estimates of leaf area index. Errors in the simulation of evapotranspiration were greatest during and just after the soil–thaw period in spring. It is recommended, therefore, to further investigate the simulation of evapotranspiration from frozen soils.

ACKNOWLEDGEMENTS

I would like to express my sincere gratitude and appreciation to all who supported and contributed in the completion of this thesis. I would first like to express my sincere gratitude to my supervisor, Dr. Andrew Ireson for his unwavering support, constructive advices, and feedback on the paper, and also for his comments on this thesis. I am also particularly grateful to my current and past committee members, Dr. Alan Barr, Dr. Colin Laroque, Dr. Warren Helgason, and Prof. Howard Wheater for the participation in the meetings. I would like to extend my sincere gratitude to Dr. Alan Barr for his unwavering support, constructive advices, and invaluable feedback on the paper, and also for his guidance and contribution in this research. I am also grateful to Dr. Colin Laroque for his revisions and comments on the proposal of this research and further advices for this research. It was a pleasure to work with them all. I would also like to acknowledge Dr. Cherie Westbrook for accepting to undertake the role of being an external examiner.

I would like to thank the funding organizations: Natural Science and Engineering Research Council (NSERC), Changing Cold Region Network (CCRN), CREATE for Water Security and the Canada Excellence Research Chair in Water Security, School of Environment and Sustainability for providing the financial support to complete this research. I would also like to appreciate all instructors, staffs, my colleagues at GIWS, and my friends who have supported me along the way.

Finally, I would like to express my profound gratitude to my family for providing me with unfailing support, love, and continuous encouragement. This accomplishment would not have been possible without them.

TABLE OF CONTENTS

LIST OF FIGURES

LIST OF TABLES

LIST OF ABBREVIATIONS

BERMS	Boreal Ecosystem Research and Monitoring Sites
CABLE	Community Atmosphere Biosphere Land Exchange
CLASS	Canadian Land Surface Scheme
CLASS–CTEM	Coupled Canadian Land Surface Scheme and Canadian Terrestrial Ecosystem Model
JULES	Joint UK Land Environment Simulator
LAI	Leaf Area Index
LFH	Leaf–Fibre–Humic Substances in a Soil Horizon
LSSs	Land Surface Schemes
MESH	Modelisation Environmentale Communautaire–Surface and Hydrology
OA	Old Aspen
OBS	Old Black Spruce
OJP	Old Jack Pine
ORCHIDEE	Organising Carbon and Hydrology in Dynamic Ecosystems
PAR	Photosynthetically Active Radiation
SMI	Soil Moisture Index
SWE	Snow Water Equivalent

LIST OF SYMBOLS

AE	Actual Evapotranspiration
A_n	Net Canopy Photosynthesis
b_r	Parameter representing the Effect of Soil Texture and other Factors on the Root Distribution Profile
b	Vegetation Dependent Parameter
B(t)	Root Biomass as a Function of Time
B_{IC}	Blowing Snow in the Canopy
B_{IG}	Blowing Snow in the Ground
B_{OC}	Blowing Snow out of the Canopy
B_{OG}	Blowing Snow out of the Ground
C_P	Specific Heat of Air
c_s	Partial Pressure of CO_2 at the leaf surface
D	Soil Drainage
D_v	Vapor Pressure Deficit
D_0	Vegetation Dependent Parameter
DELZW1–3	Thickness of Soil Layers
d(t)	Rooting Depth as a Function of Time
E_B	Soil Evaporation
E_C	Canopy Evaporation
E_S	Sublimation from the Snowpack
ET	Evapotranspiration
F	Interflow

f (z, t)	Root Distribution as a Function of Depth and Time
f (ψ)	Depth Distributed Water Stress function
G	Groundwater
G_r	Root increment
G_H	Ground Heat
g_c	Canopy Conductance
g_s	Stomatal Conductance
g(z)	The Depth Distribution of the Roots
H	The Amount of Energy Stored in the Land Surface
h_s	Relative Humidity at the Leaf Surface
i	the Number of Soil Depth Interval
I	Infiltration
I_P	Potential Infiltration
K_t	Thermal Conductivity
K	Hydraulic Conductivity
K_E	Transfer Coefficient for Latent Heat
K_h	Transfer Coefficient for Sensible Heat
$K_{r(\psi)}$	Relative Hydraulic Conductivity
K_{sat}	Saturated Hydraulic Conductivity
K^*	Net Shortwave Radiation
K↓	Incoming Shortwave Radiation
K↑	Outgoing Shortwave Radiation
L^*	Net Longwave Radiation

$L\downarrow$	Incoming Longwave Radiation
$L\uparrow$	Outgoing Longwave Radiation
m	Vegetation Dependent Parameter
M	Snowmelt
p	pressure
PCPG	Precipitation Incident on Ground, including Snowmelt
PE	Potential Evapotranspiration
P_R	Rainfall
P_{RT}	Throughfall of Rain
P_S	Snowfall
P_{ST}	Throughfall of Snow
QFC1–3	Water Uptake from each Soil Layer by Transpiration
QFG	Water Vapour Flux from Ground
$q_s(T_s)$	Saturation Water Vapor Specific Humidity at the Leaf–Surface Temperature
q_r	Water Vapor specific Humidity at the Reference Atmospheric Level
R	Runoff
R_G	Rainfall on the Ground
R_n	Net Radiation
$R(\Delta z_i)$	Root Fraction within a Soil Depth Interval
r_a	Aerodynamic Resistance
r_c	Canopy Resistance
r_s	Stomatal Resistance

$r_{s\ min}$	Minimum Stomatal Resistance
ROFB	Base Flow from Bottom of Soil Column
ROFN	Liquid Water from Snowpack
ROFO	Overland Flow from Top of Soil Column
S_C	Canopy Interception
S_H	Sensible Heat
S_i	Depth Distributed Sink Term for each Soil Depth Interval
S_P	Energy–Limited Transpiration Rate
S_S	Soil Moisture
T	Canopy Transpiration
T_{soil}	Soil Temperature
T_0	Surface Temperature
T_S	Sky Temperature
THLIQ1–3	Volumetric Liquid Water Content of Soil Layers
THICE1–3	Volumetric Frozen Water Content of Soil Layers
V	Root Zone Volume
V_a	Volume of Air
V_{max}	Maximum Rate of Carboxylation by the Enzyme Rubisco
V_s	Volume of Soil
V_w	Volume of Water
WTRG	Water Transferred into or out of the Soil
Z	Soil Depth
z_{B_i}	Bottom of Soil Depth Interval

z_R	Rooting Depth
z_{T_i}	Top of Soil Depth Interval
Δz_i	Soil Depth Interval
α	Runoff Coefficient
α_r	Root Growth Direction Parameter
ρ_a	Air Density
λ	Latent Heat of Evaporation
λE	Latent Heat
ε_0	Surface Emissivity
ε_S	Sky Emissivity
σ	Stephan–Boltzmann Constant
δe	Vapour Pressure Deficit
Γ	CO_2 Concentration Point
ρ	Air Density
$\frac{\Delta q}{\Delta z}$	The Change of Specific Humidity with Height
$\frac{\Delta T}{\Delta z}$	The Change of Air Temperature with Height
θ	Volumetric Water Content
θ_{FC}	Field Capacity
θ_L	Liquid Water Content
θ_S	Solid Water Content
θ_{sat}	Saturated Water Content
θ_{wilt}	Wilting Point
ψ	Matric Potential

ψ_{crit}	Water Potential at which Water Stress Commences
ψ_{sat}	Saturated Water Potential/ Air Entry Pressure
ψ_w	Water Potential at which Water Stress Complete

CHAPTER 1

INTRODUCTION

1.1 Background

Evapotranspiration is the key linkage between water, energy and carbon balances. Evapotranspiration plays a key role in water balance as it returns ~ 60% of continental precipitation to the atmosphere (e.g. Oki and Kanae, 2006). It also plays a significant role in the surface energy balance, as more than one–half of the solar energy absorbed by the earth's surface is used by evapotranspiration (Trenberth *et al.*, 2009). As evapotranspiration and photosynthesis are coupled through stomata, the carbon balance is also coupled to evapotranspiration. In the following, this thesis will show the significance of evapotranspiration in water, energy and carbon balances.

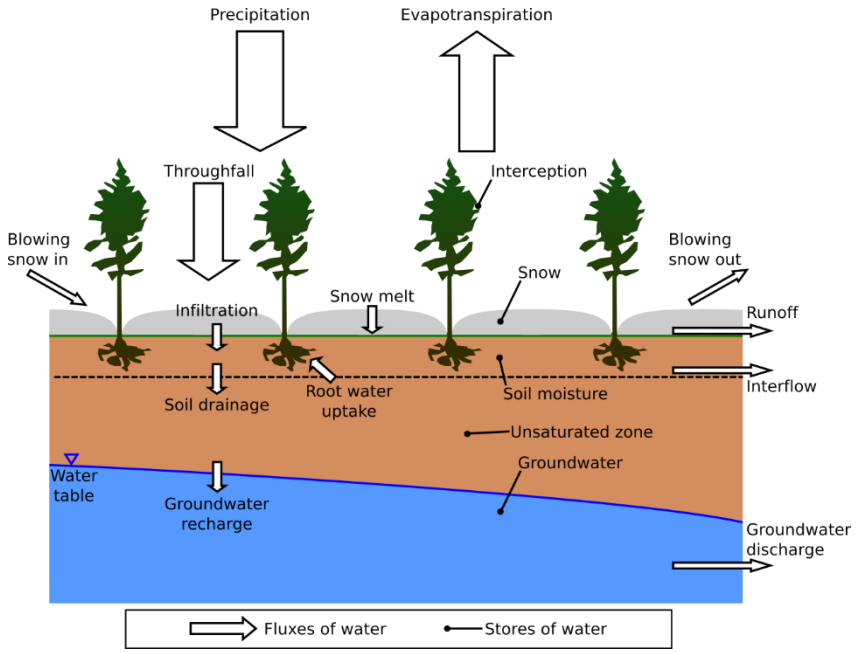

Figure 1–1 A conceptual model of the surface water balance in a seasonally frozen forest land cover.

A plausible depiction of the point scale water balance of the land surface for a seasonally frozen forest land cover is shown in Figure 1–1. There is subjectivity in how many processes are included, and the level of detail in the individual process descriptions, and this is one of the main factors that accounts for differences between land surface models. Fluxes, in units of mm d^{-1}, include rainfall (P_R), snowfall (P_S), throughfall of rain (P_{RT}) and snow (P_{ST}), snowmelt (M), blowing snow in and out of the canopy (B_{IC} and B_{OC}) and the ground (B_{IG} and B_{OG}), infiltration (I), soil drainage (D), which forms recharge to groundwater (G), interflow (F), runoff (R), and evapotranspiration (ET), which itself comprises soil evaporation (E_B), transpiration (T), canopy evaporation (E_C) and sublimation from the snowpack (E_S). ET represents an aggregated flux above the canopy is given by:

$$ET = T + E_B + E_C + E_S \tag{1.1}$$

Land surface stores, in units of mm of liquid water, include soil moisture (S_S), canopy interception (S_C) and snow (SWE). Deeper stores include unsaturated zone storage and groundwater storage, which are not considered in detail here. Conservation equations for the surface stores are given as:

$$\frac{dS_C}{dt} = P_R - P_{RT} + P_S - P_{ST} - E_C + B_{IC} - B_{OC} \tag{1.2}$$

$$\frac{dSWE}{dt} = P_{ST} - E_S + B_{IG} - B_{OG} - M \tag{1.3}$$

$$\frac{dS_S}{dt} = I - D - F - T - E_B \tag{1.4}$$

At the ground surface, the potential infiltration amount (I_P) is given by the sum of throughfall of rain and snowmelt, that is:

$$I_P = P_{RT} + M \tag{1.5}$$

And I_P is partitioned between runoff and infiltration by:

$$I = (1 - \alpha)I_P \tag{1.6}$$

Where α is defined as the runoff coefficient, which is not a constant, and depends on various dynamic factors including soil saturation, soil freeze–thaw state and the intensity of I_P.

Precipitation is partitioned between runoff and infiltration, and infiltration is partitioned between drainage, storage and evapotranspiration. Evapotranspiration is typically the second largest flux in the water balance, after precipitation (except in very wet areas where $R > ET$). Thus, ET is a critical component of the water balance which must be accurately quantified.

Furthermore, ET is the key linkage between the water and energy cycles, through the consumption of latent heat (Seneviratne *et al.*, 2006). To quantify the latent heat flux, it is necessary to consider the point scale energy balance, which for the land surface of a seasonally frozen forest land cover is presented in Figure 1–2. Fluxes, in units of Wm^{-2}, include net radiation (R_n), latent heat (λE), sensible heat (S_H), ground heat flux (G_H). λE is related to evapotranspiration (E) through the latent heat of evaporation ($\lambda = 2.45$ MJ kg^{-1} at 20℃). The dominant terms of the energy balance of the land surface are:

$$\frac{dH}{dt} = R_n - \lambda E - S_H - G_H \tag{1.7}$$

Where H is the amount of energy stored in the land surface (J m^{-2} s^{-1}). The net radiation is the sum of net shortwave radiation (K^*) and net longwave radiation (L^*). The net shortwave radiation aggregates incoming ($K\downarrow$) and outgoing ($K\uparrow$) shortwave radiation. The net longwave radiation aggregates incoming ($L\downarrow$) and outgoing ($L\uparrow$) longwave radiation.

$$R_n = K^* + L^* \tag{1.8}$$

$$K^* = K\downarrow - K\uparrow \tag{1.9}$$

$$L^* = L\downarrow - L\uparrow \tag{1.10}$$

The outgoing shortwave radiation ($K\uparrow$) depends on incoming shortwave radiation ($K\downarrow$) and the albedo(α). The incoming longwave radiation ($L\downarrow$) depends on sky temperature (T_s) and sky emissivity (ε_s). The outgoing longwave radiation ($L\uparrow$) depends on surface temperature (T_0) and surface emissivity (ε_0). σ is the Stephan–Boltzmann constant (5.67×10^{-8} Wm^{-2} K^{-4}).

$$K\uparrow = \alpha K\downarrow \tag{1.11}$$

$$L\downarrow = \varepsilon_s \sigma T_s^4 \tag{1.12}$$

$$L\uparrow = \varepsilon_0 \sigma T_0^4 \tag{1.13}$$

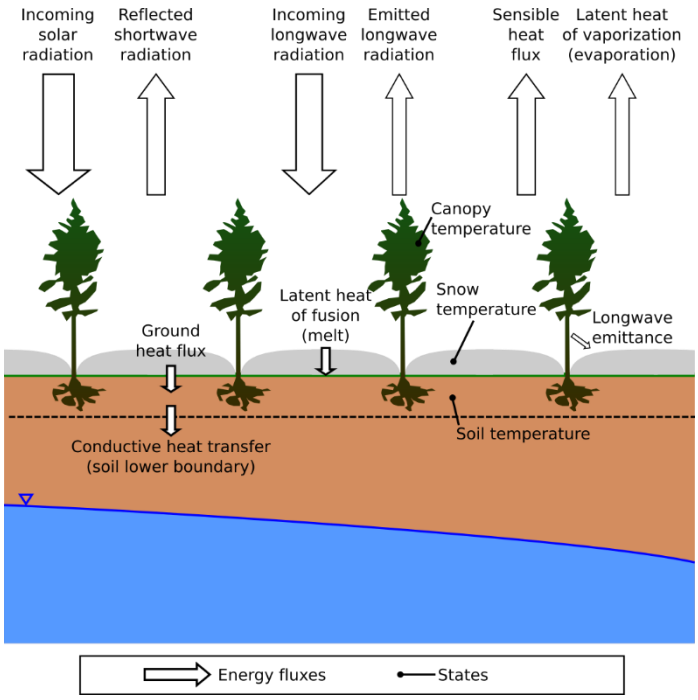

Figure 1–2 A conceptual model of the energy balance in a seasonally frozen forest land cover.

Latent and sensible heat flux can be given by:

$$\lambda E = \lambda \rho K_E \frac{\Delta q}{\Delta z} \quad (1.14)$$

$$S_H = \rho c_p K_h \frac{\Delta T}{\Delta z} \quad (1.15)$$

Where λ is the latent heat of evaporation (J kg^{-1}), ρ is the air density (kg m^{-3}), c_p is the specific heat of air (J kg^{-1} K^{-1}), $\frac{\Delta q}{\Delta z}$ is the change of specific humidity, and $\frac{\Delta T}{\Delta z}$ is the change of air temperature with height (K). K_E and K_h are transfer coefficients related to the processes such as atmospheric turbulence.

Ground heat flux is the loss of energy by heat conduction through the lower boundary, and it is expressed as follows:

$$G_H = -k_t \frac{\partial T_{soil}}{\partial z} \quad (1.16)$$

Where k_t is the thermal conductivity (W m^{-1} K^{-1}), T_{soil} is the soil temperature (K), and Z is the soil depth (m).

As is shown in the conceptual framework (Figure 1–3), the evapotranspiration regime can be defined as an energy–limited evapotranspiration regime and/or soil moisture–limited evapotranspiration (emphasized in e.g. Koster *et al.*, 2004, 2009; Seneviratne *et al.*, 2006; Teuling *et al.*, 2009). In the energy–limited condition, the soil water content is greater than the critical water content so that evapotranspiration is independent of soil water content. In the soil–moisture limited condition, soil moisture can be between the critical water content and wilting point or below the wilting point. Between the critical water content and wilting point, soil moisture considerably restricts evapotranspiration. Below wilting point, plants cannot extract water from soil matrix.

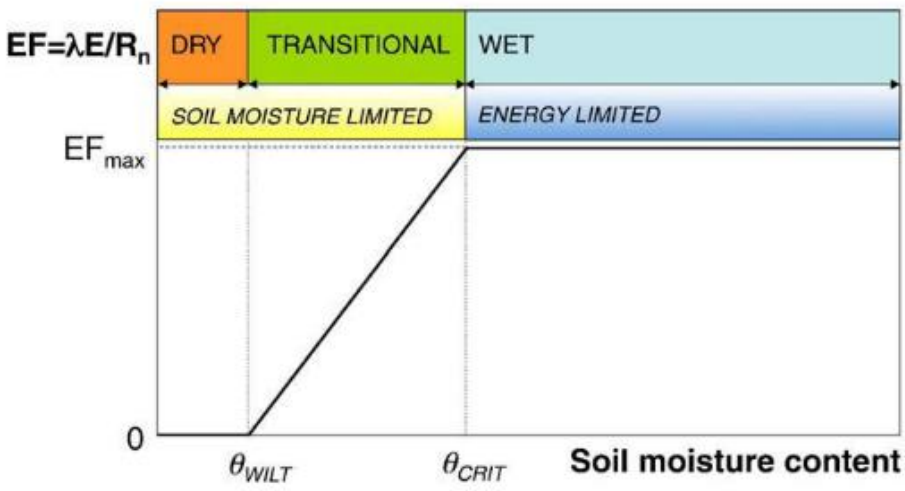

Figure 1–3 The conceptual framework of the definition of evapotranspiration regimes as a function of soil moisture (Seneviratne *et al.*, 2010).

Transpiration, often the largest component of evapotranspiration, is the key linkage between the water and carbon cycles, through the exchanges of water and CO_2 through the plants stomata (e.g. Jarvis, 1976; Cowan, 1978; Farquhar and Sharkey, 1982; Collatz *et al.*, 1991; Leuning, 1995; Katul *et al.*, 2009; Berry *et al.*, 2010; Fisher, 2013; Fatichi *et al.*, 2016). Errors in simulating evapotranspiration lead to errors in both the energy balance and the carbon balance, and therefore present problems for climate models and plant growth models.

The greatest global warming on Earth is anticipated to be at high latitudes, including boreal forests (IPCC, 2001). As 17% of the global vegetated surface is in boreal forest regions (e.g. Whittaker, 1975; Jarvis *et al.*, 1997), understanding the boreal–forest water, energy and carbon balances is critical to reduce uncertainty in the prediction of climate change in the future (Nakai *et al.*, 2013). In the southern boreal forest in Saskatchewan, Canada, flux towers are located in mature black spruce, aspen and jack pine sites (Sellers *et al.*, 1997; Barr *et al.*, 2006). These three sites are equipped with instruments to measure hydro–metrological data.

All modelling efforts to date, as detailed in the literature review below, have shown significant errors in simulating *ET* at the southern edge of the boreal forest in Saskatchewan, Canada, known as Boreal Ecosystem Research and Monitoring Sites (BERMS). This motivates me to focus on the improvement of the understanding of controls on *ET* in seasonally frozen forests, which will result in the improvement of water, energy and carbon balance and therefore the prediction of climate change in the future. As the climate changes and droughts increase in frequency and severity, it is all the more critical that models be reliable and capable of predicting future climate changes and its effects on future terrestrial ecosystems. This demonstrates the critical need for models that can realistically simulate *ET*.

1.2 Statement of research purpose, objectives, questions and hypotheses

1.2.1 Research purpose

The overall purpose of this research is to improve the understanding of controls on evapotranspiration from forest canopies in seasonally frozen soils by critically examining field observations and outputs from state–of–the–art models.

1.2.2 Research objectives

- Perform a set of CLASS and coupled CLASS–CTEM baseline model runs to simulate point scale evapotranspiration from the Old Jack Pine BERMS in the southern boreal forest.
- Analyse models outputs during and after the melt period to provide insights into the controls on the evapotranspiration process in forests on seasonally frozen soils.
- Critically assess the capacity of these models to simulate melt period evapotranspiration process, considering the impact of soil hydraulic properties and vegetation characteristics (rooting depth/distribution, leaf area index and canopy conductance).

1.2.3 Research questions

This research explores the following research question:

What are the critical controls on evapotranspiration from forests with seasonally frozen soils?

Sub–questions:

- What are the effects of frozen soils, infiltration, storage and drainage on forest evapotranspiration in spring (i.e. during the snowmelt period, soil–thaw period and ensuing post–thaw transition)?
- What are the effects of canopy conductance, leaf area index and root distribution/depth on controlling evapotranspiration in spring?

1.2.4 Hypotheses

This research explores the following hypotheses:

- Soil hydrological processes during the snowmelt period through early summer when frozen soils are thawed are poorly represented in land surface schemes, and this can explain errors in simulated evapotranspiration.
- Errors in the parametrization of vegetation characteristics, namely canopy conductance, leaf area index, and root depth and distribution can explain the errors in simulated evapotranspiration in spring.

1.3 Thesis structure

The next chapter is a literature review on the deficiencies of land surface schemes, how evapotranspiration is controlled by soil properties and processes including frozen soil processes, the role of plant characteristics and plant water uptake processes, and the summary of knowledge gaps. Chapter 3 is a manuscript which includes a description of the study site, modelling methods, and

results associated with the sensitivity of water balance components to soil hydraulic properties, rooting depth and root distribution, leaf area index and canopy conductance during the spring melt period. Chapter 4 summarizes the findings of this thesis.

CHAPTER 2

LITERATURE REVIEW

2.1 Overview

As explained in the introduction, *ET* is a critical process in water balance, energy balance and carbon balance models. Accurate quantification of *ET* is necessary for hydrological, climate and plant growth models, and sometimes these models are coupled together in the form of land surface models (Jacquemin and Noilhan, 1990; Braud *et al.*, 1995; Cresswell and Paydar, 2000). These models are applied to predict future water availability and water resource management, climate change and climate change impacts, fire risk and forest management. Land Surface Schemes (LSSs) that have been applied in the southern boreal forest in Canada (Figure 2–1) have systematic limitations in simulating *ET*. For example, Horton (2012) found that the UK LSS called JULES had deficiencies in representing the amount of infiltration from melting snow in the spring, soil temperatures and evapotranspiration at the BERMS Old Jack Pine (OJP), Old Aspen (OA) and Old Black Spruce (OBS) sites. Davison *et al.* (2016) and Mamo (2015) found that the Canadian LSS called CLASS, implemented within the hydrological model MESH, was unable to accurately simulate *ET* for OBS and OJP, even after calibration. The model overestimated *ET* for both sites, but with larger errors at OJP, compared to the observations.

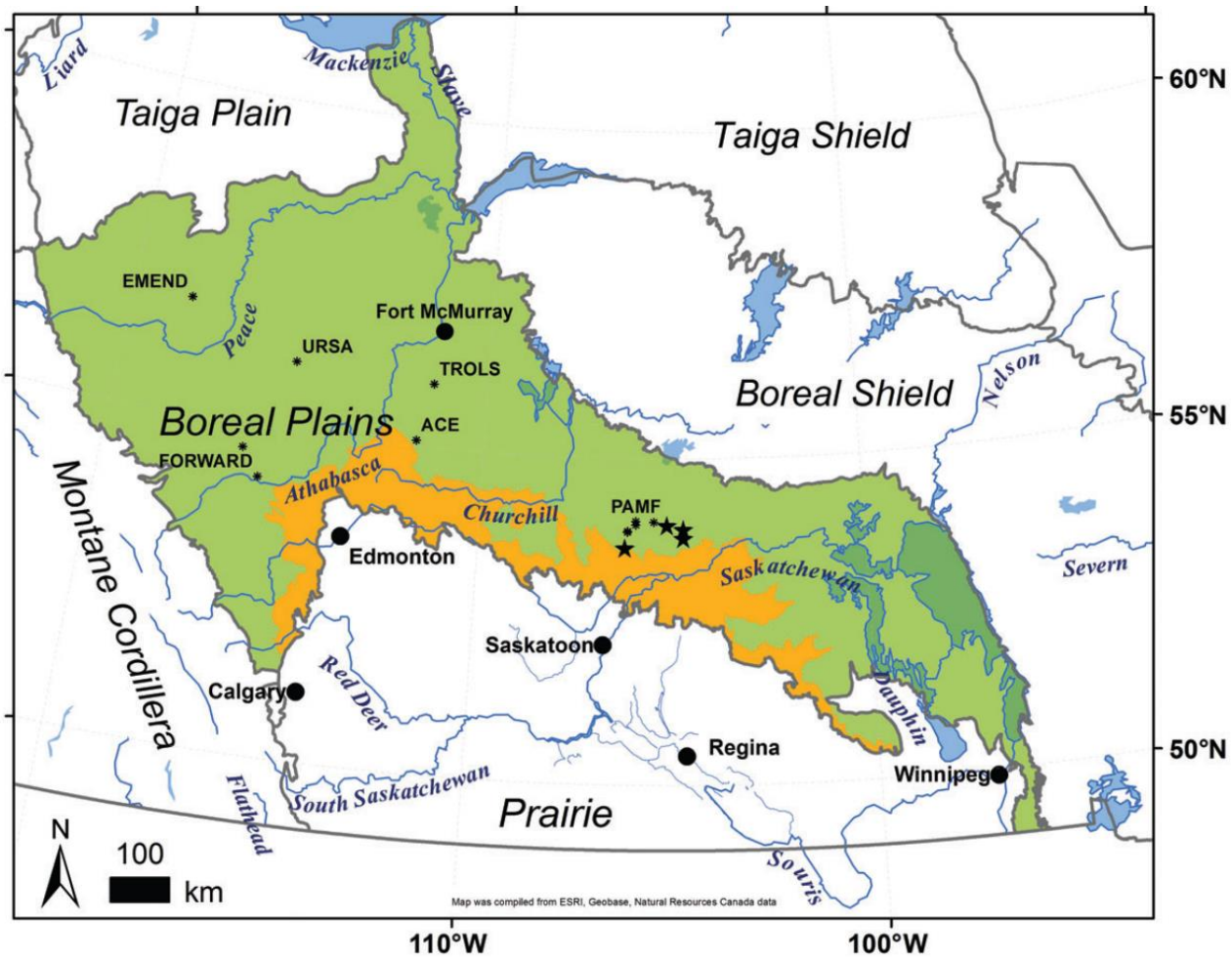

Figure 2–1 The BERMS sites, shown as stars, which include Old Jack Pine (OJP), Old Black Spruce (OBS) and Old Aspen (OA), where long–term records from flux towers are available (Ireson *et al.*, 2015).

In the proposed research, I seek to understand the processes leading to the poor simulation of *ET*. The aim of this literature review is to identify current challenges and knowledge gaps associated with the simulation of *ET*, with a particular focus on simulating *ET* in seasonally frozen forests. In such environments, a specific combination of cold regions processes and tree–water relations dominates the evapotranspiration process. *ET* is controlled by atmospheric demand for water, root–zone moisture content and the characteristics of the plant (Allen *et al.*, 2006). *ET* is sensitive to soil and vegetation properties, which are variable in time and space and therefore introduce large uncertainties. This is captured in my research questions and hypotheses, and this literature review,

which is organized as follows. The first section focuses on the deficiencies of current land surface schemes. The second section describes how *ET* is controlled by soil properties and processes, including frozen soil processes. The third section describes the role of plant characteristics and plant water uptake processes on *ET*. The review ends with a brief summary of knowledge gaps.

2.2 Deficiencies of land surface schemes

The deficiencies of land surface schemes to simulate water and carbon fluxes have been demonstrated in drought conditions by the Joint UK Land Environment Simulator (JULES; Best *et al.*, 2011), the Organising Carbon and Hydrology in Dynamic Ecosystems (ORCHIDEE; Krinner *et al.*, 2005) and the Community Atmosphere Biosphere Land Exchange (CABLE; Wang *et al.*, 2011). Ukkola *et al.* (2016) evaluated the performance of 14 LSSs (CABLE–SLI, CABLE–GW, CABLE–2.0, CHTESSEL, COLASSiB, ISBA–3L, ISBA–dif, JULES–3.1, JULES–altP, Mosaic, NOAH 2.7, NOAH 3.2, NOAH 3.3, ORCHIDEE) to simulate water and energy fluxes during water stress conditions. They found that all 14 LSSs have systematic biases in the simulation of water and energy fluxes in drought conditions (Figure 2–2). As shown in Figure 2–2, 14 LSSs are incapable to capture observed *ET* during the whole year.

Snow and ice affect land surface processes, especially in northern latitudes, where a critical component of the water balance is the partitioning of snowmelt into runoff and infiltration in the spring (Luo et al. 2003). Luo *et al.* (2003) found that the ability of LSSs to accurately simulate hydrological processes depends on the correct representation of snow process. Pitman *et al.* (1999) and Mitchell and Warrilow (1987) thought that frozen soil significantly affect the simulation of soil moisture and runoff. However, the inclusion of frozen soil in LSSs had negligible effects on soil moisture and runoff (Cherkauer and Lettenmaier, 1999; Pitman *et al.*, 1999; Luo *et al.*, 2003). Horton (2012) showed that JULES overestimated the amount of infiltration into the soil profile

resulting in the overestimation of soil moisture content during wet period at all sites (Figure 2–3). As a matter of fact, soil thaw happens after snow melt leads to runoff over frozen soil (Carey and Quinton, 2004; Ireson *et al.*, 2013). But, JULES stores snow melt in the snow pack as unfrozen water and make it accessible to infiltrate into the soil profile after soil thaw, leading to an overly large increase in soil moisture (Horton, 2012). Pomeroy *et al.* (1999) found that snow sublimation includes 38–45% of annual snow fall for spruce canopies of Wold Creek. However, JULES inappropriately represented the amount of sublimation leading to the increased soil moisture response during snow melt period (Horton, 2012). The ability of land surface schemes to capture subsurface hydrological processes is critical (Maxwell *et al.*, 2007; Clark *et al.*, 2015).

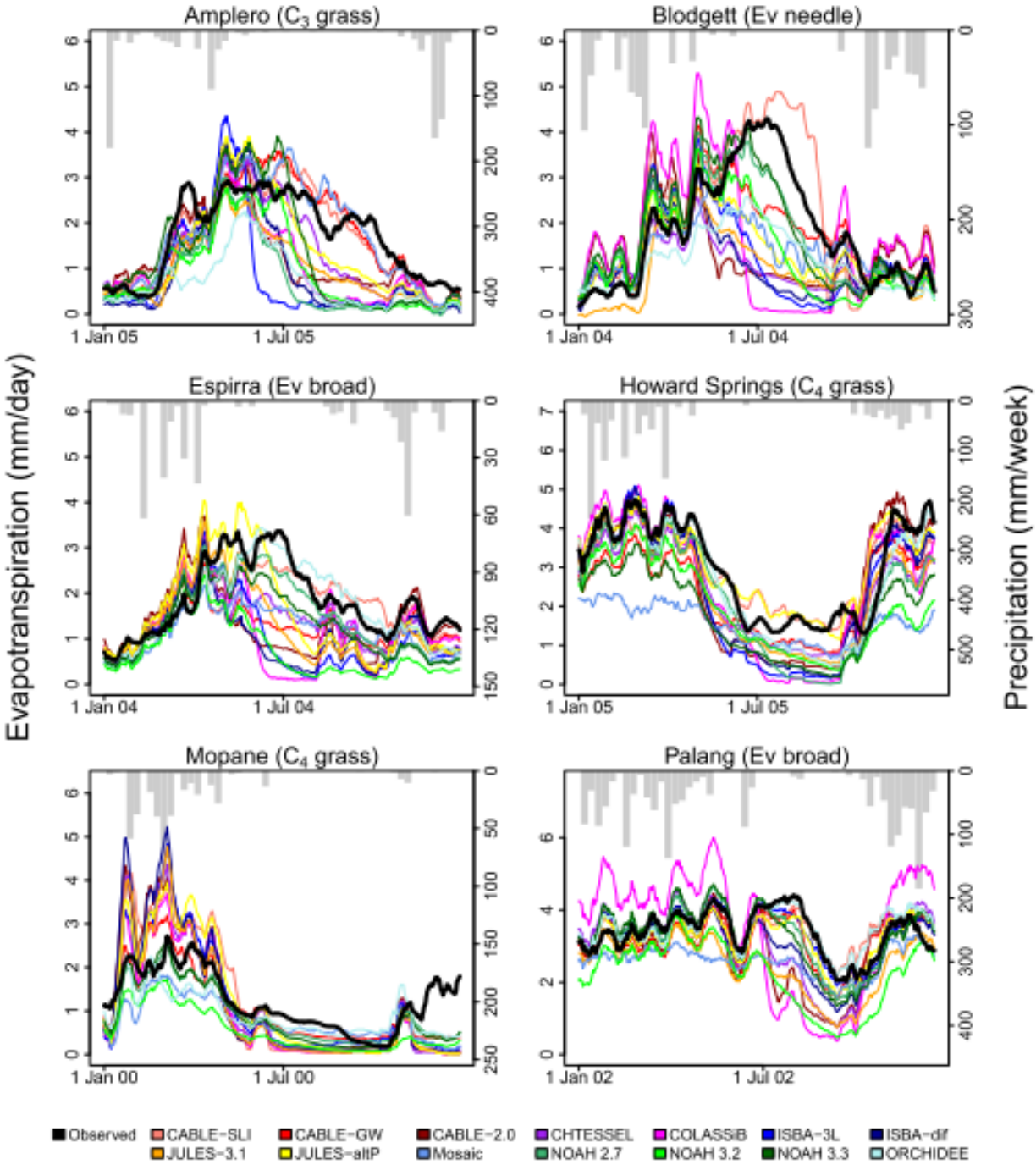

Figure 2–2 Simulated and observed evapotranspiration for a one year period (Ukkola *et al.*, 2016).

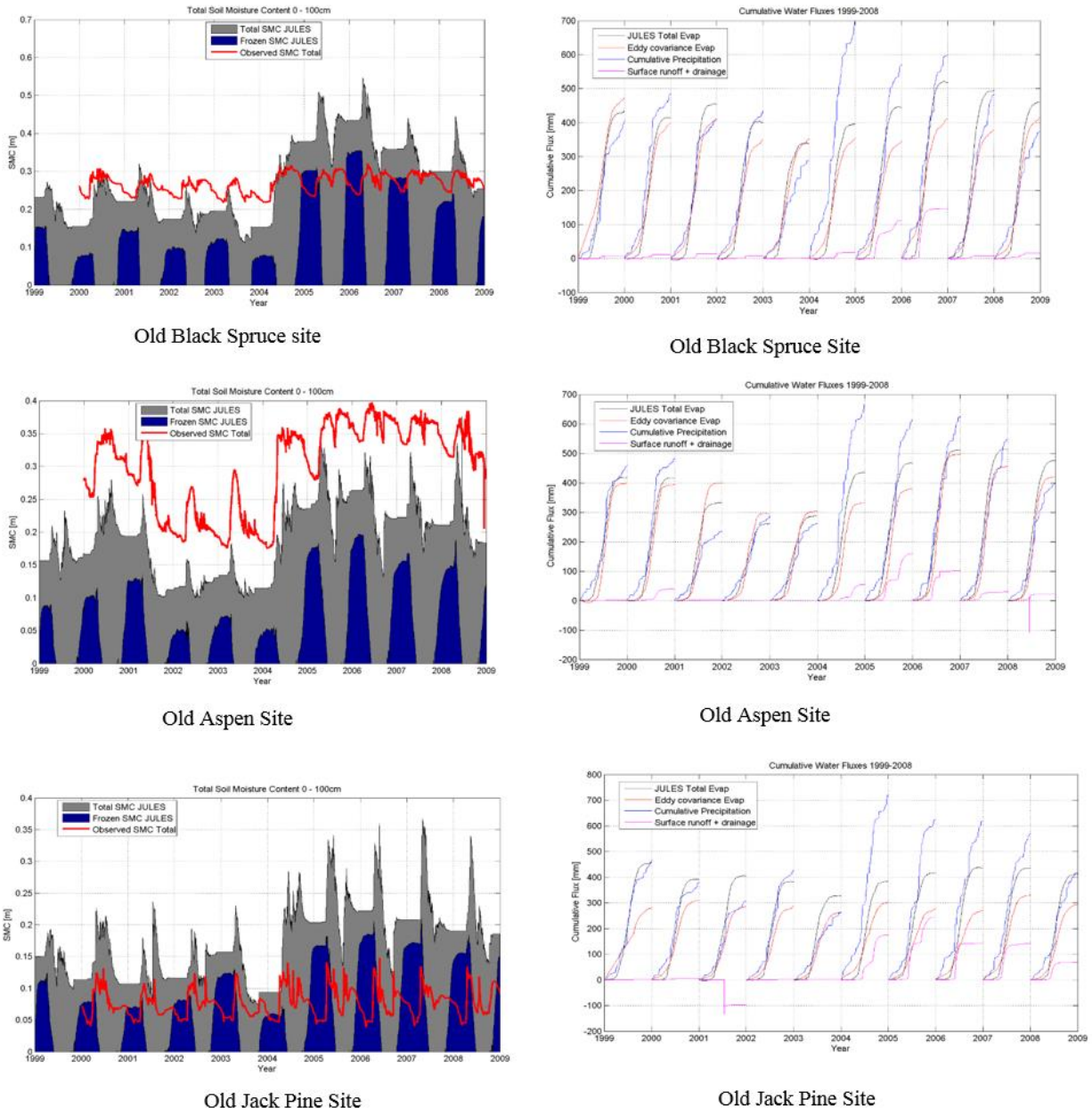

Figure 2–3 Observed and modelled soil moisture content and cumulative water fluxes using default, respectively (Horton, 2012).

Land surface schemes applied in the BERMS have been unable to correctly model *ET* in spring. For example, Davison *et al.* (2016) and Mamo (2015) applied the Canadian Land Surface Scheme (CLASS; Verseghy, 1991; Verseghy *et al.*, 1993) within the hydrologic land surface modeling platform Modelisation Environmentale Communautaire (MEC)–Surface and Hydrology

(MESH; Pietroniro *et al.*, 2007) in the White Gull Creek basin located 60 km northeast of Prince Albert, Saskatchewan, at the southern end of the Canadian boreal forest. They found an overestimation of *ET* in comparison with observations in all four model configurations at Old Black Spruce and Old Jack Pine sites (Figure 2–4 and 2–5). The results showed that the overestimation of *ET* at the OJP site is far more than that at the OBS site. Yetemen *et al.* (2015) applied coupled Canadian Land Surface Scheme and Canadian Terrestrial Ecosystem Model (CLASS–CTEM) at the OJP BERMS and found the incapability of the model to accurately simulate *ET*. In addition to CLASS–CTEM, Nazarbakhsh *et al.* (2017) applied Canadian Land Surface Scheme (CLASS) to the OJP site and compared the performance of CLASS with CLASS–CTEM. The results showed both models overestimate *ET*, and the performance of CLASS–CTEM is worse than that of CLASS in the simulation of *ET* (Figure 2–6). Horton (2012) evaluated the performance of the Joint UK Land Environment Simulator (JULES) at the OJP, OBS and OA BERMS in the Canadian boreal forest. They showed that JULES overestimated the amount of infiltration into the soil profile resulting in the overestimation of soil moisture content and *ET* during wet period at all sites. These studies have demonstrated the incapability of LSSs to simulate *ET*.

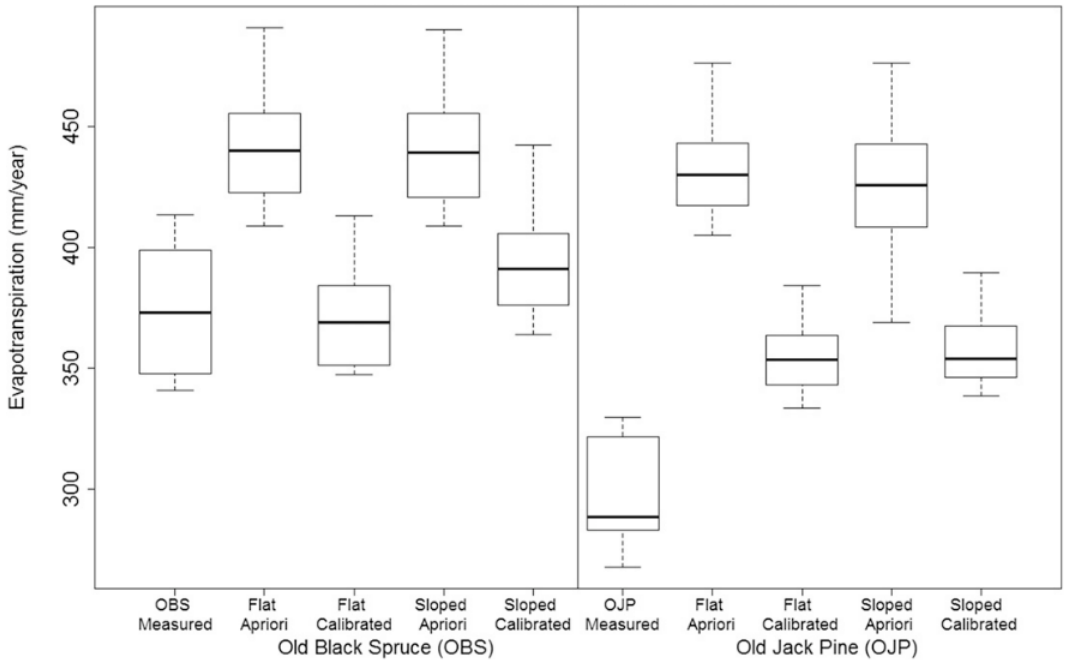

Figure 2–4 Box plots of annual ET for OBS and OJP measurements and four model configuration outputs for 2001–2008 (Davison *et al.*, 2016).

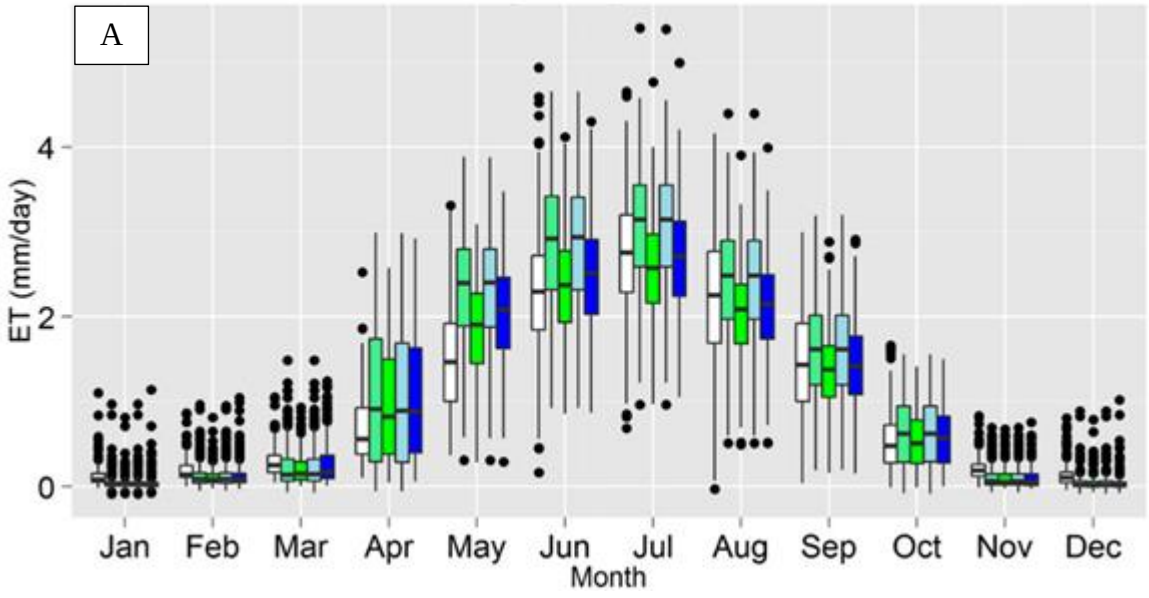

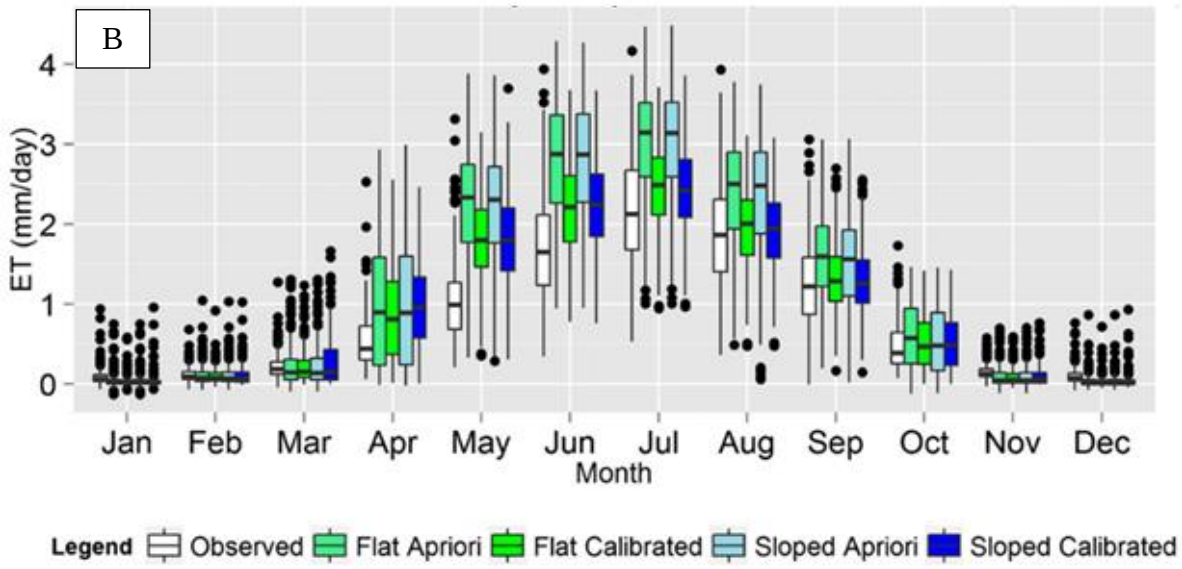

Figure 2–5 Box plots of daily evapotranspiration for A) Old Black Spruce and B) Old Jack Pine observations and model outputs on a monthly basis from January 1, 2001 to September 30, 2009, respectively (Davison *et al.*, 2016).

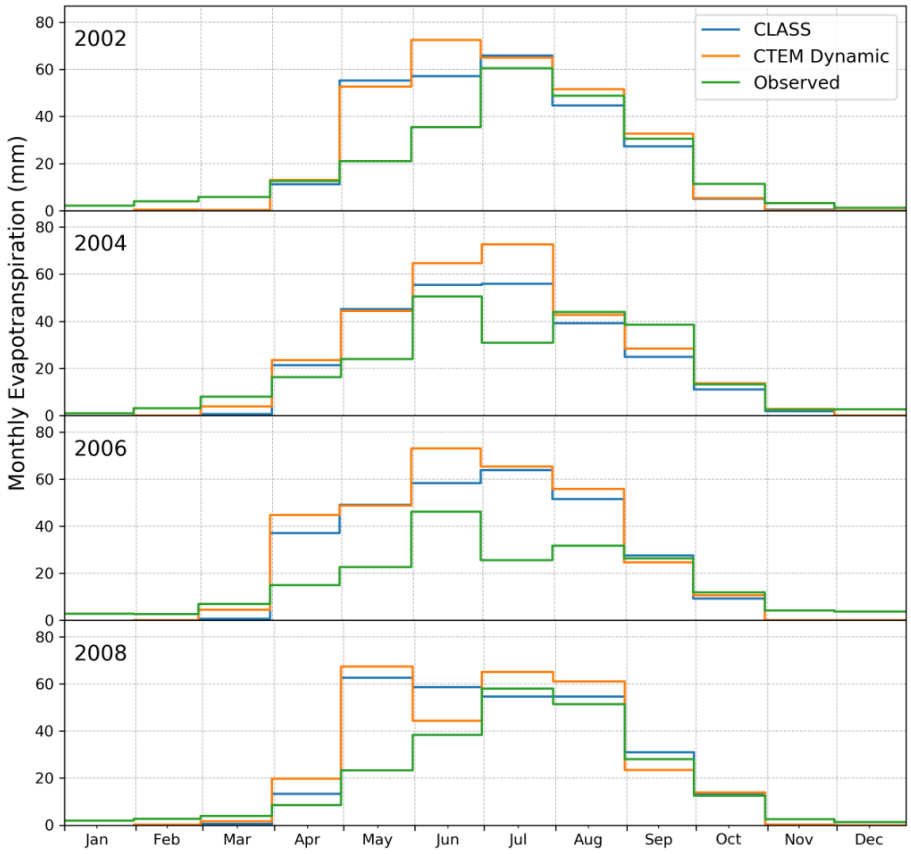

Figure 2–6 Monthly observed and simulated evapotranspiration applying CLASS and coupled CLASS–CTEM (Nazarbakhsh *et al.*, 2017).

2.3 Controls on evapotranspiration

2.3.1 Soil properties and processes

Evapotranspiration is dependent on soil moisture when the soil–plant continuum cannot keep up with the transpiration demand, starting in spring and ending in the fall before snow cover. The soil properties in unfrozen and frozen conditions influence how much moisture is available to the plants as root water uptake, by controlling how much water infiltrates into and drains out of the root zone, dependent in part on the hydraulic conductivity, and by controlling how much water is retained in the soil, dependent on the soil storage capacity and retention properties. These properties are characteristics of the soil, and subject to heterogeneity and variability from site to site, and strongly impacted by the frozen state of the soil.

Soil hydraulic properties divide into two categories. First, soil hydraulic properties are associated with water storage in the soil, measured by the volumetric water content (θ (-)). Second, soil hydraulic properties are related to water transmission through soil layers, measured by the hydraulic conductivity (K (m d^{-1})). These properties are both related to the matric potential (ψ (m)), which expresses to how tightly water is held in the soil by capillary and adsorptive forces and is equivalent to the pressure head. ψ is always negative, and a low negative value relates to a dry soil, while the value goes to zero at saturation.

Water content (θ) is defined as:

$$\theta = \left(\frac{V_w}{V}\right) \tag{2.1}$$

$$V = V_w + V_a + V_s \tag{2.2}$$

Where V_w (m^3) is the volume of water in V (m^3) which is the sum of the volume of water, air (V_a) and soil (V_s). V can be expressed as the root zone volume (e.g. Jackson *et al.*, 1996; Schenk and Jackson, 2002) or from the land surface to the water table depth.

The relationship between water content and matric potential is represented using a soil moisture characteristics curve (Figure 2–7). When matric potential declines, the largest pores start to empty and then afterward smaller pores if they are not blocked from draining. The threshold of soil dewatering is the largest pore in the soil. The soil pressure head of largest active pore is known as the air entry pressure. Below the air entry pressure, soil water is released.

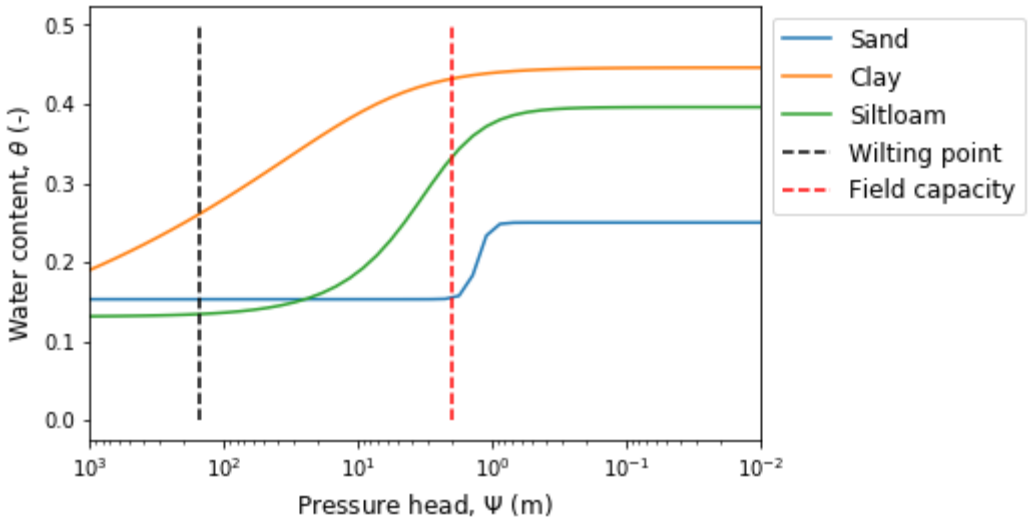

Figure 2–7 Water retention curves for three soil types (i.e. sandstone, silt loam and clay).

The available water for plants is between wilting points (θ_{wilt}) and field capacity (θ_{FC}). Plants cannot take up water when the water content is below the wilting point as it is strongly held by soil particles. When the water content is above the field capacity, water is drained by gravity. Both field capacity and wilting point depend on soil properties such as soil texture, and wilting point also depends on vegetation type (Sperry *et al.*, 2002; Hupet *et al.*, 2005). For example, shrubs or Mediterranean trees can absorb water at the water potential of –4 or –5 MPa (Damesin and Rambal, 1995; Rambal *et al.*, 2003); however, temperate oaks can take up water at the water potential of –2

MPa (Breda *et al.*, 1995). Saturated moisture content (θ_{sat}), is the maximum moisture content of the soil volume, when all pores are filled with water. Soil moisture potential at saturation, field capacity and wilting point are –0.01 m, –1 to –3 m, and –150 m, respectively. Soil moisture index is defined as below. For any values more than field capacity and less than wilting point, soil moisture index is set to 1 and 0, respectively.

$$SMI = \begin{cases} 1 & \theta > \theta_{FC} \\ \dfrac{\theta - \theta_{wilt}}{\theta_{FC} - \theta_{wilt}} & \theta_{FC} \geq \theta \geq \theta_{wilt} \\ 0 & \theta_{wilt} \geq \theta \end{cases} \quad (2.3)$$

Plant transpiration and soil evaporation strongly depend on water transfer in the soil profile (Garrigues *et al.*, 2018). Water transmission through soil profiles also demonstrate the change in hydraulic conductivity with declining pressure head (Figure 2–8). The $K(\psi)$ equation is defined as follows:

$$K(\psi) = K_{sat} K_r(\psi) \quad (2.4)$$

Where K_{sat} and $K_r(\psi)$ are saturated hydraulic conductivity and relative hydraulic conductivity, respectively. $K_{r(\psi)}$ is a scaling factor which varies with θ or ψ between 0 and 1, with lower numbers for drier soils.

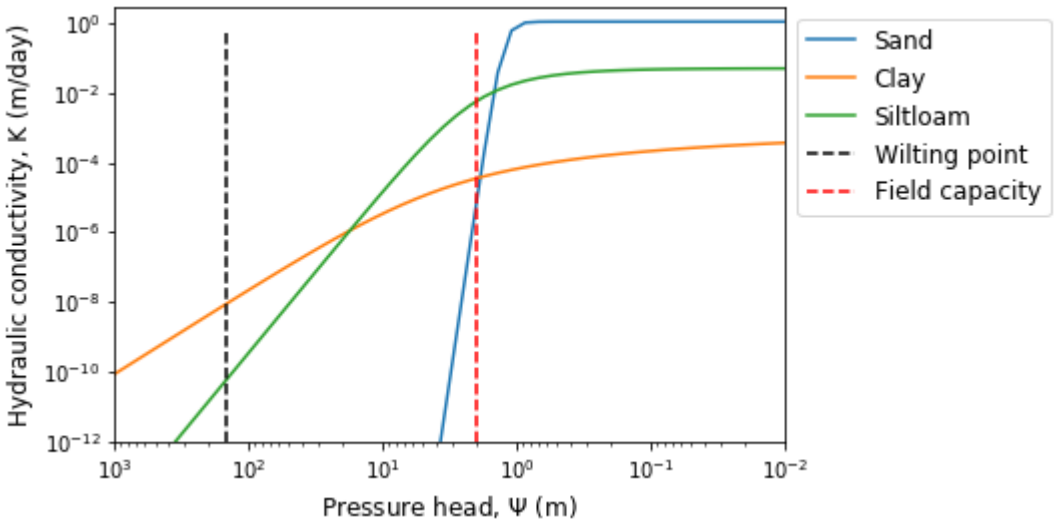

Figure 2–8 The K(ψ) curves for three soil types (i.e. sand, silt loam and clay).

Water and energy balances have dominant linkage with snow and freeze–thaw processes in the soil. In the northern hemisphere, 55–60% of the land surface has frozen soil in winter (Zhang *et al.*, 1999). Frozen soils include small liquid water–filled pores, medium ice–filled pores, large air–filled pores and liquid water around soil particles (Stähli *et al.*, 1999). The amount of water, ice and air filled pores depend on pore size distribution and water content in the soil profile before freezing (Watanabe and Wake, 2009). The hydraulic conductivity and consequently infiltration rates of frozen soils is less than those of unfrozen soils due to ice–filled pores resulting in decreased pore space and increased tortuosity (Stähli *et al.*, 1999). Infiltration rate into frozen soil is known as a dominant hydrological process in cold regions (Fang and Pomeroy, 2007; Ireson *et al.*, 2013), which may significantly affect the amount of evapotranspiration in seasonally frozen forests. In addition to the importance of frozen soil on soil hydrology and runoff, snow plays a critical role for the accurate simulation of surface and subsurface hydrology in spring. Snow has an influence on water availability for runoff and infiltration, the availability of energy for evapotranspiration via snow albedo, and the soil temperature and frozen state via insulation. Snow cover, acting as an insulator, causes a delay in soil thawing (Lunardini, 1981). Slow water release from seasonally frozen soil

increases soil moisture content during spring (Viereck *et al.*, 1983, 1986). Therefore, snow and soil freeze–thaw processes have significant effects on soil moisture in cold regions (Cuntz and Haverd, 2017). The accurate presentation of heat and water transport during freeze–thaw processes in the soil and snow may lead to the improvement of simulating ET.

Heat and water transport in the soil can be accurately represented by the precise representation of soil hydraulic properties and processes. When soils freeze, water in the soil pores transitions to ice progressively as the temperature drops, due to the phenomenon of freezing point depression (Williams and Smith, 1989). Under frozen conditions, the hydraulic properties are modified, influencing the hydrological processes (such as infiltration vs runoff partitioning) and overall water balance (Hillel, 1998). Infiltration and drainage are impeded (Benninghoff, 1952; Wolff *et al.*, 1977; Ford and Bedford, 1987), and then sharply increase following thaw (Hayashi *et al.*, 2003; Watanabe *et al.*, 2013). Infiltration rates can be limited further by the refreezing of infiltrated water during melt period (Stähli *et al.*, 1999), which happens in a shallow layer (0–0.1 m) (Appels *et al.*, 2018). The infiltration capacity of frozen soil relies on ice content, air–filled porosity, soil structure, the number of freezing and thawing cycles (Stadler *et al.*, 1997; Stähli *et al.*, 1999; Nyberg *et al.*, 2001). Air–filled macropores at freezing make pathways for infiltration into deeper soil (Flury *et al.*, 1994; Stadler *et al.*, 2000; Stähli *et al.*, 2004). The number of freeze and thaw processes, soil type and structural conditions and soil temperature may cause cracks in the underlying frozen soil layers allowing snow melt to drain beyond rooting zone. Cracks, dead root passages, soil structural aggregates and worm holes make the frozen soil permeable (Koren *et al.*, 1999). These studies demonstrate that accurate parameterization of soil hydraulic properties can improve the simulation of ET.

2.3.2 Plant water uptake processes

Transpiration is a dominant component of ET, and is dependent on the ability of the plant to draw water into its root system. This depends on the spatial distribution of the roots, in particular how deep they reach into the soil to access the deeper soil water stores. It also depends on the ability of the plant to transmit water from the roots to the leaves, and the capacity of the leaf canopy to transpire water to the atmosphere, which in turn is dependent on the stomatal conductance and leaf area index. In this section, the roles of plant characteristics on ET are addressed.

2.3.2.1 Tree phenology

There are tree phenological controls on photosynthesis and transpiration, which are particularly dynamic during the spring melt period. Vegetation cycles for all ecosystems include inactive and active periods (Aalto *et al.*, 2014). Evergreen conifers have down– and up– regulations of photosynthesis in autumn and spring (Ensminger *et al.*, 2004). In autumn, the process of cold–hardening is started by short day lengths and low temperatures (Huner *et al.*, 1993; Lindgren and Hallgren, 1993). Plant growth is impeded at low temperatures, and photosynthesis is completely suppressed in the cold season, known as the dormancy stage (Ottander *et al.*, 1995; Ensminger *et al.*, 2008). Evergreen conifers have adaptations to keep their green foliage during the extreme cold winter (Oquise *et al.*, 2001; Savitch *et al.*, 2002; Slaney, 2006). Changes in temperature are the driving factor to release plants from dormancy (Hänninen *et al.*, 2007; Rohde and Bhalerao, 2007). During the spring period, plants undergo processes of dehardening (waking up) and budbreak (Kramer, 1994; Saxe *et al.*, 2001). During this period, two phases demonstrate the plants' recovery from dormancy: reactivation of plants' metabolism and onset of plants growth. The first phase is a quiescent phase in which environmental conditions activate genetic expression and producing enzymatic pathways for the growth stage (Heide, 1993; Rohde and Bhalerao, 2007; Sutinen *et al.*,

2009) – no visible signs of plants growth. Photosynthesis is recovered in spring when temperature is above freezing (Ottander *et al.*, 1995; Ensminger *et al.*, 2008), and the rate of recovery relies on soil temperature (Ensminger *et al.*, 2008) and air temperature (Lundmark et al. 1988). This phase (biomass growth) is known as the growth phase. The timing of spring thaw and autumn freeze up determines the carbon–uptake period of boreal evergreen conifers (Goulden *et al.*, 1998; Monson *et al.*, 2005).

2.3.2.2 Root distribution and water uptake model

Root distribution plays a dominant role in root water uptake models. Researchers typically use two methods for calculating root water uptake: macroscopic and microscopic. The microscopic method considers detailed and dynamic root geometry, which is difficult to measure (e.g. Passioura 1988; Hainsworth and Aylmore 1989; Vrugt *et al.*, 2001). This approach simulates water uptake towards individual roots (e.g. Personne *et al.*, 2003). In contrast, the macroscopic method considers the whole root system as a single unit to calculate the root water uptake in models (e.g. Molz and Remson 1970; Nimah and Hanks 1973; Feddes *et al.*, 1976; Feddes 1978; Afshar and Marino 1979; Molz 1981; Marino *et al.*, 1988; Wu *et al.*, 1999; Li *et al.*, 1999; Vrugt *et al.*, 2001; Kumar *et al.*, 2013 and 2014). In this method, water movement is calculated based on numerical solutions to the Darcy–Richards equation and contains a sink term to represent plant root water uptake (Celia and Boulout 1990):

$$\frac{\partial}{\partial Z}\left[K(\Psi)\left(\frac{\partial \psi}{\partial Z}+1\right)\right]+S(z,t)=\frac{\partial \Theta}{\partial t} \qquad (2.5)$$

Where S (d^{-1}) is a depth distributed sink term. In the Feddes *et al.* (1976) model, the S term is given as a function of the depth distribution of the roots ($g(z)$) (dimensionless, the volume of

roots per volume of soil), and a depth distributed water stress function ($f(\psi)$). $g(z)$ can take the form of an exponential decay function, for example:

$$g(z) = \frac{1}{L} e^{-z/L} \tag{2.6}$$

Where L is a parameter (m). The root increment (G_r) from z_{T_i} to z_{B_i} is:

$$G_r = \int_{z=z_{T_i}}^{z_{B_i}} g dz = e^{-\frac{1}{L} z_{T_i}} - e^{-\frac{1}{L} z_{B_i}} \tag{2.7}$$

Root fraction within a soil depth interval (Δz_i), $R(\Delta z_i)$, can be represented as below:

$$R(\Delta z_i) = \begin{cases} 0 & z_R \leq z_{T_i} \\ \dfrac{e^{-\frac{1}{L} z_{T_i}} - e^{-\frac{1}{L} z_R}}{1 - e^{-\frac{1}{L} z_R}} & z_{T_i} < z_R \leq z_{B_i} \\ \dfrac{e^{-\frac{1}{L} z_{T_i}} - e^{-\frac{1}{L} z_{B_i}}}{1 - e^{-\frac{1}{L} z_R}} & z_R > z_{B_i} \end{cases} \tag{2.8}$$

Where z_{T_i} and z_{B_i} are the top and bottom of soil depth interval, respectively. z_R and i are the rooting depth and the number of soil depth interval, respectively.

$f(\psi)$ can be given by:

$$f(\psi) = \begin{cases} 1 & \psi > \psi_{crit} \\ \dfrac{\psi - \psi_w}{\psi_{crit} - \psi_w} & \psi_{crit} \geq \psi \geq \psi_w \\ 0 & \psi_w \geq \psi \end{cases} \tag{2.9}$$

Where ψ_{crit} and ψ_w correspond with the threshold at which water stress commences, and the threshold at which water stress is complete, i.e. wilting point, as ψ is reduced (i.e. as the soil dries), respectively. Note, f can also be expressed as a function of θ or SMI instead of ψ. Now the uptake from a given soil layer (S_i), can be given by:

$$S_i = R(\Delta z_i)\, f(\psi_i)\, \frac{S_P}{\Delta z_i} \tag{2.10}$$

Where $R(\Delta z_i)$ is the fraction of roots within soil depth interval and S_p is the energy–limited transpiration rate, a measure of the atmospheric demand for water. If S_i is integrated with depth, we get the actual evapotranspiration (AE), given by:

$$AE = \sum_{i=1}^{n} S_i \Delta z_i \tag{2.11}$$

Where $AE \leq PE$. In general the sink term can be made to account for the root distribution, the water pressure head, osmotic pressure and meteorological conditions (Feddes *et al.*, 1976; Prasad, 1988).

Researchers have developed root water uptake models based on different root distribution patterns in the soil profile. First, a uniform root density distribution in various soil depths has been considered in the macroscopic root water uptake models (Feddes *et al.*, 1978; Prasad, 1984). Reasoning that root density and thus potential root water uptake decrease with depth, Hoogland *et al.* (1981) offered a linear relationship between maximum uptake and depth. As indicated by Prasad (1988), anomalies remain between the observed and simulated soil moisture extraction when the linear root water uptake model is applied. In other research, non–linear root distribution patterns decreasing with depth have been developed to improve root water uptake models (e.g. Dwyer *et al.*, 1988; Prasad, 1988; Ojha and Rai, 1997; Li *et al.*, 1999; Wu *et al.*, 1999). These studies demonstrate that the more realistic root distribution pattern is considered to be a nonlinear model. Arora and Boer (2003) proposed root distribution and rooting depth as an exponential function of root biomass with time variation as follows:

$$f(z,t) = 1 - \exp[-\frac{b_r}{B^{\alpha_r}(t)} z] \tag{2.12}$$

$$d(t) = \frac{3B^{\alpha_r}(t)}{b_r} \quad (2.13)$$

Where f (z, t) is root distribution as a function of depth and time, d (t) is rooting depth as a function of time, B(t) is root biomass as a function of time, α_r is the root growth direction parameter, and b_r is the parameter representing the effect of soil texture and other factors on the root distribution profile. In this method, the root distribution function is parametrized based on root biomass and applied in dynamic vegetation models. This approach proposed an increase in root distribution and rooting depth as a function of root biomass. This research illustrates the significance of root distribution in the simulation of root water uptake. Errors in root distribution functions may lead to errors in root water uptake models and then the simulation of *ET*.

Although root distribution and density have been found to decrease with increasing soil depth (Arora and Boer, 2003) (Figure 2–9), some studies have uncovered anomalies, with highly distributed and dense root systems found in different soil layers. For example, Van Rees and Jackson (1994) reported that the root distribution of a jack pine stand in Brunisol soil extended to at least 120 cm soil depth (Figure 2–10). According to their records, root length density decreased up to 45 cm soil depth and then increased in 45–60 cm depth and thereafter decreased to 120 cm soil depth (Figure 2–10). Jack pine trees are strongly tap–rooted (Muller-Dombois, 1964; Rowe and Acton, 1985), with their taproots reported from 1.0 to 2.9 m (Bannan, 1940; Strong and La Roi, 1983; Stone and Kalisz, 1991). In a study by Van Rees and Jackson (1994), the root weight density of jack pine increased from LFH layer to 15 cm soil depth, then decreased in 45 cm soil depth, increased in 60 cm depth, again decreased in 105 cm soil depth and increased in 120 cm soil depth. The authors reported low concentrations of root biomass (1%) for the jack pine stand in the forest floor. These studies suggest that uncertainty remains about root distribution within the soil profile.

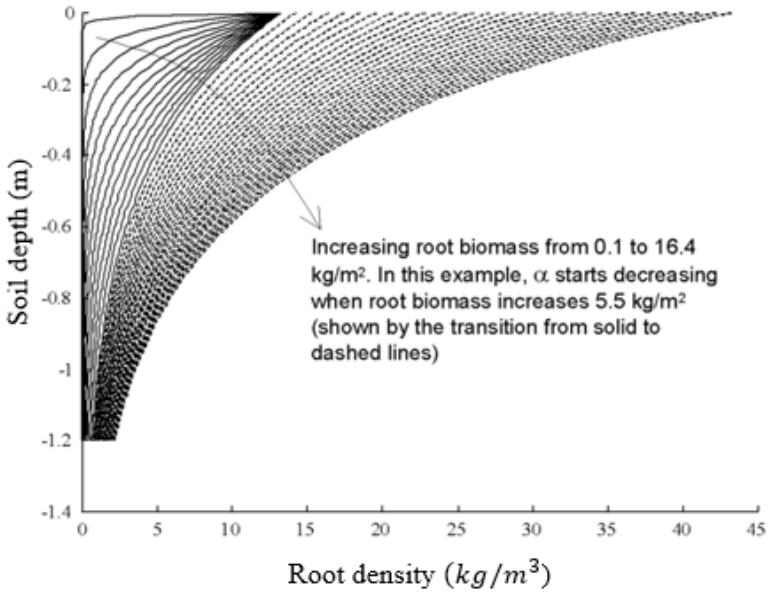

Figure 2–9 The distribution of root density and biomass in the soil profile (Arora and Boer, 2003).

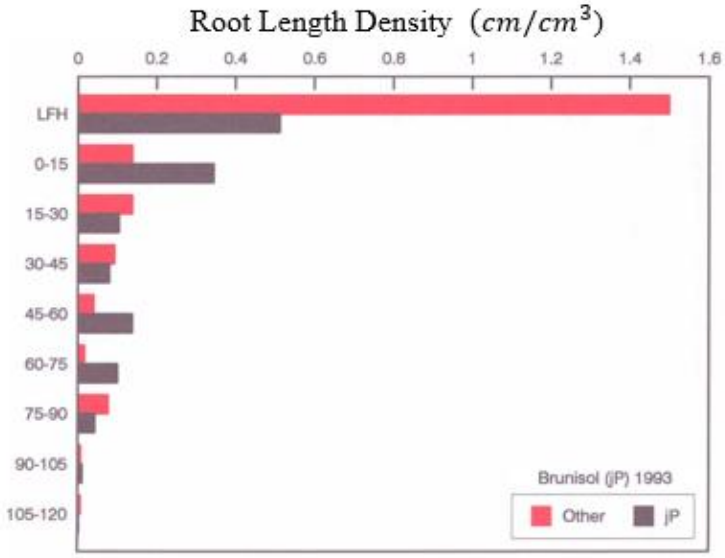

Figure 2–10 Root length density for jack pine stand growing on the Brunisol soil (Van Rees and Jackson, 1994).

2.3.2.3 Soil frost phenomena and root water uptake

In high latitudes, interactions between soil frost phenomena and vegetation are essential to be understood as they have dynamic effects on each other (Benninghoff, 1952). Plant roots are directly

affected by frozen soils (Harvey and Lipman, 1935). In northern regions, not only the long duration of frozen conditions but also repeated freeze and thaw cycles have destructive effects on plant roots. Deep and wide cracks in soils along with extreme damage to roots occur by sudden and rapid drop in temperature in soil free–snow (Harvey and Lipman, 1935). Physical site conditions are significantly affected by low soil temperatures. In addition to profound biochemical changes within plants during a year, root resistance and water viscosity are increased by low soil temperatures and thereby impede trees' biological activities and plants water uptake (Wolff *et al.*, 1977; Lawrence and Oechel, 1983; Goldstein *et al.*, 1985). Trees' root located in frozen soil cannot take up water (Benninghoff, 1952). Although numerous root water uptake models have been developed, these models still have limitations due to difficulties with accurate parametrizations. These parameters depend on field measurements, which are not only tedious and time consuming to collect, but also have high uncertainty.

2.3.2.4 Stomatal conductance and evapotranspiration

In addition to rooting depth and root distribution, stomatal conductance controls transpiration and as a result of that latent heat loss (Huang *et al.*, 2017) as the canopy transpiration (*T*) is derived as follows:

$$T = \rho_a \left[\frac{q_s(T_s) - q_r}{r_a + r_c} \right] \tag{2.14}$$

Where ρ_a is the air density (kg m^{-3}), $q_s(T_s)$ is the saturation water vapor specific humidity at the leaf–surface temperature, and q_r is the water vapor specific humidity at the reference atmospheric level, r_a is the aerodynamic resistance (s m^{-1}), and r_c is the canopy resistance (s m^{-1}).

The role of stomatal resistance (r_s) on simulating evapotranspiration is critical as stomata couple the exchange of carbon and water between the plants and the atmosphere. The calculation of

stomatal resistance given in Arora (2003), which is based on the Jarvis approach (1976), is as follows:

$$r_s = r_{s\,min} f(PAR) f(T) f(\delta e) f(\psi) \tag{2.15}$$

Where $f(PAR)$, $f(T)$, $f(\delta e)$, and $f(\psi)$ are the dependency factors of r_s on solar radiation (Photosynthetically Active Radiation, *PAR*) (W m^{-2}), temperature (℃), vapour pressure deficit (mbar), and soil matric potential (m), respectively, and are given by:

$$f(PAR) = \max(1, \left(\frac{500}{PAR}\right) - 1.5) \tag{2.16}$$

$$f(\delta e) = \max(1, \frac{\Delta e}{5}) \tag{2.17}$$

$$f\ (\psi) = \max(1, \frac{\psi}{40}) \tag{2.18}$$

$$f(T) = \begin{cases} 1\,, & 40\ ℃ > T_a > 0\ ℃ \\ \dfrac{5000}{r_{s\,min}}, & T_a \geq 40\ ℃\ or\ T_a \leq 0\ ℃ \end{cases} \tag{2.19}$$

When all environmental controls are non–limiting, stomatal resistance equals to minimum stomatal resistance ($r_{s\,min}$); otherwise it is higher. As shown in the above equations, stomatal resistance depends on numerous parameters. Errors in assigning these parameters may significantly lead to errors in the calculation of stomatal resistance and therefore errors in the simulation of *ET*.

In order to scale up stomatal resistance at leaf level (r_s) to canopy resistance(r_c), Leaf Area Index (*LAI*) is used. *LAI* is defined as the whole one–sided green leaf area per unit of ground surface (Chen and Cihlar, 1996). *LAI* is a dimensionless amount. In numerous land surface schemes, *LAI* is a critical parameter for the simulation of water and carbon balances. Evapotranspiration, gross photosynthesis, canopy interception, energy and mass balance rely on *LAI*. The appropriate quantification of *LAI* is difficult due to considerable temporal and spatial variability (Bréda, 2003).

The canopy resistance, then, is given by:

$$r_c = \frac{r_s}{LAI} \tag{2.20}$$

Which can also be expressed in terms of conductance as:

$$g_c = g_s LAI \tag{2.21}$$

$$g_c = \frac{1}{r_c} \; ; g_s = \frac{1}{r_s} \tag{2.22}$$

Where g_s and g_c are the stomatal conductance (m s^{-1}) and canopy conductance (m s^{-1}), respectively. The Ball *et al.* (1987) canopy conductance formulation is as follows:

$$g_c = m\frac{A_n h_s p}{c_s} + b\ LAI \tag{2.23}$$

Where g_c is the canopy conductance (µmol CO_2 m^{-2} s^{-1}), $A_n$is the net canopy photosynthesis rate (µ mol CO_2 m^{-2} s^{-1}), h_s is the relative humidity at the leaf surface, p is the pressure (Pa), c_s is the partial pressure of CO_2 at the leaf surface (Pa), LAI is the leaf area index, m and b are vegetation dependent parameters. The Leuning (1995) canopy conductance model is given by:

$$g_c = m\frac{A_n p}{(c_s - \Gamma)}\frac{1}{(1 + \frac{D_v}{D_0})} + b\ LAI \tag{2.24}$$

Where Γ is the CO_2 compensation point (Pa), which is the CO_2 partial pressure when photosynthetic uptake is equal to the leaf respiratory losses, D_v is the vapor pressure deficit (Pa), and D_0 is a vegetation dependent parameter (Pa).

Researchers have demonstrated the inadequacy of the aforementioned parameterizations for simulating transpiration due to not considering other limiting factors which are associated with plants physiology. This deficiency results in overestimation of *ET* in Land Surface Schemes (e.g. Henderson-Sellers *et al.*, 1996; Seneviratne *et al.*, 2002).

2.4 Conclusion and gaps

This literature review has presented an overview of plant characteristics, subsurface hydrological processes in seasonally frozen forests and identified the crucial challenges and main questions that need to be addressed to improve the predictions of *ET* using land surface schemes in seasonally frozen forests. We show that land surface schemes applied to this environment to date have failed to simulate *ET*, and have associated errors in simulating water, carbon and energy balances. To improve the simulation of *ET* in seasonally frozen forests using land surface schemes, researchers need to focus on the following factors. First, land surface schemes should have the capability to capture subsurface hydrological processes in a manner that the amount of soil water storage in each rooting zone soil layer and water flow in different soil layers are accurately represented. Second, vegetation properties (e.g. root depth/distribution, leaf area index and canopy conductance) should be accurately represented in land surface schemes. To adequately simulate *ET*, the proposed research will consider the parametrization of plant characteristics and soil hydraulic properties. As seasonally frozen soils present a particular challenge due to their snowmelt–dominated hydrology and the impact of soil freezing on the soil hydraulic properties and plant root water uptake, this study will consider the important role of frozen soils and snow melt processes in the simulation of *ET*.

CHAPTER 3

CONTROLS ON EVAPOTRANSPIRATION FROM SEASONALLY FROZEN FORESTS

Status: Submitted November 2018. Under Review

Citation: Nazarbakhsh, M., Ireson, A.M., Barr, A.G. (under review)
Controls on evapotranspiration from seasonally frozen forests, Hydrological Processes.

3.1 Abstract

The exchanges of water, energy and carbon between the land surface and the atmosphere are tightly coupled, so that errors in simulating evapotranspiration lead to errors in simulating both the water and carbon balances. Seasonally frozen soils present a particular challenge due to the snowmelt–dominated hydrology and the impact of soil freezing on the soil hydraulic properties and plant root water uptake. Land surface schemes that have been applied in high latitudes often have problems with simulating the snowpack and runoff. Models applied at the Boreal Ecosystem Research and Monitoring Sites (BERMS) in central Saskatchewan have consistently over–predicted evapotranspiration as compared with flux–tower estimates. We assessed the performance of two Canadian land surface schemes (CLASS and CLASS–CTEM) for simulating point–scale evapotranspiration at an instrumented jack pine sandy upland site in the southern edge of the boreal forest in Saskatchewan, Canada. Looking systematically at soil properties and vegetation characteristics, we found that the dominant control on evapotranspiration was canopy conductance, and that errors in the soil hydraulic properties, root distribution and leaf area index could not, individually, account for the model biases. Although canopy conductance and leaf area index are dependent, we can confidently rule out the possibility that errors in leaf area index can explain bias in ET – given the fact that at this site we have site specific estimates of leaf area index. We also

show that the model ET bias was largest during and just after the soil–thaw period in spring, and recommend further exploration of the effects of spring thaw on plant root water uptake in these models.

Key words:

Land Surface Schemes, Seasonally Frozen Soils, Evapotranspiration, Snowmelt, Soil Hydraulic Properties, Vegetation Characteristics, Eco–hydrology, Boreal Forest

3.2 Introduction

Evapotranspiration, ET, is a critical process in the land surface water, energy and carbon balances. Accurate quantification of ET is necessary for hydrological, climate and plant growth models, and the joint application of these models in the form of land surface models or Land Surface Schemes, LSSs (Jacquemin and Noilhan, 1990; Braud *et al.*, 1995; Cresswell and Paydar, 2000). Many studies have been undertaken to assess the performance of LSSs to quantify water, energy and carbon fluxes as compared with flux–tower observations (e.g. Henderson-Sellers *et al.*, 1993; Best *et al.*, 2015). Ukkola *et al.* (2016) assessed the performance of 14 LSSs (CABLE–SLI, CABLE–GW, CABLE–2.0, CHTESSEL, COLASSiB, ISBA–3L, ISBA–dif, JULES–3.1, JULES–altP, Mosaic, NOAH 2.7, NOAH 3.2, NOAH 3.3, ORCHIDEE) to simulate water and energy fluxes during drought conditions, and found that the models systematically underestimated ET during water stress conditions (and hence overestimated the "evaporative–drought"). The six sites used in this study (a subset of the 20 sites used by PALS and PLUMBER, Best *et al.* (2015)) were all in temperate climate locations (latitudes no greater than 42^{o} N).

In more northern latitudes, land surface processes are increasingly influenced by snow and ice, and the partitioning of snowmelt into runoff and infiltration in the spring is a critical component of the water balance (Luo *et al.*, 2003). Most past studies in such conditions have focussed on the

importance of snow accumulation and ablation processes (Essery *et al.*, 2009; Rutter *et al.*, 2009). Schlosser *et al.* (2000) reported on the PILPs study that compared 21 LSSs at a seasonally frozen site. They found considerable differences in ET and runoff between the models, in particular during the melt period, and concluded that differences in the representation of snow melt processes and frozen soil moisture were critical to the performance of the models. Luo *et al.* (2003) continued this study to look at the simulation of frozen soil, but found the inclusion of frozen soils within the model did not make a big difference on soil moisture processes. They concluded, again, that snow processes were of critical importance. Cherkauer and Lettenmaier (1999) and Pitman *et al.* (1999) ran large scale models (the Global Soil Wetness Project and VIC, respectively) for the McKenzie and Mississippi river basins, respectively, and both concluded that while frozen soil physics did affect runoff and infiltration processes, the impacts on large scale simulations of runoff were negligible. More recently, Ganji *et al.* (2017) applied the CLASS model with different frozen soil infiltration representations to 21 watersheds in northeastern Canada and showed that this had a significant impact on streamflow. Simulations were improved, as compared with observed streamflow, when the infiltration capacity of the frozen soils was reduced, resulting in more runoff generation.

A number of LSSs have been applied to the Boreal Ecosystem Research and Monitoring sites, BERMS, in the southern part of the boreal forest in Saskatchewan, Canada. These sites include Old Jack Pine, OJP (53.92 °N, 104.69 °W) (Barr *et al.*, 2006), Old Aspen, OA (53.63 °N, 106.2 °W) (Black *et al.*, 1996; Barr *et al.*, 2006), and Old Black Spruce, OBS (53.98 °N, 105.12 °W) (Barr *et al.*, 2006), sites, two of which (OBS and OJP) are located in the White Gull Creek basin located 60 km northeast of Prince Albert, Saskatchewan. Bartlett *et al.* (2003) applied an earlier version of CLASS (v2.6) to the BERMS sites, and found that ET was overestimated by the model, and they

concluded that this was due to the parameterization of canopy conductance. Horton (2012) found that the joint UK Land Environment Simulator, JULES, overestimated the available snowmelt for infiltration in the spring leading to the overestimation of soil moisture content and ET during the wet periods following spring melt at all of the flux tower sites. Davison *et al.* (2016) and Mamo (2015) found that Canadian Land Surface Scheme (CLASS; Verseghy, 1991; Verseghy *et al.*, 1993) implemented within the hydrologic land surface modeling platform Modelisation Environmentale Communautaire (MEC)–Surface and Hydrology (MESH; Pietroniro *et al.*, 2007) consistently overestimated ET for the OBS and OJP sites, even when the soil and routing parameter were calibrated. Yetemen *et al.* (2015) demonstrated the overestimation of ET at the OJP site by the coupled Canadian Land Surface Schemes and Canadian Terrestrial Ecosystem Model (CLASS–CTEM; Arora, 2014). Chen *et al.* (2016) applied NOAH–MP to the OA site and found that ET was overestimated in the spring and underestimated in the summer, except during drought conditions, when it was slightly overestimated. They also found that the simulations were improved by including an organic soil layer. In all of these studies, ET has been overestimated by the models, in particular during the spring melt period, suggesting that this may be a generic limitation of LSSs in seasonally frozen environments.

The objective of this paper is to assess the controls on evapotranspiration from forest canopies in seasonally frozen soils. We apply the Canadian Land Surface Scheme (CLASS, version 3.6) and the coupled Canadian Land Surface Scheme and Canadian Terrestrial Ecosystem Model (CLASS–CTEM, version 1.2). We will first compare the performance of these models with observations of evapotranspiration from the flux tower at the OJP BERMS site. Next, we will investigate how soil properties and vegetation characteristics impact the hydrological processes, and in particular ET, in both of these models.

3.3 Methods

3.3.1 Study site

The research site is the Boreal Ecosystem Research and Monitoring Sites (BERMS) Old Jack Pine (OJP) site, located at the southern edge of the Canadian boreal forest east of Prince Albert National Park, Saskatchewan, Canada (53.92 °N, 104.69 °W, and altitude 579.3 m). The dominant tree species is jack pine (*Pinus banksiana Lamb.*) with a stand density of 1190 stem ha^{-1} (Amiro *et al.*, 2006; Barr *et al.*, 2006). The jack pine–dominated forest is on well– or rapidly–drained dry and sandy textured soil, which is nutrient poor (Acton *et al.*, 1998; Barr *et al.*, 2012). The water table is located at least 5 metres below the soil surface (Barr *et al.*, 2012). Over the period 1999 to 2011, the average precipitation and evapotranspiration are 502 and 307 mm $year^{-1}$, respectively (Ireson *et al.*, 2015). Snowfall is between 21% and 31% of precipitation, and snow cover remains for about four months (Ireson *et al.*, 2015). The mean annual temperature (1981–2010) is 3–4℃ with corresponding means of –10℃ and 20℃ for January and July, respectively (Ireson *et al.*, 2015). From 1999 to 2008, the depth of soil freezing was greater than 1 m at the OJP site (Ireson *et al.*, 2015).

3.3.2 Modelling tools

This research applied two models: the Canadian Land Surface Scheme (CLASS, version 3.6) and the coupled Canadian Land Surface Scheme and Canadian Terrestrial Ecosystem Model (CLASS–CTEM, version 1.2). CLASS simulates the water and energy balance of the soil, vegetation and snowpack (Verseghy, 1991, 2011; Verseghy *et al.*, 1993). In this study, we perform simulations using a single grid cell with a single land cover tile representative of the jack pine forest as an evergreen needleleaf forest plant functional type. CLASS considers static vegetation, whereby the root distribution and canopy height are fixed, and leaf area index (LAI) changes seasonally at a

prescribed rate based on accumulated temperature. CLASS–CTEM, in addition to the water and energy balance, also simulates the carbon balance (Arora, 2003, 2014; Arora and Boer, 2005; Melton and Arora, 2016). The model is comprised of three vegetation pools consisting of leaves, stems and roots, and two dead carbon pools consisting of litter and soil organic matter. Vegetation is dynamic, and the roots, canopy height and leaves all respond seasonally and interannually to the assimilation and allocation of carbon. There are some other differences between CLASS and CLASS–CTEM, such as how the canopy conductance is parameterised. To control for differences between the models caused by vegetation dynamics (that is, differences in LAI, canopy height and root distribution), we also used a modified configuration of CLASS–CTEM, where these vegetation characteristics were fixed, known hereafter as CLASS–CTEM Static. Both models contain three soil layers, with a total depth of 4.1 metres and are driven by forcing data with a 30–minute time step. CTEM simulates all terrestrial ecosystem processes at a daily time step, except for photosynthesis and leaf respiration simulated at half–hourly time steps.

3.3.3 Observed data

Half–hourly values of shortwave radiation, longwave radiation, precipitation, temperature, specific humidity, wind speed, and pressure are required to drive the models. Flux tower estimates of evapotranspiration (Barr *et al.*, 2006, 2012) were used to assess the performance of the model. All of these data were obtained from the OJP flux tower site (available from http://giws.usask.ca/meta).

3.3.4 Analysis of model outputs

In this study, we investigate how rainfall and snowmelt are partitioned between ET, runoff, drainage and storage, as depicted in Figure 3–1. We focus our analysis on the simulated soil water balance, which is constructed from model output variables as described here.

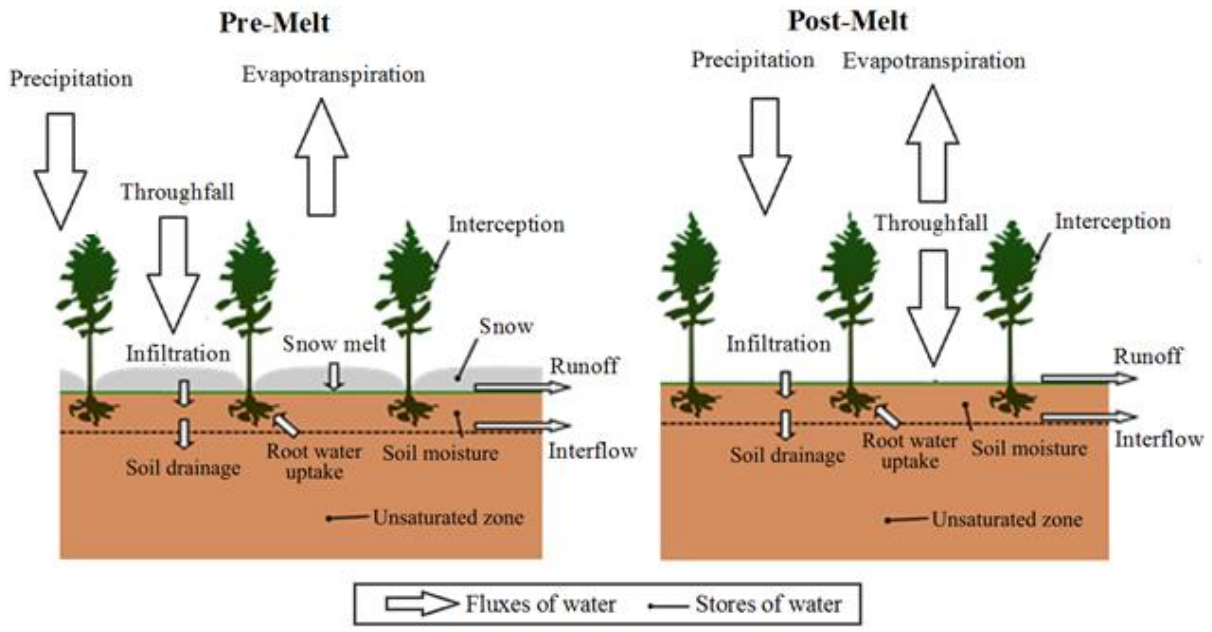

Figure 3–1 Conceptual diagram of the pre– and post– melt soil water balance from a seasonally frozen forest.

The water balance equation is:

$$\Delta S = \Delta S_L + \Delta S_S = I - D - ET \tag{3.1}$$

Where ΔS, ΔS_L and ΔS_S (L) are the change in total, liquid and solid (ice) soil water storage in the root zone , and I, D and ET (L) are time integrated fluxes of infiltration, drainage (that is downward vertical percolation out of the base of the soil column) and evapotranspiration (that is ground evaporation plus transpiration). We assumed that interflow was zero, and verified that this was the case from the model outputs. The storage terms are given by depth integrating the liquid/solid water contents, θ_L and θ_S (-), e.g.:

$$\Delta S_{L,j} = \sum_{i=1}^{3} \left(\theta_{L\,i,j} - \theta_{L\,i,j-n} \right) \Delta z_i \tag{3.2}$$

where i and j are indices in depth and time, respectively, and Δz_i (L) is the layer thickness. n is an index value greater than or equal to 1, which allows us to calculate the changes in storage over

different time periods – for example, daily changes in storage are obtained by setting $n = 48$. The time integrated fluxes are given by:

$$D = \sum_{j=1}^{n} D_j \Delta t \quad (3.3)$$

where j and n have the same meaning as in Equation 3.2, D_j is the model outputted flux (L T^{-1}) (in this example drainage) and Δt is the model calculation timestep, which was 30–minutes. Infiltration was calculated as:

$$I = R_G + M - F \quad (3.4)$$

where R_G (L), M (L) and F (L) are rainfall on the ground (throughfall, which includes canopy unloading), snowmelt and surface runoff, respectively. The snow and canopy water balances are not included here, as these are not our focus. However, when we compare the model with observed ET fluxes from the flux tower, we include sublimation and evaporation from the canopy in the total ET term.

The variables in Equations 3.1–3.4 are obtained from the CLASS/CLASS–CTEM output variables listed in Table 3–1.

Table 3–1 Canadian Land Surface Scheme variables.

Variable name	Descriptions	Units
PCPG	Precipitation incident on ground, including snowmelt	kg m^{-2} s^{-1}
ROFN	Liquid water from snowpack, i.e. snowmelt	kg m^{-2} s^{-1}
WTRG	Water transferred into or out of the soil	kg m^{-2} s^{-1}
ROFO	Overland flow from top of soil column	kg m^{-2} s^{-1}
ROFB	Base flow from bottom of soil column, i.e. drainage	kg m^{-2} s^{-1}
QFG	Water vapour flux from ground, i.e. soil evaporation	kg m^{-2} s^{-1}
QFC1–3	Water uptake from each soil layer by transpiration	kg m^{-2} s^{-1}
THLIQ1–3	Volumetric liquid water content of soil layers	m^3 m^{-3}
THICE1–3	Volumetric frozen water content of soil layers	m^3 m^{-3}
DELZW1–3	Thickness of soil layers	m

The CLASS/CLASS–CTEM output variables are related to the symbols in our water balance equations by the following:

$$\text{PCPG} + \text{WTRG} = R_G + M \quad (3.5)$$

$$\text{ROFN} + \text{WTRG} = M \quad (3.6)$$

$$\text{THLIQ1} = \theta_{L1} \quad (3.7)$$

$$\text{THICE1} = \theta_{S1} \quad (3.8)$$

$$\text{ROFO} = F \quad (3.9)$$

$$\text{ROFB} = D \quad (3.10)$$

$$\text{QFG} + \text{QFC1} + \text{QFC2} + \text{QFC3} = ET \quad (3.11)$$

$$\text{DELZW1} = \Delta z_1 \quad (3.12)$$

Note that 1 kg m^{-2} is equal to 1 mm, and we work in units of mm (storage) and mm d^{-1} (fluxes).

3.3.5 Assessment of the dominant controls on evapotranspiration

Land Surface Schemes have large numbers of free parameters (sometimes including parameters that are hard coded and thus easily overlooked, Mendoza *et al.*, 2015) whose values are uncertain. Sensitivity analysis can be used to understand how certain parameters affect certain model outputs (Slater *et al.*, 2001; Sieber and Uhlenbrook, 2005; Bastidas *et al.*, 2006). However, this can be challenging when the number of parameters is large (Cadero *et al.*, 2018), when the influences of different parameters are not independent, and when we are potentially interested in multiple output metrics. Here, we applied a simple mechanistic approach to assess the dominant controls on ET, by focussing not on individual parameters (such as the root distribution exponent parameter), but on emergent characteristics (such as the actual proportions of roots in each soil layer that are determined by the root exponent parameter, as well as other parameters). We consider separately the role of soil hydraulic properties and plant characteristics (abiotic and biotic factors,

respectively, Fatichi *et al.*, 2015). Soil properties influence how much water infiltrates into the soil, how much drains out of the root zone, and consequently how much is available to the plants as root water uptake. Plant characteristics determine the transpiration flux, a dominant component of ET; critical plant characteristics are the root distribution, canopy conductance and leaf area index. The premise of our study is that, a–priori, it is not possible to say which of these factors is most important, and therefore where efforts to improve the models should be focussed. All of the "characteristics" we look at depend in turn on a number of parameters and relationships. For example, in CLASS–CTEM, the canopy conductance depends on numerous factors including the vapor pressure deficit, leaf area index, the maximum rate of carboxylation by the enzyme Rubisco, the canopy temperature, parameters defining the lower and upper temperature limits for photosynthesis, a soil moisture stress term and the ambient CO_2 concentration (Arora, 2003, 2014). It is important to understand the contribution of each of these factors, but that is not our objective here — we look only at the overall impact of changing the canopy conductance.

Below we describe the different model configurations that were used to explore the dominant controls on ET.

3.3.5.1 Soil hydraulic properties

Soil hydraulic properties in CLASS and CLASS–CTEM are parameterized based on soil texture using pedotransfer functions (Saxton and Rawls, 2006) and the Clapp and Hornberger parametric model (Clapp and Hornberger, 1978) that defines the relationship between water content, θ (-), matric potential, ψ (L), and hydraulic conductivity, K (L T^{-1}). Such approaches are widely used in LSSs (Looy *et al.*, 2017) but can constrain the parameter space unrealistically. Here, we consider two baseline parameter sets: one based on local direct observations of the soil hydraulic properties (Cuenca *et al.*, 1997), and the second based on local observations of soil texture,

combined with the CLASS pedotransfer function. The observed soil hydraulic properties from Cuenca *et al.* (1997) are given for the van Genuchten–Mualem (Van Genuchten, 1980) model (shown in Table 3–2), so equivalent Clapp and Hornberger parameters (shown in Table 3–3) were obtained by optimization, with the result shown in Figure 3–2. For the second case, the soil texture of the OJP site is 93–96% sand, 2–3% clay, with 10% organic matter in the top 10 cm, and the bulk density is estimated 1.45 (g cm^{-3}), and the corresponding soil hydraulic properties are given in Table 3–3. The major difference between the two baseline parameter sets is that the saturated hydraulic conductivity is lower from direct observations (1.46 m d^{-1}) compared with the texture–based parameter (2.17 m d^{-1}). In addition to these two parameter sets, we also varied individual parameters in a univariate sensitivity analysis. The range of parameters considered are given in Table 3–3.

Table 3–2 Soil hydraulic properties using the van Genuchten–Mualem model measured at site (Cuenca *et al.*, 1997).

K_{sat} (m d^{-1})	η	α (m^{-1})	θ_r (m^3 m^{-3})	θ_{sat} (m^3 m^{-3})
1.46	1.56	7.81	0.03	0.40

Table 3–3 Soil hydraulic properties using the Clapp and Hornberger model.

Types	K_{sat} (m d^{-1})	θ_p (m^3 m^{-3})	b	ψ_{sat} (m)
Texture–based parameters	2.17	0.37	3.35	–0.044
Fit to observations	1.46	0.4	2.26	–0.026
Range of each parameter used in the sensitivity analysis	0.001–10	0.15–0.55	no change	0.001–10

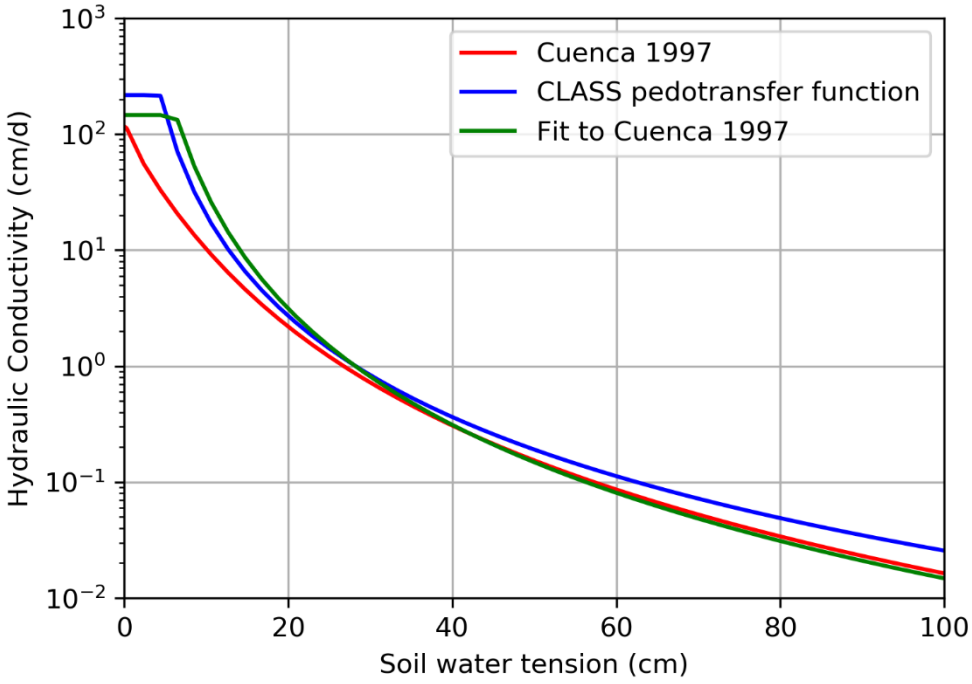

Figure 3–2 Cuenca et al. (1997); CLASS pedotransfer function; Fit to Cuenca et al. (1997).

3.3.5.2 Rooting depth and root distribution

Transpiration, the dominant component of ET, depends on the spatial distribution of the roots, in particular how deep they reach to access the deeper soil water stores. By default the CLASS and CLASS–CTEM models have three soil layers with depths of 0.1, 0.25, and 3.75 m, though it is possible to use alternative configurations with more soil layers. By default, the root density declines exponentially with depth. Due to the differences in layer thicknesses, this means that the actual proportion of roots in each layer, by default, works out to be approximately even for CLASS and this study's implementation of CLASS–CTEM. To assess the sensitivity to root depth and distribution, considered three cases. First, we performed three model runs with the maximum root depth set to reach the base of each of the three layers in turn – i.e. 0.1 m, 0.35 m, and 4.1 m. Next, we used a finer soil discretization, with 10 layers, so that we could explore the sensitivity of the root

depth at a finer resolution. Finally, we explored the root distribution in the three–layer model, by applying 100% of the root distribution to one layer at a time. This is the most extreme variation in root distribution that is possible in a three–layer model.

3.3.5.3 Leaf Area Index

Transpiration is also strongly dependent on LAI (Bonan, 1993; Chen *et al.*, 1997). Here, for the CLASS and CLASS–CTEM static model runs, we assumed a constant value for LAI that does not change seasonally. We took a baseline value of 2.7 for LAI, which was based on local observations (Chen *et al.*, 1997; Griffis *et al.*, 2003; Barr *et al.*, 2006), and considered a range of values from 0.9 to 8.1 in the sensitivity analysis.

3.3.5.4 Canopy conductance

As described above, CLASS and CLASS–CTEM have different parameterisations of canopy conductance. Here, we only modified the bulk canopy conductance for each model, by factors of 0.6, 0.8, 1.2, and 1.4. This was achieved for CLASS by multiplying the minimum stomatal resistance by these factors. It was achieved for CLASS–CTEM by multiplying the parameter b and m used in the coupled photosynthesis and canopy conductance model (Leuning, 1995) by these factors.

3.4 Results

3.4.1 Model performance

As shown in Figure 3–3, all three models, that is CLASS, CLASS–CTEM and CLASS–CTEM Static, overestimate ET in comparison with observations from the OJP flux tower. The overestimation of ET using all three models is maximum during the spring and early summer. We found that the difference in ET simulated with dynamic and static versions of CLASS–CTEM was

negligible. The simulation of ET using both configurations of CLASS–CTEM with baseline parameters was worse than the simulation of ET using CLASS.

We show in Figure 3–4 that for the baseline CLASS model configuration, the annual and seasonal soil water balance is successfully closed for the period 2000 to 2010 using the variables that we extracted from the model outputs, as described in Section 3.3.4. There may be terms that we have ignored, such as storage of ponded water on the land surface, but these are negligible to the water balance, and can be ignored. Figure 3–5 shows the daily water balance for the spring period in 2005 (as an example), showing again that the model water balance is closed and showing the detailed time series response of the storage and fluxes. We see that in the baseline configuration, there is negligible runoff, with all rainfall on the ground and snowmelt infiltrating into the soil. There are differences between the observed and simulated timing of soil thaw, but all of the snowmelt occurs while the soils are still frozen (both observed and modelled). Simulated ET starts increasing shortly after snowmelt, in April, while observed soils are fully thawed, but the modelled soils are still partially frozen.

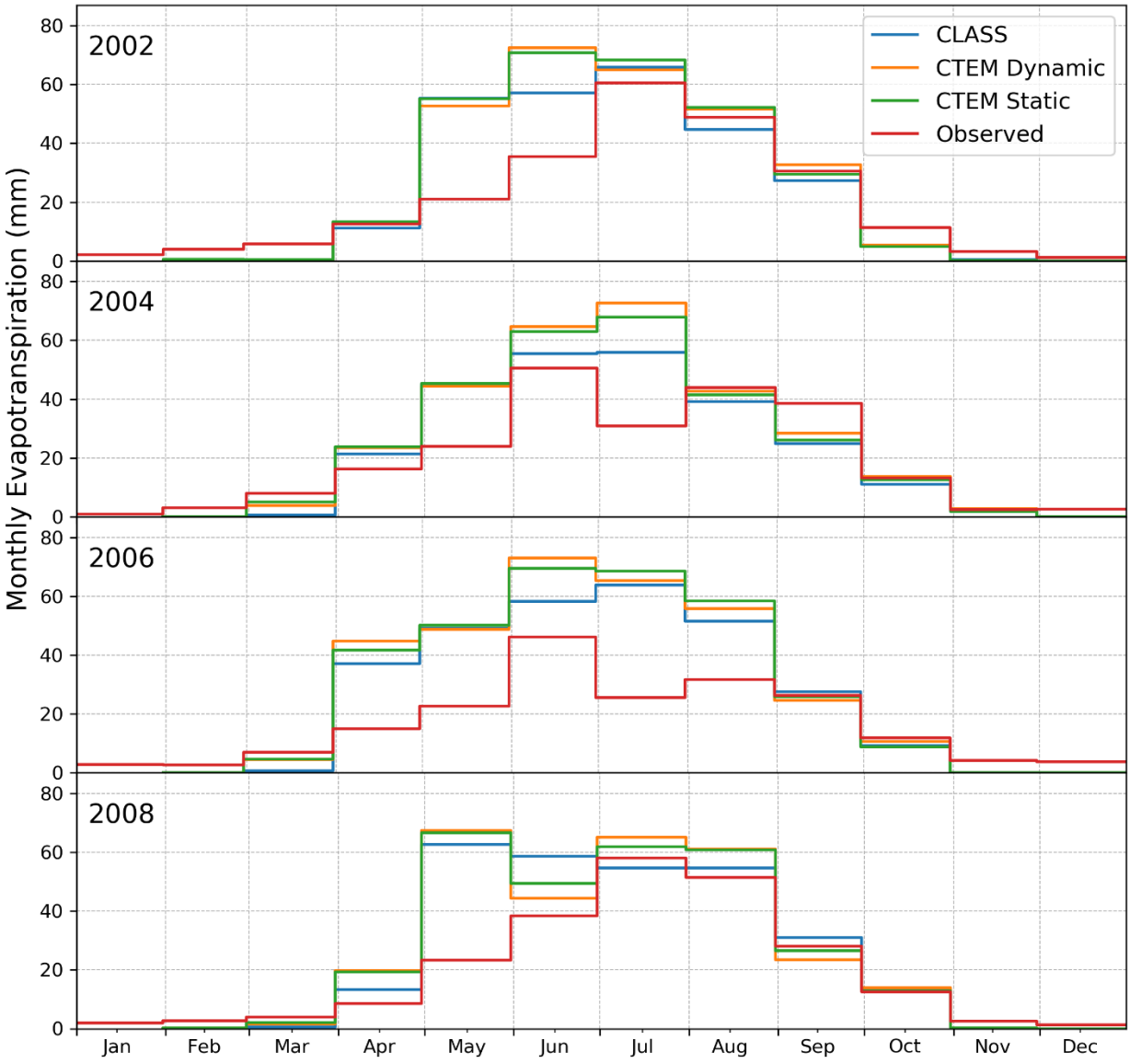

Figure 3–3 The comparison of monthly observed evapotranspiration with simulated evapotranspiration using three Land Surface Schemes, including CLASS, CLASS–CTEM with static vegetation, and CLASS–CTEM with dynamic vegetation, for a range of representative years.

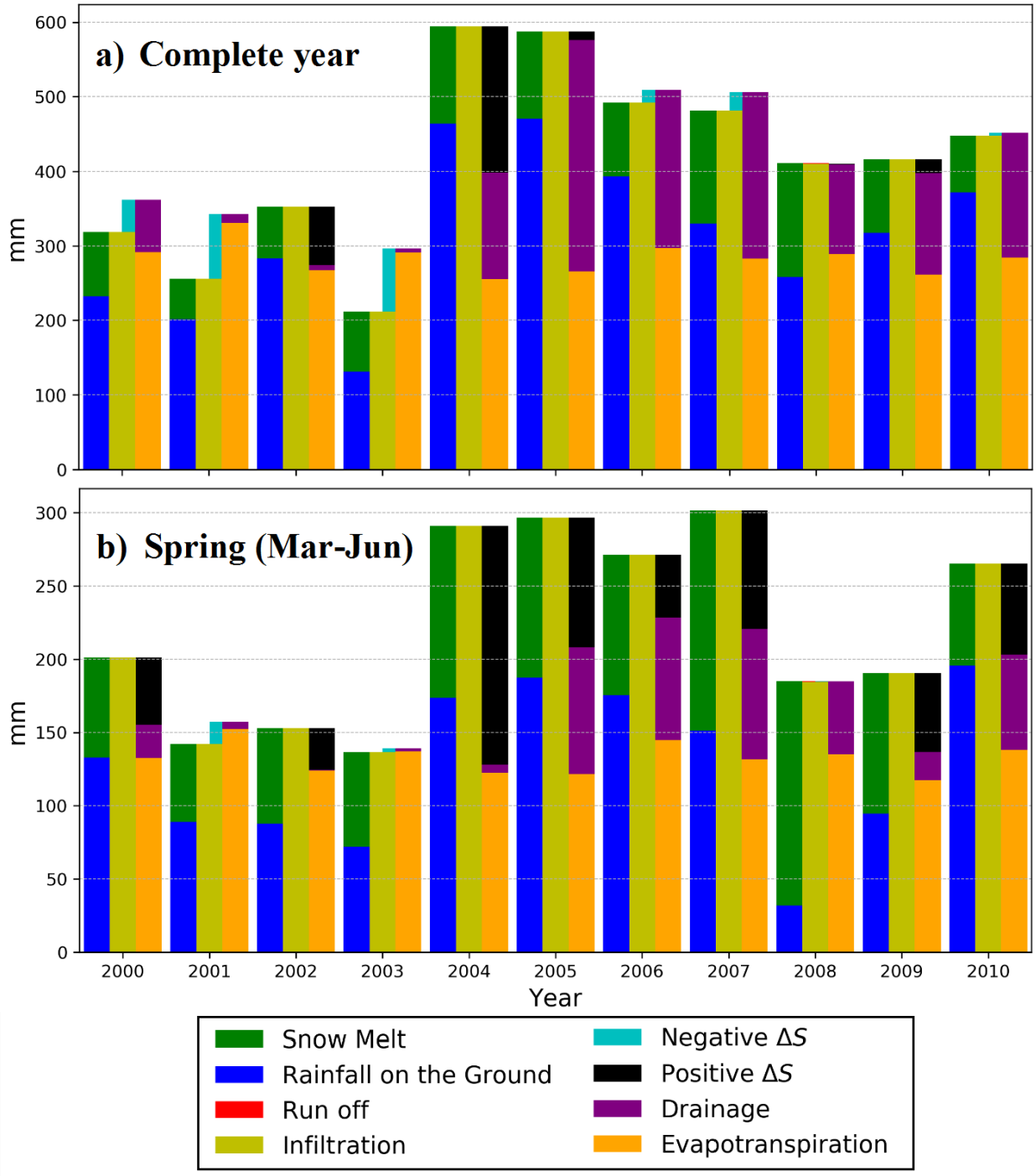

Figure 3–4 The water balance components of the CLASS model for the period of simulation, considering a) complete years (Jan–Dec) and b) the spring melt period (March–June).

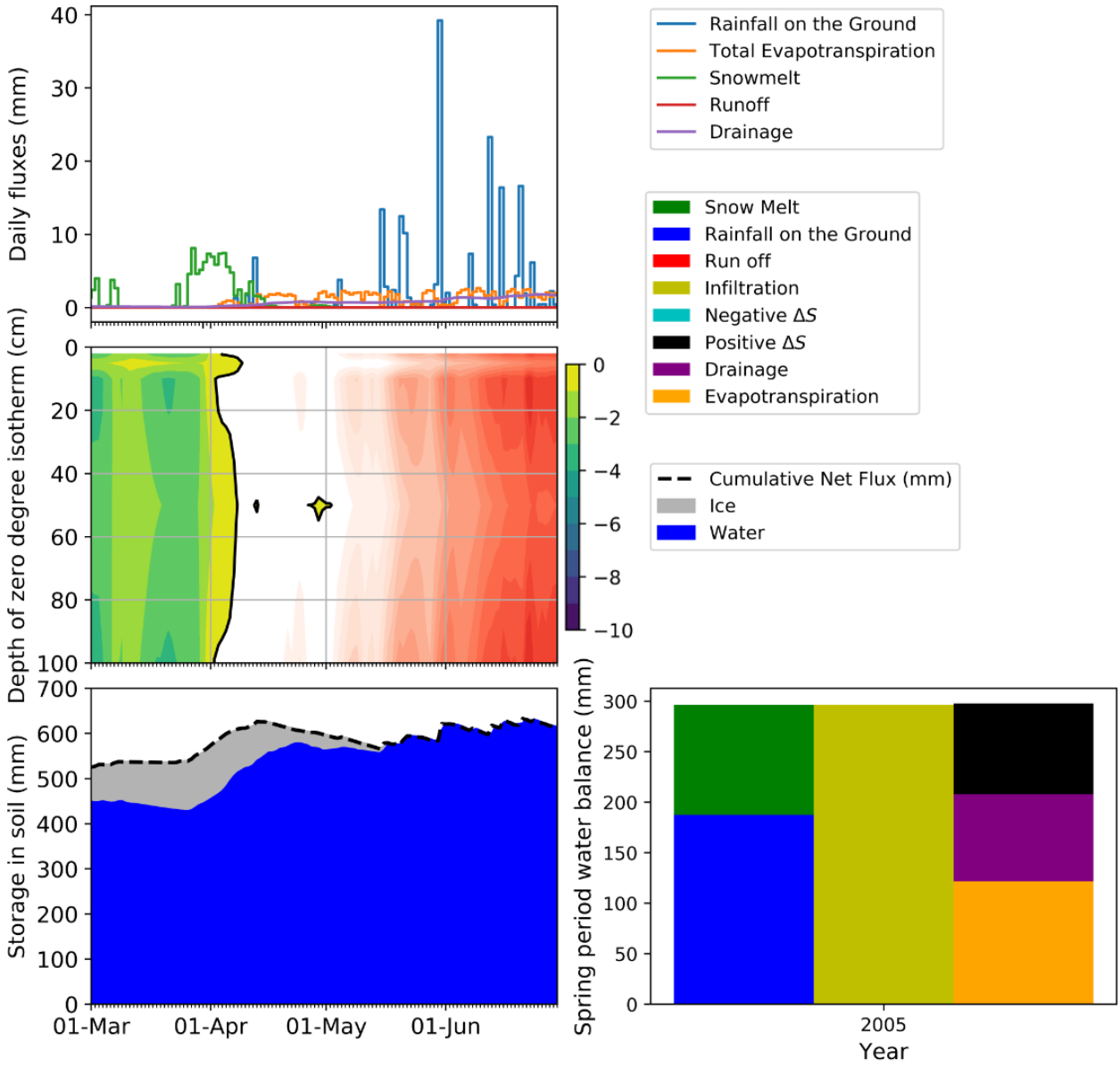

Figure 3–5 Observed soil freezing depth and simulated detailed water balance during the spring melt period using CLASS for the year 2005.

3.4.2 Controls on evapotranspiration

3.4.2.1 Soil hydraulic properties

The effect of different soil hydraulic properties on the water balance during the spring melt period (March to June) is shown in Figure 3–6. “Standard” and “Cuenca” represent the texture–

based parameters and the observed parameters (Table 3–3). The standard/texture–based parameters are taken as the baseline for the individual parameter sensitivity analysis. The Cuenca/observed parameter configuration results in the largest ET simulated, and therefore the worst result compared with observations. Water balance components are only sensitive to saturated hydraulic conductivity (K_{sat}) when the value drops below the value of 0.1 m day^{-1} and runoff is generated, so that infiltration and drainage are significantly reduced, and ET is moderately reduced. Above 0.1 m d^{-1}, saturated hydraulic conductivity has no impact on the water balance. Increased saturated water content (θ_{sat}) causes an increase in simulated ET and a decrease in simulated drainage, while simulated infiltration and runoff are conservative. The air–entry pressure or saturated water potential (Ψ_{sat}) impacts drainage and change in storage, but has only a small impact on ET, with ET reducing slightly when the air entry pressure is large.

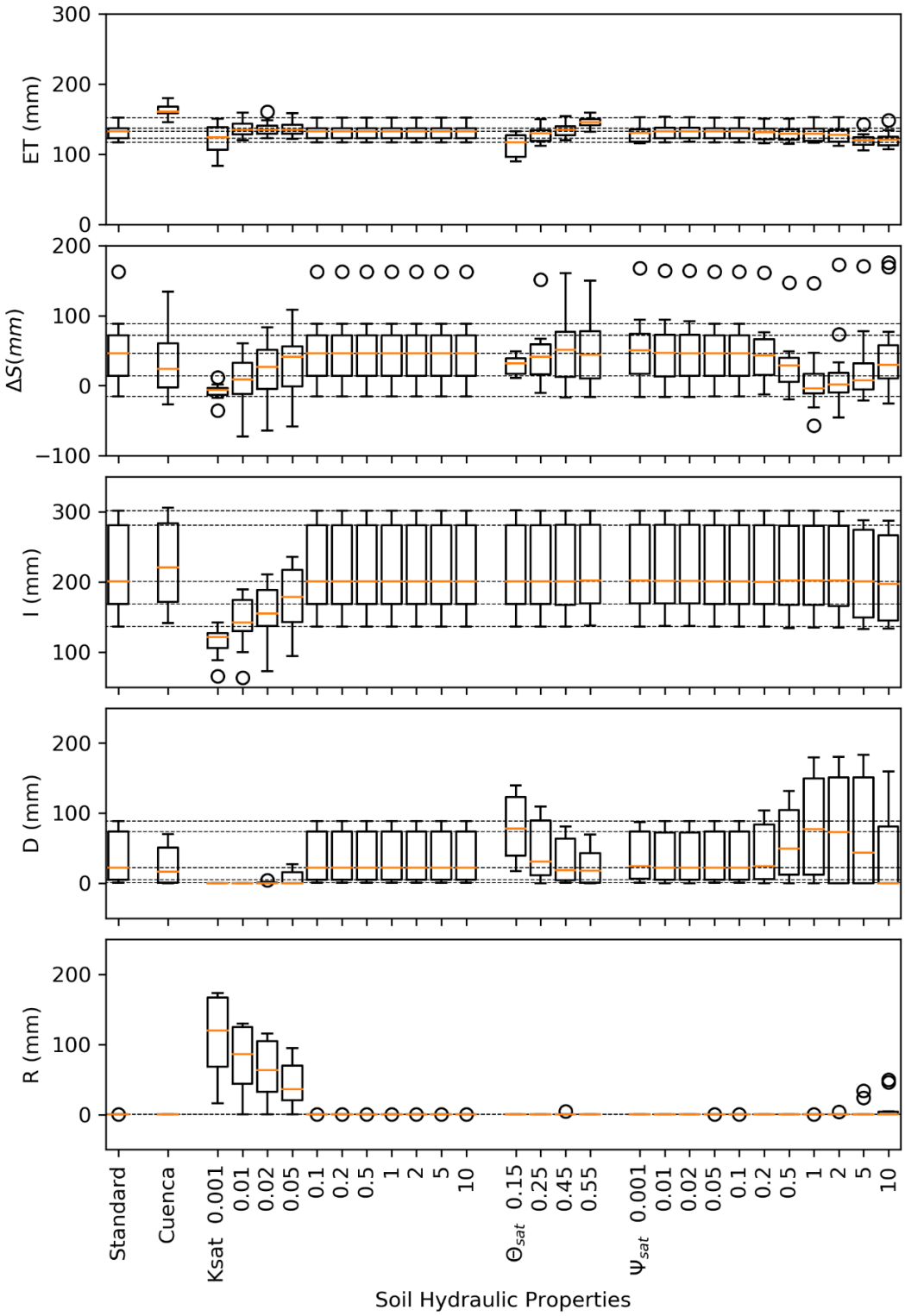

Figure 3–6 The sensitivity of water balance components to soil hydraulic properties applying CLASS. Boxplots show the quartiles of the various water balance components accumulated over the spring period for years 2000 to 2010.

3.4.2.2 Rooting depth and root distribution

Figure 3–7 shows how the water balance during the spring melt period is affected by rooting depth and root distribution for the standard run, and the three cases considered (described above). The effect of the finer soil layer discretization on the water balance is negligible. When the root depth is less than 0.6 m, ET is reduced, but only moderately. For root depths greater than 0.6 m, the water balance in insensitive to the root depth. When all the roots are in the top layer, the effect is the same as restricting the soil depth to 0.1 m (as would be expected). When all the roots are in the second layer, ET is increased, and when all the roots are in the third layer, ET is roughly the same as the standard model run.

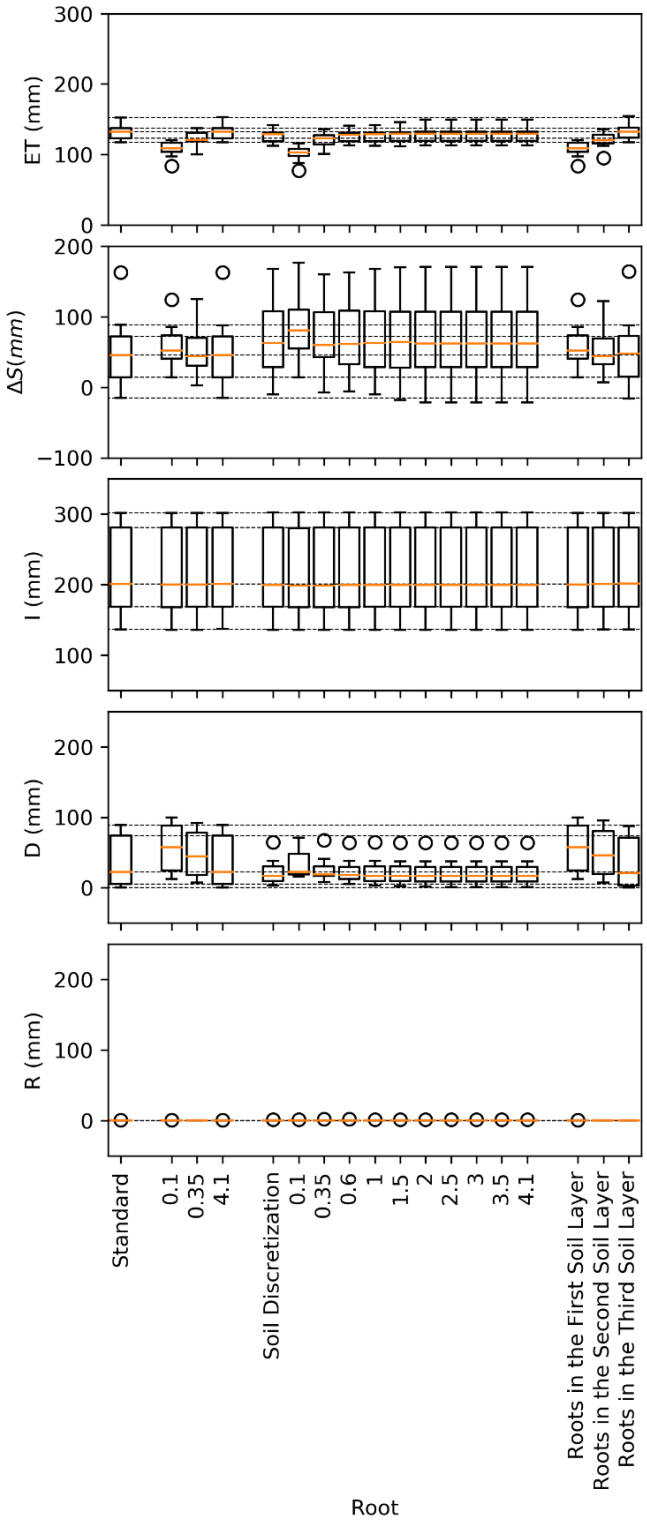

Figure 3–7 The sensitivity of simulated evapotranspiration to soil discretization, different rooting depths, and different root distributions applying CLASS. Boxplots show the quartiles of the evapotranspiration accumulated over the spring period for years 2000 to 2010.

3.4.2.3 Leaf Area Index

Figure 3–8 shows the impact of LAI on the simulated water balance during the spring melt period using both CLASS and CLASS–CTEM Static. Varying LAI not only affects simulated ET, but also infiltration, drainage, and storage change. Increased LAI results in a reduction in infiltration due to an increase in interception. For LAI > 3, the simulated ET is roughly conservative using CLASS. For LAI < 3 there is a progressive reduction in ET with reducing LAI. The response is the same in CLASS–CTEM Static, and in Figure 3-8 we only show the effect of doubling and halving the LAI with CLASS–CTEM Static.

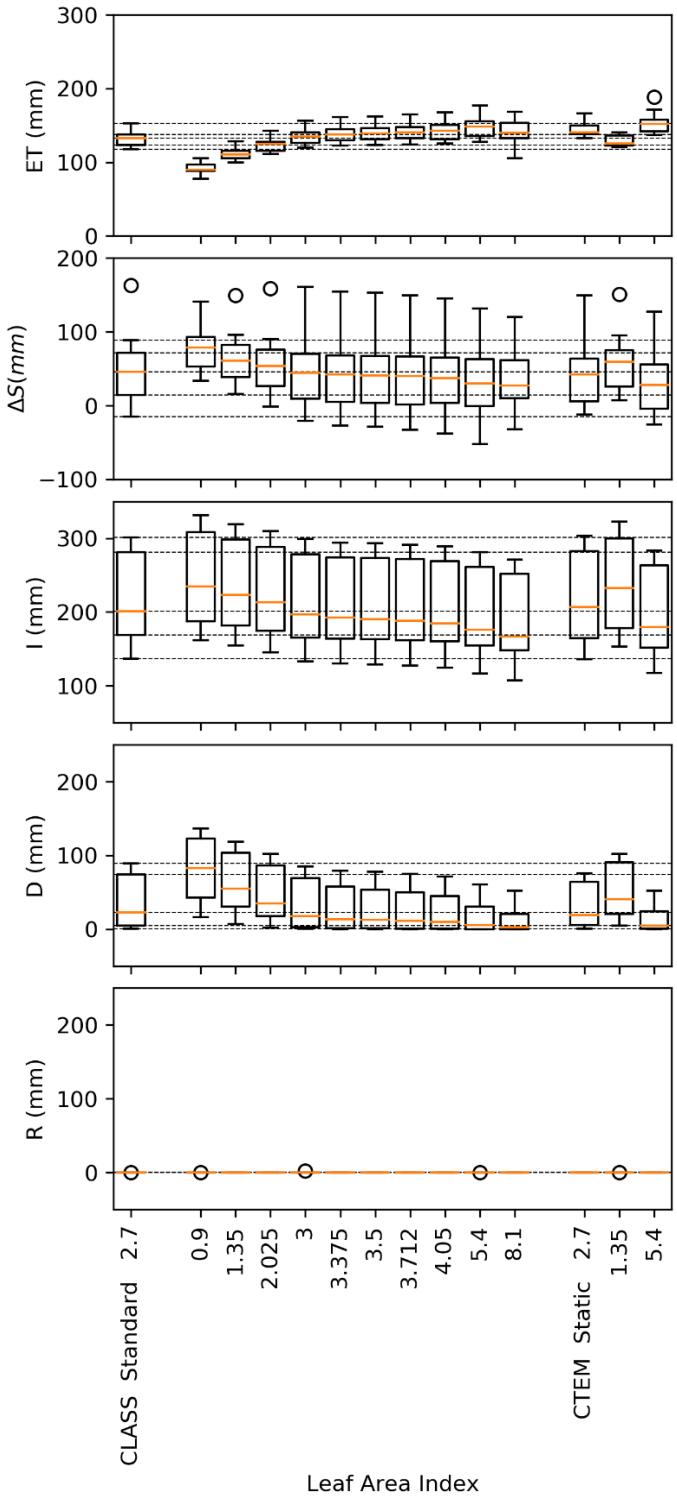

Figure 3–8 The sensitivity of water balance components to leaf area index using CLASS, CLASS–CTEM with static vegetation and CLASS–CTEM with dynamic vegetation. Boxplots show the quartiles of the various water balance components accumulated over the spring period for years 2000 to 2010.

3.4.2.4 Canopy conductance

Figure 3–9 shows the sensitivity of the water balance to canopy conductance during the spring melt period. Canopy conductance has a direct and nearly proportional effect on the simulated ET for both CLASS and CLASS–CTEM Static. When ET is reduced by reducing canopy conductance, there is a corresponding reduction in the change in storage and an increase in drainage.

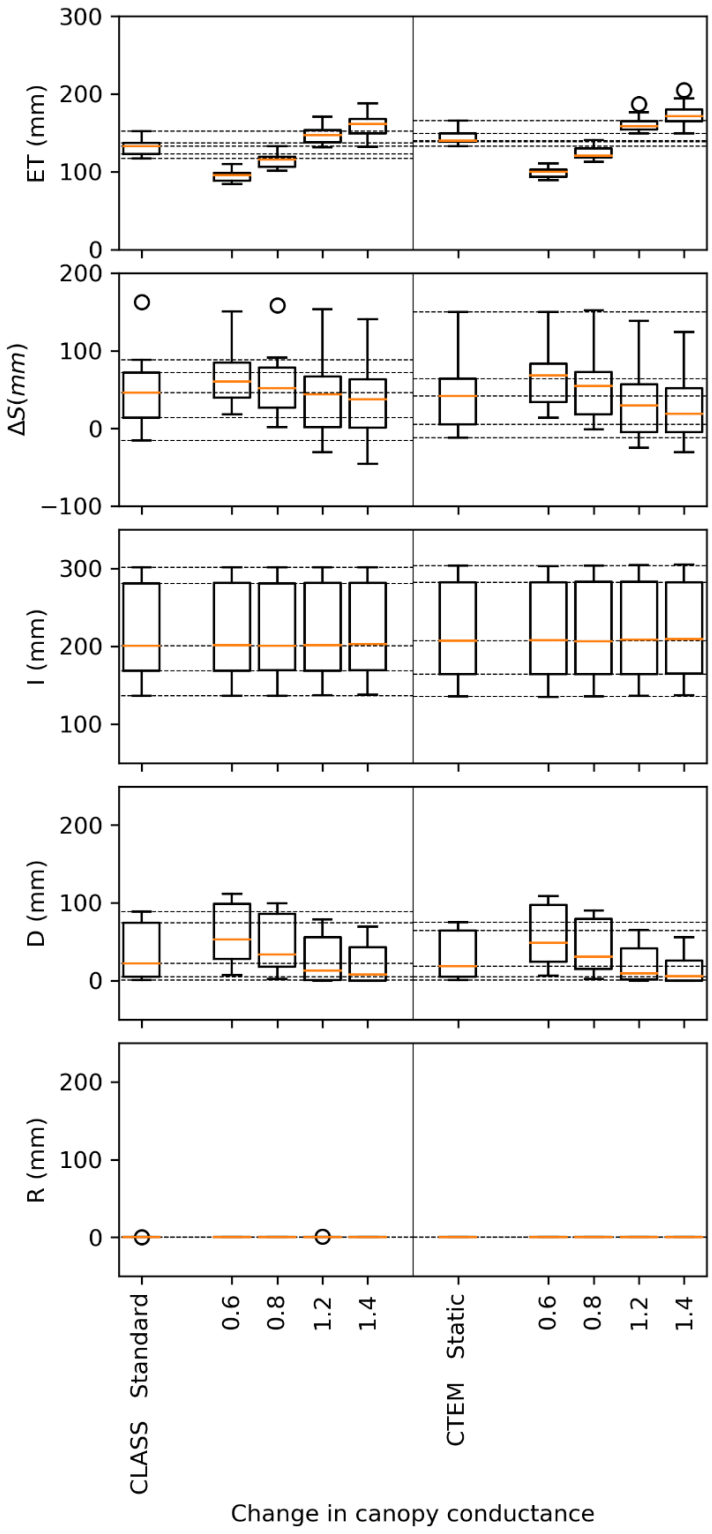

Figure 3–9 The sensitivity of water balance components to change in canopy conductance using CLASS, and CLASS–CTEM with static vegetation. Boxplots show the quartiles of the various water balance components accumulated over the spring period for years 2000 to 2010.

3.5 Discussion

The LSSs examined in this research all overestimated ET in the spring period (Figure 3–3), which was consistent with other studies in this region (Yetemen *et al.*, 2015), including studies with different models (Hejazi and Woodbury, 2011; Horton, 2012; Davison *et al.*, 2016). Although flux–tower measurements do contain biases (e.g. Leuning *et al.*, 2012), the large and systematic errors in the land surface model simulations cannot be explained by errors in observations (Haughton *et al.*, 2016). An unexpected result from the models is that negligible runoff was generated during spring snowmelt; all of the snowmelt infiltrated into the frozen ground. This may or may not be physically correct, but it was anticipated that there would be some snowmelt runoff while the soils were frozen. This issue was raised by Ganji *et al.* (2017), who showed that streamflow predictions in the spring were poor for the same reasons — too much infiltration occurred. Ganji *et al.* (2017) explored alternative infiltration algorithms, and found that restricting infiltration did improve streamflow simulations. We were unable to test those alternative infiltration algorithms in the version of CLASS and CLASS–CTEM that we had available to us, but it is likely that this would also have a strong impact on ET. Nonetheless, since the configurations of the models that we tested are those being used (e.g. Teufel *et al.*, 2018), it remains a useful exercise to examine the controls in the models on simulated ET.

Note, all of the simulations were run for CLASS and CLASS–CTEM Static, and unless otherwise stated, we obtained negligible differences in sensitivity between the different models, and provide results only for the CLASS result.

We found that, as expected, the soil hydraulic properties had significant impacts on infiltration runoff, drainage, and changes in storage, but the response of ET was relatively insensitive, which was not expected (Figure 3–6). We found that lowering the hydraulic conductivity resulted in a

reduction in infiltration, which was generally accompanied by a reduction in drainage, and ET stayed relatively constant (until the lowest value of hydraulic conductivity, where ET was reduced somewhat). The largest reduction in ET was achieved by reducing the saturated water content. Reducing the saturated water content did not impact infiltration, but led to an increase in drainage, with less water from the spring melt going into storage and a moderate reduction in ET. The air–entry pressure (ψ_{sat}) impacted drainage and the amount of water going into storage but had a negligible impact on infiltration and ET. Overall, we can fairly confidently rule out the possibility that errors in the soil hydraulic properties alone can explain the bias in ET — especially given the fact that at this site we have site specific estimates of these properties (Cuenca *et al.*, 1997), and we have to deviate wildly from these measured parameters to achieve reductions in ET.

Another fairly surprising result was that the root distribution had a relatively small impact on ET (Figure 3–7). Firstly, we restricted the total root depth, and we found that we did reduce ET with shallower roots, but the shallowest root depth of 0.1 m still only led to modest reductions in ET, insufficient to explain the model errors. We also used 10 soil layers to allow for a finer resolution of root depth, and we found that roots deeper than 0.6 m had no further impacts on ET. The most extreme difference in root distribution that is possible in a 3–layer model is to assign all the roots to one of the three soil layers. We restricted all the roots in the third layer, and the results were as same as the baseline run, and when the roots were restricted in the shallower layers, there were modest reductions in ET. It is not realistic; however, to assign a root depth of 0.1 m for a jack pine stand, since these trees are strongly tap–rooted (Muller-Dombois, 1964; Sims, 1964; Rowe and Acton, 1985), with their taproots reported from 1.0 to 2.9 m (Bannan, 1940; Fowells, 1965; Strong and La Roi, 1983; Stone and Kalisz, 1991). We therefore can conclude that errors with the root

depth alone cannot explain the model errors, which again, was not expected at the outset of this study.

Changes in leaf area index did have a larger impact on ET using both CLASS and CLASS–CTEM Static (Figure 3–8). With CLASS, ET increased progressively with LAI up until a maximum value of 3, beyond which simulated ET was conservative. Higher LAI also led to reductions in infiltration (due to interception losses) and drainage. LAI at the OJP site, has a measured value of 2.5–2.7 (Chen *et al.*, 1997; Griffis *et al.*, 2003; Barr *et al.*, 2006). Given this, it is unlikely that errors in LAI could be solely responsible for the errors in ET.

The largest impact on the simulation of ET was associated with changes in canopy conductance (Figure 3–9). Although canopy conductance and leaf area index are dependent, we can confidently rule out the possibility that errors in leaf area index can explain bias in ET – given the fact that at this site we have site specific estimates of leaf area index. Canopy conductance was the most direct control on ET, with changes in ET that were nearly in proportion to the changes in canopy conductance. Canopy conductance depends on numerous model parameters, including minimum stomatal resistance (r_{smin}) for CLASS and the PFT–dependent maximum rate of carboxylation by the enzyme rubisco (v_{max}) for coupled CLASS–CTEM. To reduce simulated ET, we would have to reduce the canopy conductance by changing r_{smin} or v_{max}, and we can do this with realistic values that are better suited to this site than the models' default values. Zheng *et al.* (2017) reported the value of 25 $\mu mols^{-1}m^{-2}$ for the maximum carboxylation rate normalized to 25℃ at BERMS OJP site. However, the default value for the v_{max} of evergreen needleleaf is considered 42 $\mu mols^{-1}m^{-2}$ in CLASS–CTEM.

Note, tree phenology is particularly dynamic during the spring melt period, as described in the section 2.3.2.1, and it may have important implications for transpiration. While tree phenology

process is represented in the CLASS–CTEM for nine plant functional types, the role of tree phenology on spring transpiration has not been critically examined in this thesis.

CLASS and CLASS–CTEM Static showed broadly the same response to changes in soil hydraulic properties and vegetation properties. CLASS–CTEM also simulates how LAI, canopy height and root distribution change, which we switched off in CLASS–CTEM Static. We found that the effect on the water balance of including dynamic vegetation in CLASS–CTEM was negligible at our study site.

3.6 Conclusions

Simulating the soil water balance in seasonally frozen conditions can be challenging, in particular due to the complexities of the snow accumulation and melt processes, and the frozen soil physics. Past studies of the southern Boreal Plains Ecozone have consistently found biases in simulated ET, compared with flux tower estimates. We have shown that CLASS and CLASS–CTEM models overestimate ET at the BERMS OJP site, and that the errors are largest during the melt period and early summer. An investigation of the controls on ET found that the model errors could not be explained by errors in the soil hydraulic properties, root distribution or leaf area index individually — though all of these characteristics do have important impacts on the water balance. The canopy conductance parameterisation could potentially explain the errors in simulated ET, and reducing the canopy conductance by calibration could improve simulation errors. Although canopy conductance and leaf area index are dependent, we can confidently rule out the possibility that errors in leaf area index can explain bias in ET – given the fact that at this site we have site specific estimates of leaf area index. We also noted that the ET model bias was greatest during and just after

the soil–thaw period in spring, with significant ET modeled while the soils were still frozen — an important aspect of the model to explore further.

3.7 Acknowledgments

We gratefully acknowledge that funding for this research was provided by the NSERC CCRN program.

CHAPTER 4

CONCLUSIONS AND RECOMMENDATIONS FOR FUTURE WORK

4.1 Conclusions

This thesis investigated the sensitivity of ET to soil and vegetation properties to improve the understanding of controls on ET from seasonally frozen forests. Past studies have demonstrated that land surface schemes overestimated ET at the BERMS OJP site in comparison with flux towers observations during the melt period and early summer (Hejazi and Woodbury, 2011; Horton, 2012; Yetemen *et al.*, 2015; Davison *et al.*, 2016). The results of this thesis are consistent with the past research in this region. In this study, two land surface schemes, including CLASS and CLASS–CTEM, are used. CLASS and CLASS–CTEM use static and dynamic vegetation, respectively. To control for differences between these land surface schemes caused by vegetation dynamics — that is, differences in LAI, canopy height, and root distribution, we also used a modified configuration of CLASS–CTEM, where these characteristics were fixed, known as CLASS–CTEM Static. The results from the models demonstrated that all of the snowmelt infiltrated into the frozen ground, with negligible runoff generation. The near–zero runoff during snowmelt was unexpected. In seasonally frozen conditions, it can be challenging to simulate the soil water balance, especially due to the complexities of the snow accumulation and melt processes, and the frozen soil physics. To improve the understanding of controls on ET from seasonally frozen forests, this study considered the sensitivity of ET to soil hydraulic properties and vegetation characteristics. The results demonstrate that bias in the simulation of ET cannot be explained by errors in the soil hydraulic properties, rooting depth, root distribution, or leaf area index individually although these characteristics do have important effects on the water balance. Changes in canopy conductance have shown the largest impact on the simulation of ET. Given this, the canopy conductance

parameterisation could potentially explain the observed errors in simulated ET, and reducing the canopy conductance by calibration could improve simulation errors. Although canopy conductance and leaf area index are dependent, we can confidently rule out the possibility that errors in leaf area index can explain bias in ET – given the fact that at this site we have site specific estimates of leaf area index. The study showed negligible differences in sensitivity between the different models. Given that, the effect on the water balance of including dynamic vegetation in CLASS–CTEM was negligible at this study site.

4.2 Recommendations for future work

Although the parameterization of canopy conductance could potentially explain the model errors, errors in the simulation of ET were greatest in the spring–melt period. It is recommended, therefore, to further investigate the simulation of evapotranspiration from frozen soils.

The understanding of controls on ET associated with other aspects of these models still remains limited. In this study, the sensitivity of ET to a limited number of important parameters has been assessed. Sensitivity analyses give insights into how model parameters, initial and boundary conditions affect model behaviors. It is recommended to choose a multivariate approach to assess the sensitivity of ET to different sets of parameters, initial and boundary conditions, and their interactions.

Although the importance of canopy conductance model on the simulation of ET has been demonstrated for the Old Jack Pine site, it would be worthwhile to extend the analysis to the Old Black spruce and Old Aspen sites. This would give deep insights into controls on ET as it would consider the effects of different plant functional types, soil properties and environmental conditions on ET.

If errors between observed and simulated water fluxes continue to be significant, in spite of canopy conductance parametrizations for each plant functional type, it would be necessary to reformulate the representation of the canopy conductance model. This would result in the improvement of water fluxes at regional and global scales.

In addition to deficiencies of land surface schemes to simulate ET in the spring–melt period, land surface models have shown systematic errors in the simulation of ET during water–stressed conditions (Ukkola *et al.*, 2016). It is recommended, therefore, to also focus on the improvement of simulating water fluxes in drought conditions.

REFERENCES

Aalto J, Kolari P, Hari P, Kerminen VM, Schiestl–Aalto P, Aaltonen H, Levula J, Siivola E, Kulmala M, Bäck J. 2014. New foliage growth is a significant, unaccounted source for volatiles in boreal evergreen forests. *Biogeosciences* **11** (5): 1331–1344 DOI: 10.5194/bg-11-1331-2014.

Acton DF, Padbury GA, Stushnoff CT. 1998. Boreal plain ecozone. In the ecoregions of Saskatchewan. Regina, SK: Canadian Plains Research Center, Saskatchewan Environment and Resource Management.

Afshar A, Marino MA. 1979. Model for simulation soil–water content considering evapotranspiration–reply. *Hydrology* **40** (3–4): 393–395.

Allen RG, Pereira LS, Raes D, Smith M. 2006. FAO irrigation and draiange paper (crop evapotranspiration). *European Journal of Agronomy* **34** (3): 144–152.

Amiro BD, Barr AG, Black TA, Iwashita H, Kljun N, McCaughey JH, Morgenstern K, Murayama S, Nesic Z, Orchansky AL, et al. 2006. Carbon, energy and water fluxes at mature and disturbed forest sites, Saskatchewan, Canada. *Agricultural and Forest Meteorology* **136** (3–4): 237–251 DOI: 10.1016/j.agrformet.2004.11.012.

Appels WM, Coles AE, McDonnell JJ. 2018. Infiltration into frozen soil: from core–scale dynamics to hillslope–scale connectivity. *Hydrological Processes* **32** (1): 66–79.

Arora V. 2014. User guide for running stand–alone versions of Canadian Land Surface Scheme (CLASS 3.6) and Canadian Terrestrial Ecosystem Model (CTEM 2.0) in a coupled mode. *Manual for Coupled CLASS–CTEM.*

Arora VK. 2003. Simulating energy and carbon fluxes over winter wheat using coupled land surface and terrestrial ecosystem models. *Agricultural and Forest Meteorology* **118** (1–2): 21–47 DOI: 10.1016/S0168-1923(03)00073-X.

Arora VK, Boer GJ. 2003. A representation of variable root distribution in dynamic vegetation models. *American Meterological Society* **7** (6): 1–19.

Arora VK, Boer GJ. 2005. A parameterization of leaf phenology for the terrestrial ecosystem component of climate models. *Global Change Biology* **11** (1): 39–59.

Ball JT, Woodrow IE, Berry JA. 1987. A model predicting stomatal conductance and its contribution to the control of photosynthesis under different environmental conditions. In *Progress in Photosynthesis Research* 221–224.

Bannan MW. 1940. The Root systems of Northern Ontario conifers growing in sand. *American Journal of Botany* **27** (2): 108–114.

Barr AG, van der Kamp G, Black TA, McCaughey JH, Nesic Z. 2012. Energy balance closure at the BERMS flux towers in relation to the water balance of the White Gull Creek watershed 1999-2009. *Agricultural and Forest Meteorology* **153**: 3–13 DOI: 10.1016/j.agrformet.2011.05.017.

Barr AG, Morgenstern K, Black TA, McCaughey JH, Nesic Z. 2006. Surface energy balance closure by the eddy–covariance method above three boreal forest stands and implications for the measurement of the CO2 flux. *Agricultural and Forest Meteorology* **140** (1–4): 322–337 DOI: 10.1016/j.agrformet.2006.08.007.

Bartlett PA, Harry McCaughey J, Lafleur PM, Verseghy DL. 2003. Modelling evapotranspiration

at three boreal forest stands using the CLASS: tests of paramterizations for canopy conductance and soil evaporation. *International Journal of Climatology* **23** (4): 427–451 DOI: 10.1002/joc.884.

Bastidas LA, Hogue TS, Sorooshian S, Gupta H V., Shuttleworth WJ. 2006. Parameter sensitivity analysis for different complexity land surface models using multicriteria methods. *Geophysical Research* **111** (D20): 1–19.

Benninghoff WS. 1952. Interaction of vegetation and soil frost phenomena. *Arctic* **5** (1): 34–44.

Berry JA, Beerling DJ, Franks PJ. 2010. Stomata: Key players in the earth system, past and present. *Current Opinion in Plant Biology* **13** (3): 233–240.

Best MJ, Abramowitz G, Johnson HR, Pitman AJ, Balsamo G, Boone A, Cuntz M, Decharme B, Dirmeyer PA, Dong J, et al. 2015. The plumbing of land surface models: benchmarking model performance. *Hydrometeorology* **16** (3): 1425–1442 DOI: 10.1175/JHM-D-14-0158.1.

Best MJ, Proyer M, Clark DB, Rooney GG, Essery RLH, Menard CB, Edwards JM, Hendry MA, Gedney N, Mercado LM, et al. 2011. The Joint UK Land Environment Simulator (JULES), model description–part 1: energy and water fluxes. *European Geosciences Union* **4** (1): 677–699.

Black TA, Den Hartog G, Neumann HH, Blanken PD, Yang PC, Russell C, Nesic Z, Lee X, Chen SG, Staebler R, et al. 1996. Annual cycles of water vapour and carbon dioxide fluxes in and above a boreal aspen forest. *Global Change Biology* **2** (3): 219–229 DOI: 10.1111/j.1365-2486.1996.tb00074.x.

Bonan GB. 1993. Importance of leaf area index and forest type when estimating photosynthesis in

boreal forests. *Remote Sensing of Environment* **43** (3): 303–314 DOI: 10.1016/0034-4257(93)90072-6.

Braud I, Dantas–Antonino AC, Vauclin M. 1995. A stochastic approach to studying the influence of the spatial variability of soil hydraulic properties on surface fluxes, temperature and humidity. *Hydrology* **165** (1–4): 283–310.

Breda N, Granier A, Barataud F, Moyne C. 1995. Soil water dynamics in an oak stand. I. soil moisture, water potential and water uptake by roots. *Plant and Soil* **172** (1): 17–27.

Bréda NJJ. 2003. Ground–based measurements of leaf area index: a review of methods, instruments and current controversies. *Experimental Botany* **54** (392): 2403–2417.

Budhathoki S. 2017. Modelling snowmelt infiltration processes in seasonally frozen ground (master's thesis). University of Saskatchewan, Saskatoon, Saskatchewan.

Cadero A, Aubry A, Brun F, Dourmad JYY, Salaün Y, Garcia–Launay F. 2018. Global sensitivity analysis of a pig fattening unit model simulating technico–economic performance and environmental impacts. *Agricultural Systems* **165**: 221–229 DOI: 10.1016/J.AGSY.2018.06.016.

Carey SK, Quinton WL. 2004. Evaluating snowmelt runoff generation in a discontinuous permafrost catchment using stable isotope, hydrochemical and hydrometric data. *Hydrology Research* **35** (4–5): 309–324.

Celia MA, Bouloutas ET. 1990. A General Mass–Conservative Numerical Solution for the Unsaturated Flow Equation. *Water Resources Research* **26** (7): 1483–1496.

Chen JM, Cihlar J. 1996. Retrieving leaf area index of boreal conifer forests using landsat TM

images. *Remote Sensing of Environment* **55** (2): 153–162.

Chen JM, Rich PM, Gower ST, Norman JM, Plummer S. 1997. Leaf area index of boreal forests: Theory, techniques, and measurements. *Geophysical Research* **102** (D24): 29429–29443.

Chen L, Li Y, Chen F, Barr A, Barlage M, Wan B. 2016. The incorporation of an organic soil layer in the Noah–MP land surface model and its evaluation over a boreal aspen forest. *Atmospheric Chemistry and Physics* **16** (13): 8375–8387 DOI: 10.5194/acp-16-8375-2016.

Cherkauer KA, Lettenmaier DP. 1999. Hydrologic effects of frozen soils in the upper Mississippi river basin. *Geophysical Research* **104** (D16): 19599–19610.

Clapp RB, Hornberger GM. 1978. Empirical equations for some soil hydraulic properties. *Water Resources Research* **14** (4): 601–604 DOI: 10.1029/WR014i004p00601.

Clark MP, Fan Y, Lawrence DM, Adam JC, Bolster D, Gochis DJ, Hooper RP, Kumar M, Leung LR, Mackay DS, et al. 2015. Improving the representation of hydrologic processes in earth system models. *Water Resources Research* **51** (8): 5929–5956.

Collatz GJ, Ball JT, Grivet C, Berry JA. 1991. Physiological and environmental regulation of stomatal conductance, photosynthesis and transpiration: a model that includes a laminar boundary layer. *Agricultural and Forest Meteorology* **54** (2–4): 107–136.

Cowan IR. 1978. Stomatal behaviour and environment. *Advances in Botanical Research* **4**: 117–228.

Cresswell HP, Paydar Z. 2000. Functional evaluation of methods for predicting the soil water characteristic. *Hydrology* **227** (1–4): 160–172.

Cuenca RH, Stangel DE, Kelly SF. 1997. Soil water balance in a boreal forest. *Geophysical*

Research **102** (D24): 29355–29365 DOI: 10.1029/97jd02312.

Cuntz M, Haverd V. 2017. Physically accurate soil freeze–thaw processes in a global land surface scheme. *Advances in Modeling Earrth systems* **10** (1): 54–77.

Damesin C, Rambal S. 1995. Field study of leaf photosynthetic performance by a Mediterranean deciduous Oak tree (Quercus Pubescens) during a severe summer drought. *New Phytologist* **131** (2): 159–167.

Davison B, Pietroniro A, Fortin V, Leconte R, Mamo M, Yau MK. 2016. What is Missing from the prescription of hydrology for land surface schemes? *Hydrometeorology* **17** (7): 2013–2039.

Dwyer LM, Stewart DW, Balchin D. 1988. Rooting characteristics of corn, soybeans and barley as a function of available water and soil physical characteristics. *Canadian Journal of Soil Science* **68** (1): 121–132.

Ensminger I, Schmidt L, Lloyd J. 2008. Soil temperature and intermittent frost modulate the rate of recovery of photosynthesis in Scots pine under simulated spring conditions. *New Phytologist* **177** (2): 428–442 DOI: 10.1111/j.1469-8137.2007.02273.x.

Ensminger I, Sveshnikov D, Campbell DA, Funk C, Jansson S, Lloyd J, Shibistova O, Öquist G. 2004. Intermittent low temperatures constrain spring recovery of photosynthesis in boreal Scots pine forests. *Global Change Biology* **10** (6): 995–1008 DOI: 10.1111/j.1365-2486.2004.00781.x.

Essery R, Rutter N, Pomeroy J, Baxter R, Stahli M, Gustafsson D, Barr A, Bartlett P, Elder K. 2009. SNOWMIP2: an evaluation of forest snow process simulations. *American Meteorological Society* **90** (8): 1120–1136.

Fang X, Pomeroy JW. 2007. Snowmelt runoff sensitivity analysis to drought on the Canadian prairies. *Hydrological Processes* **21** (19): 2594–2609.

Farquhar GD, Sharkey TD. 1982. Stomatal conductance and photosynthesis. *Annual Review of Plant Physiology* **33** (1): 317–345.

Fatichi S, Katul GG, Ivanov VY, Pappas C, Paschalis A, Consolo A, Kim J, Burlanso P. 2015. Abiotic and biotic controls of soil moisture spationtemporal variability and the occurrence of hysteresis. *Water Resources Research* **51**: 3505–3524 DOI: 10.1002/2014WR015608.

Fatichi S, Pappas C, Ivanov VY. 2016. Modeling plant–water interactions: an ecohydrological overview from the cell to the global scale. *Wiley Interdisciplinary Reviews: Water* **3** (3): 327–368.

Feddes RA. 1978. Simulation of field water use and crop yield. Wiley. New York.

Feddes RA, Bresler E., Neuman SP. 1974. Field test of a modified numerical model for water uptake by root systems. *Water Resources Research* **10** (6): 1199–1206.

Feddes RA, Kowalik P, Kolinska-Malinka K, Zaradny H. 1976. simulation of field water uptake by plants using a soil water dependent root extraction function. *Hydrology* **31** (1–2): 13–26.

Fisher JB. 2013. Land–Atmosphere interactions: Evapotranspiration, in Encyclopedisa of Remote Sensing, editied by E. Njoku. Springer. Germany.

Flury M, Flühler H, Jury WA, Leuenberger J. 1994. Susceptibility of soils to preferential flow of water: a field study. *Water Resources Research* **30** (7): 1945–1954.

Ford J, Bedford BL. 1987. The hydrology of Alaskan wetlands , U.S.A.: a review. *Arctic and Alpine Research* **19** (3): 209–229.

Fowells HA. 1965. Silvics of forest trees of the United States. *Agriculture Handbook No. 271. U.S. Dept. of Agriculture, Forest Service, Washington, D.C.*

Ganji A, Sushama L, Verseghy D, Harvey R. 2017. On improving cold region hydrological processes in the Canadian Land Surface Scheme. *Theoretical and Applied Climatology* **127** (1–2): 45–59 DOI: 10.1007/s00704-015-1618-4.

Garrigues S, Boone A, Decharme B, Olioso A, Albergel C, Calvet J–C, Moulin S, Buis S, Martin E. 2018. Impacts of the soil water transfer parameterization on the simulation of evapotranspiration over a 14–year mediterranean crop succession. *Hydrometeorology* **19** (1): 3–25.

Goldstein GH, Brubarker LB, Hinckley TM. 1985. Water relations of white spruce (Picea glauca (Moench) Voss) at tree line in north central Alaska. *Canadian Journal of Forest Research* **15** (6): 1080–1087.

Goulden, M. L., Wofsy SC, Harden, J. W., Trumbore, S. E., Crill, P. M., Gower ST, Fries, T., Daube, B. C., Fan, S. –M., Sutton, D. J., Bazzaz, A., Munger JW. 1998. Sensitivity of boreal forest carbon balance to soil thaw. *Science* **279** (5348): 214–217.

Griffis TJ, Black TA, Morgenstern K, Barr AG, Nesic Z, Drewitt GB, Gaumont–Guay D, McCaughey JH. 2003. Ecophysiological controls on the carbon balances of three southern boreal forests. *Agricultural and Forest Meteorology* **117** (1–2): 53–71 DOI: 10.1016/S0168-1923(03)00023-6.

Hainsworth JM, Aylmore LAG. 1989. Non–uniform soil water extaction by plant roots. *Plant and Soil* **113** (1): 121–124.

Hänninen H, Slaney M, Linder S. 2007. Dormancy release of Norway spruce under climatic warming: testing ecophysiological models of bud burst with a whole-tree chamber experiment. *Tree Physiology* **27** (2): 291–300 DOI: 10.1093/treephys/27.2.291.

Harvey RB, Lipman JG. 1935. An annotated bibliography of the low temperature relations of plants. *Soil Science* **41** (2): 164.

Haughton N, Abramowitz G, Pitman AJ, Or D, Best MJ, Johnson HR, Balsamo G, Boone A, Cuntz M, Decharme B, et al. 2016. The plumbing of land surface models: is poor performance a result of methodology or data quality? *Hydrometeorology* **17** (6): 1705–1723 DOI: 10.1175/JHM-D-15-0171.1.

Hayashi M, Van Der Kamp G, Schmidt R. 2003. Focused infiltration of snowmelt water in partially frozen soil under small depressions. *Hydrology* **270** (3–4): 214–229.

Heide OM. 1993. Dormancy release in beech buds (Fagus sylvatica) requires both chilling and long days. *Physiologia Plantarum* **89** (1): 187–191 DOI: 10.1111/j.1399-3054.1993.tb01804.x.

Hejazi A, Woodbury AD. 2011. Evaluation of Land Surface Scheme SABAE-HW in simulating snow depth, soil temperature and soil moisture within the BOREAS site, Saskatchewan. *Atmosphere–Ocean* **49** (4): 408–420 DOI: 10.1080/07055900.2011.587238.

Henderson–Sellers A, McGuffie K, Pitman AJ. 1996. The project for intercomparison of land–surface parametrization schemes (PILPS): 1992 to 1995. *Climate Dynamics* **12** (12): 849–859.

Henderson–Sellers A, Yang Z–L, Dickinson RE. 1993. The project for intercomparison of land–surface parameterization schemes. *American Meteorological Society* **74** (7): 1335–1349 DOI: 10.1175/1520-0477(1993)074<1335:TPFIOL>2.0.CO;2.

Hillel D. 1998. Environmental soil physics: fundamentals, application and environmental considerations. Academic Press. New York.

Hoogland JC, Feddes RA, Belmans C. 1981. Root water uptake model depending on soil water pressure head and maximum extraction rate. In *International Symposium on Water Supply and Irrigation* 123–136.

Horton AJ. 2012. An evaluation of the Joint UK Land Environment Simulator (JULES) model performance applied to three sites in the canadian boreal forest (master's thesis). Imperial College London, London, England.

Huang Y, Jiang J, Ma S, Ricciuto D, Hanson PJ, Luo Y. 2017. Soil thermal dynamics, snow cover, and frozen depth under five temperature treatments in an ombrotrophic bog: Constrained forecast with data assimilation. *Geophysical Research: Biogeosciences* **122** (8): 2046–2063.

Huner NPA, Öquist G, Hurry VM, Krol M, Falk S, Griffith M. 1993. Photosynthesis, photoinhibition and low temperature acclimation in cold tolerant plants. *Photosynthesis Research* **37** (1): 19–39 DOI: 10.1007/BF02185436.

Hupet F, Trought MCT, Greven M, Green SR, Clothier BE. 2005. Data requirements for identifying macroscopic water stress parameters : a study on grapevines. *Water Resource Research* **41** (6): 1–15.

IPCC, 2001. Climate change 2001 : impacts, adaptation, and vulnerability. Intergovernmental Panal on Climate Change. Cambridge University Press.

Ireson AM, Barr AG, Johnstone JF, Mamet SD, van der Kamp G, Whitfield CJ, Michel NL, North RL, Westbrook CJ, DeBeer C, Chun KP, Nazemi A, Sagin J. 2015. The changing water cycle:

the boreal plains ecozone of western canada. *Wiley Interdisciplinary Reviews: Water* **2**: 505–521.

Ireson AM, van der Kamp G, Ferguson G, Nachshon U, Wheater HS. 2013. Hydrogeological processes in seasonally frozen northern latitudes: understanding, gaps and challenges. *Hydrogeology* **21** (1): 53–66.

Jackson RB, Canadell J, Ehleringer JR, Mooney HA, Sala OE, Schulze ED. 1996. A global analysis of root distributions for terrestrial biomes. *Oecologia* **108** (3): 389–411.

Jacquemin B, Noilhan J. 1990. Sensitivity study and validation of a land surface parameterization using the hapex–mobilhy data set. *Boundary–Layer Meteorology* **52** (1–2): 93–134.

Jarvis PG. 1976. The interpretation of the variations in leaf water potential and stomatal conductance found in canopies in the field. *Philosophical Transactions of the Royal Society* **273** (927): 593–610.

Jarvis PG, Massheder JM, Hale SE, Moncrieff JB, Rayment M, Scott SL. 1997. Seasonal variation of carbon dioxide, water vapor, and energy exchanges of a boreal black spruce forest. *Geophysical Research* **102** (D24): 28,953–28,966.

Katul GG, Palmroth S, Oren R. 2009. Leaf stomatal responses to vapour pressure deficit under current and CO2–enriched atmosphere explained by the economics of gas exchange. *Plant, Cell and Environment* **32** (8): 968–979.

Koren V, Schaake J, Mitchell K, Duan QY, Chen F, Baker JM. 1999. A parameterization of snowpack and frozen ground intended for NCEP weather and climate models. *Geophysical Research* **104** (D16): 19569–19585.

Koster RD, Dirmeyer PA, Guo Z, Bonan G, Chan E, Cox P, Gordon CT, Kanae S, Kowalczyk E, Lawrence D, et al. 2004. Regions of Strong Coupling Between Soil Moisture and Prediction. *Science* **305** (August): 1138–1140 DOI: 10.1126/science.1100217.

Koster RD, Schubert SD, Suarez MJ. 2009. Analyzing the concurrence of meteorological droughts and warm periods, with implications for the determination of evaporative regime. *Climate* **22** (12): 3331–3341.

Kramer K. 1994. A modelling analysis of the effects of climatic warming on the probability of spring frost damage to tree species in The Netherlands and Germany. *Plant, Cell & Environment* **17** (4): 367–377 DOI: 10.1111/j.1365-3040.1994.tb00305.x.

Krinner G, Viovy N, de Noblet-Ducoudré, N., Ogée J, Polcher J, Friedlingstein P, Ciais P, Sitch S, Prentice IC. 2005. A dynamic global vegetation model for studies of the coupled atmosphere–biosphere system. *Global Biogeochemical Cycles* **19** (1): 1–33.

Kumar R, Shankar V, Jat MK. 2013. Efficacy of nonlinear root water uptake model for a multilayer crop root zone. *Irrigation and Drainage Engineering* **139** (11): 898–910.

Kumar R, Shankar V, Jat MK. 2014. Sensitivity analysis of nonlinear model parameters in a multilayer root zone. *Hydrologic Engineering* **19** (2): 462–471.

Lawrence WT, Oechel WC. 1983. Effects of soil temperature on the carbon exchange of taiga seedlings. II. photosynthesis, respiration, and conductance. *Canadian Journal of Forest Research* **13** (5): 850–859.

Leuning R. 1995. A critical appraisal of a combined stomatal–photosynthesis model for C3 plants. *Plant, Cell and Environment* **18** (4): 339–355.

Leuning R, van Gorsel E, Massman WJ, Isaac PR. 2012. Reflections on the surface energy imbalance problem. *Agricultural and Forest Meteorology* **156**: 65–74 DOI: 10.1016/j.agrformet.2011.12.002.

Li KY, Boisvert JB, Jong R De. 1999. An exponential root–water–uptake model. *Canadian Journal of Soil Science* **79** (2): 333–343.

Lindgren K, Hallgren JE. 1993. Cold acclimation of Pinus contorta and Pinus sylvestris assessed by chlorophyll fluorescence. *Tree Physiology* **13** (1): 97–106 DOI: 10.1093/treephys/13.1.97.

Looy VK, Bouma J, Herbst M, Koestel J, Minasny B, Mishra U, Montzka C, Nemes A, Pachepsky YA, Padarian J, et al. 2017. Pedotransfer functions in earth system science: challenges and perspectives. *Reviews of Geophysics* **55** (4): 1199–1256 DOI: 10.1002/2017RG000581.

Lunardini VJ. 1981. Heat transfer in cold climate. Van Nostrand Reinhold Company. New York.

Luo L, Robock A, Vinnikov KY, Schlosser CA, Slater AG, Boone A, Braden H, CoxOX P, Rosnay PD, Dickinson RE, et al. 2003. Effects of frozen soil on soil temperature, spring infiltration, and runoff: results from the PILPS 2(d) experiment at Valdai, Russia. *Hydrometeorology* **4** (2): 334–351.

Mamo M. 2015. Exploring the ability of a distributed hydrological land surface model in simulating hydrological processes in the boreal forest environment (master's thesis). University of Saskatchewan, Saskatoon, Saskatchewan.

Marino MA, Tracy JC. 1988. Flow of water through root–soil environment. *Irrigation and Drainage Engineering* **114** (4): 588–604.

Maxwell RM, Chow FK, Kollet SJ. 2007. The groundwater–land–surface–atmosphere connection:

soil moisture effects on the atmospheric boundary layer in fully–coupled simulations. *Advances in Water Resources* **30** (12): 2447–2466.

Melton JR, Arora VK. 2016. Competition between plant functional types in the Canadian Terrestrial Ecosystem Model (CTEM) v. 2.0. *Geoscientific Model Development* **9** (1): 323–361.

Mendoza PA, Clark MP, Barlage M, Rajagopalan B, Samaniego L, Abramowitz G, Gupta H. 2015. Are we unneccessarily constraining the agility of complex process–based models? *Water Resource Research* **51**: 716–728.

Mitchell JFB, Warrilow DA. 1987. Summer dryness in northern mid–latitudes due to increased CO2. *Nature* **330** (19): 238–240.

Molz FJ. 1981. Models of water transport in the soil–plant system: a review. *Water Resources Research* **17** (5): 1245–1260.

Molz FJ, Remson I. 1970. Extraction term models of soil moisture use by transpiration plants. *Water Resources Research* **6** (5): 1346–1356.

Monson RK, Sparks JP, Rosenstiel TN, Scott–Denton LE, Huxman TE, Harley PC, Turnipseed AA, Burns SP, Backlund B, Hu J. 2005. Climatic influences on net ecosystem CO2 exchange during the transition from wintertime carbon source to springtime carbon sink in a high–elevation, subalpine forest. *Oecologia* **146** (1): 130–147 DOI: 10.1007/s00442-005-0169-2.

Muller–Dombois D. 1964. Effect of depth to water table on height growth of tree seedlings in a greenhouse. *Forest Science* **10** (3): 306–316.

Nakai T, Kim Y, Busey RC, Suzuki R, Nagai S, Kobayashi H, Park H, Sugiura K, Ito A. 2013. Characteristics of evapotranspiration from a permafrost black spruce forest in interior Alaska.

Polar Science **7** (2): 136–148.

Nazarbakhsh M, Ireson A, Barr A, Melton J. 2017. Trade–offs between soil and vegetation characteristics in controlling the boreal forest water balance. Oral presentation at the *Canadian Geophysical Union*, Vancouver, BC.

Nimah MN, Hanks RJ. 1973. Model for estimating soil water, plant, and atmospheric interrelations: I. description and sensitivity. *Soil Science Society of America Journal* **37** (4): 522–527.

Nyberg L, Stahli M, Mellander PE, Bishop KH. 2001. Soil frost effects on soil water and runoff dynamics along a boreal forest transect: 1. Field investigations. *Hydrological Processes* **15** (6): 909–926.

Ojha CSP, Rai AK. 1997. Nonlinear root–water uptake model. *Irrigation and Drainage Engineering* **122** (4): 198–202.

Oki T, Kanae S. 2006. Global hydrological cycles and world water resources. *Science* **313** (5790): 1068–1072.

Oquise G, Gardestrom P, Huner NPA. 2001. Metabolic changes during cold acclimation and subsequent freezing and thawing. In Conifer Cold Hardiness , Vol.1 , ed. S.J. Colombo , pp. 137–163. Dordrecht:Kluwer.

Ottander C, Campbell D, Öquist G. 1995. Seasonal changes in photosystem II organisation and pigment composition in Pinus sylvestris. *Planta* **197** (1): 176–183 DOI: 10.1007/BF00239954.

Passioura JB. 1988. Water transport in and to roots. *Annual Review of Plant Biology* **39** (1): 245–265.

Personne E, Perrier A, Tuzet A. 2003. Simulating water uptake in the root zone with a microscopic–

scale model of root extraction. *Agronomy* **23** (2): 153–168.

Pietroniro A, Fortin V, Kouwen N, Neal C, Turcotte R, Davison B, Verseghy D, Soulis ED, Caldwell R, Evora N, et al. 2007. Development of the MESH modelling system for hydrological ensemble forecasting of the Laurentian Great lakes at the regional scale. *Hydrology and Earth System Sciences* **11** (4): 1279–1294.

Pitman AJ, Slater AG, Desborough CE, Zhao M. 1999. Uncertainty in the simulation of runoff due to the parameterization of frozen soil moisture using the Global Soil Wetness Project methodology. *Geophysical Research Atmospheres* **104** (D14): 16879–16888 DOI: 10.1029/1999JD900261.

Pomeroy J, Hedstrom N, Parviainen J. 1999. The snow mass balance of Wolf Creek , Yukon : effects of snow sublimation and redistribution. *Wolf Creek Research Basin Workshop*, Yukon.

Prasad R. 1984. Influence of time step in the simulation modelling of evapotranspiration. *Sadhana, Academy Proceedings in Engineering Sciences* **7** (2): 91–118.

Prasad R. 1988. A linear root water uptake model. *Hydrology* **99** (3–4): 297–306.

Rambal S, Ourcival JM, Joffre R, Mouillot F, Nouvellon Y, Reichstein M, Rocheteau A. 2003. Drought controls over conductance and assimilation of a Mediterranean evergreen ecosystem: scaling from leaf to canopy. *Global Change Biology* **9** (12): 1813–1824.

Rohde A, Bhalerao RP. 2007. Plant dormancy in the perennial context. *Trends in Plant Science* **12** (5): 217–223 DOI: 10.1016/j.tplants.2007.03.012.

Rowe JS, Acton DF. 1985. Taproots of jack pine (*Pinus banksiana Lamb.*) and soil tongues in Saskatchewan. *Canadian Journal of Forest Research* **15** (4): 646–650.

Rutter N, Essery R, Pomeroy J, Altimir N, Andreadis K, Baker I, Barr A, Bartlett P, Boone A, Deng H, et al. 2009. Evaluation of forest snow processes models (SnowMIP2). *Geophysical Research Atmospheres* **114** (D06111): 1–18 DOI: 10.1029/2008JD011063.

Savitch LV, Leonardos ED, Krol M, Jansson S, Grodzinski B, Huner NPA, Oquist G. 2002. Two different strategies for light utilization in photosynthesis in relation to growth and cold acclimation. *Plant, Cell and Environment* **25** (6): 761–771 DOI: 10.1046/j.1365-3040.2002.00861.x.

Saxe H, Cannell MGR, Johnsen Ø, Ryan MG, Vourlitis G. 2001. Tree and forest functioning in response to global warming. *New Phytologist* **149** (3): 369–400 DOI: 10.1046/j.1469-8137.2001.00057.x.

Saxton KE, Rawls WJ. 2006. Soil water characteristic estimates by texture and organic matter for hydrologic solutions. *Soil Science Society of America Journal* **70** (5): 1569–1578 DOI: 10.2136/sssaj2005.0117.

Schenk HJ, Jackson RB. 2002. Rooting depths, lateral root spreads and below–ground/ above–ground allometries of plants in water–limited ecosystems. *Ecology* **90** (3): 480–494.

Schlosser CA, Slater AG, Robock A, Pitman AJ, Vinnikov KY, Henderson–Sellers A, Speranskaya NA, Mitchell K, The PILPS 2(D) Contributors. 2000. Simulations of a boreal grasland hydrology at Valdai Russia: PILPS phase 2(d). *Monthly Weather Review* **128** (2): 301–321 DOI: 10.1175/1520-0493(2000)128<0301:SOABGH>2.0.CO;2.

Sellers PJ, Hall FG, Kelly RD, Black A, Baldocchi D, Berry J, Ryan M, Ranson KJ, Crill PM, Lettenmaier DP, et al. 1997. BOREAS in 1997: experiment overview, scientific results, and future directions. *Geophysical Research* **102** (D24): 28731–28769.

Seneviratne SI, Corti T, Davin EL, Hirschi M, Jaeger EB, Lehner I, Orlowsky B, Teuling AJ. 2010. Investigating soil moisture–climate interactions in a changing climate: a review. *Earth–Science Reviews* **99** (3–4): 125–161.

Seneviratne SI, Lüthi D, Litschi M, Schär C. 2006. Land–atmosphere coupling and climate change in Europe. *Nature* **443**: 205–209.

Seneviratne SI, Pal JS, Eltahir EAB, Schar C. 2002. Summer dryness in a warmer climate: a process study with a regional climate model. *Climate Dynamics* **20** (1): 69–85.

Sieber A, Uhlenbrook S. 2005. Sensitivity analyses of a distributed catchment model to verify the model structure. *Hydrology* **310** (1–4): 216–235.

Sims HP. 1964. Root development of jack pine seedlings on burned–over dry sites in southeastern Manitoba. *Canadian Forest Service* **47** (1061): 1–15.

Slaney M. 2006. Impact of Elevated Temperature and [CO_2] on Spring Phenology and Photosynthetic Recovery of Boreal Norway Spruce . Doctoral thesis, Swedish University of Agricultural Sciences, Alnarp, Sweden.

Slater AG, Schlosser CA, Desborough CE, Pitman AJ, Henderson–Sellers, A., Robock A, Vinnikov KY, Mitchell K, Boone A, Braden H, Chen F, et al. 2001. The representation of snow in land surface schemes: results from PILPS 2(d). *Hydrometeorology* **2** (1): 7–25.

Sperry J, Hacke U, Oren R. 2002. Water deficits and hydraulic limits to leaf water supply. *Plant, Cell and Environment* **25** (2): 251–263.

Stadler D, Flühler H, Jansson P–E. 1997. Modelling vertical and lateral water flow in frozen and sloped forest soil plots. *Cold Regions Science and Technology* **26** (3): 181–194.

Stadler D, Stähli M, Aeby P, Flühler H. 2000. Dye tracing and image analysis for quantifying water infiltration into frozen soils. *Soil Science Society of America Journal* **64** (2): 505–516.

Stähli M, Bayard D, Wydler H, Flühler H. 2004. Snowmelt infiltration into alpine soils visualized by dye tracer technique. *Arctic, Antarctic, and Alpine Research* **36** (1): 128–135.

Stähli M, Jansson PE, Lundin L–C. 1999. Soil moisture redistribution and infiltration in frozen sandy soils. *Water Resources Research* **35** (1): 95–103.

Stone EL, Kalisz PJ. 1991. On the maximum extent of tree roots. *Forest Ecology and Management* **46** (1–2): 59–102.

Strong WL, La Roi GH. 1983. Root–system morphology of common boreal forest trees in Alberta, Canada. *Canadian Journal of Forest Research* **13** (6): 1164–1173.

Sutinen S, Partanen J, Viher–Aarnio A, Hkkinen R. 2009. Anatomy and morphology in developing vegetative buds on detached Norway spruce branches in controlled conditions before bud burst. *Tree Physiology* **29** (11): 1457–1465 DOI: 10.1093/treephys/tpp078.

Teufel B, Sushama L, Arora VK, Verseghy D. 2018. Impact of dynamic vegetation phenology on the simulated pan–Arctic land surface state. *Climate Dynamics*: 1–16 DOI: 10.1007/s00382-018-4142-2.

Teuling AJ, Hirschi M, Ohmura A, Wild M, Reichstein M, Ciais P, Buchmann N, Ammann C, Montagnani L, Richardson AD, et al. 2009. A regional perspective on trends in continental evaporation. *Geophysical Research Letters* **36** (2): 1–5.

Trenberth KE, Fasullo JT, Kiehl J. 2009. Earth's global energy budget. *American Meterological Society* **90**: 311–323.

Ukkola AM, De Kauwe MG, Pitman AJ, Best MJ, Abramowitz G, Haverd V, Decker M, Haughton N. 2016. Land surface models systematically overestimate the intensity, duration and magnitude of seasonal–scale evaporative droughts. *Environmental Research Letters* **11** (10): 1–10.

Van Genuchten, M.T., 1980. A closed–form equation for predicting the hydraulic conductivity of unsaturated soils. *Soil Science Society of America Journal* 44(5): 892–898.

Van Rees K, Jackson D. 1994. Rooting patterns of boreal mixedwood species. A Report for the Prince Albert Model Forest. Soil Science Department. University of Saskatchewan, Saskatoon, Saskatchewan.

Verseghy D. 2011. CLASS – The Canadian land surface scheme (version 3.5). Climate research division, science and technology branch, Environment Canada, Ontario.

Verseghy DL. 1991. CLASS – A Canadian land surface scheme for GCMs. I. soil model. *International Journal of Climatology* **11** (2): 111–133.

Verseghy DL, McFarlane NA, Lazare M. 1993. CLASS–a canadian land surface scheme for GCMs, II. Vegetation model and coupled runs. *International Journal of Climatology* **13** (4): 347–370.

Viereck L, Cleve K Van, Dyrness C. 1986. Forest ecosystem distribution in the taiga environment In: Van Cleve K, Chapin FS, Flanagan PW, Viereck LA, Dryness CT (eds) Forest Ecosystems in the Alaskan Taiga. Ecological Studies (Analysis and Synthesis). Springer. New York.

Viereck LA, Dryness CT, Cleve K V., Foote MJ. 1983. Vegetation, soils and forest productivity in selected forest types in interior Alaska. *Canadian Journal of Forest Research* **13** (5): 703–720.

Vrugt JA, Wijk MT Van, Hopmans JW, Simunek J. 2001. One–, two–, and three–dimensional root

water uptake functions for transient modeling. *Water Resources Research* **37** (10): 2457–2470

Wang YP, Kowalczyk E, Leuning R, Abramowitz G, Raupach MR, Pak B, Gorsel E V., Luhar A. 2011. Diagnosing errors in a land surface model (CABLE) in the time and frequency domains. *Geophysical Research* **116** (G101034): 1–18.

Watanabe K, Wake T. 2009. Measurement of unfrozen water content and relative permittivity of frozen unsaturated soil using NMR and TDR. *Cold Regions Science and Technology* **59** (1): 34–41.

Watanabe K, Kito T, Dun S, Wu JQ, Greer RC, Flury M. 2013. Water infiltration into a frozen soil with simultaneous melting of the frozen layer. *Vadose Zone* **12** (1): 1–11.

Whittaker RH. 1975. Community structure and composition.

Williams P, Smith M. 1989. The frozen earth: fundamentals of geocryology. *Canadian Geotechnical Journal* **27** (4): 762–763.

Wolff JO, West SD, Viereck LA. 1977. Xylem pressure potential in black spruce in interior Alaska. *Canadian Journal of Forest Research* **7** (2): 422–428.

Wu J, Zhang R, Gui S. 1999. Modeling soil water movement with water uptake by roots. *Plant and Soil* **215** (1): 7–17.

Yetemen O, Ireson AM, Barr AG, Melton JR, Black TA. 2015. Modeling the ecohydrologic response of the forest–grassland ecotone in western Canada to changes in annual precipitation. Poster presentation at the *American Geophysical Union,* San Francisco, California.

Zheng T, Chen J, He L, Arain MA, Thomas SC, Murphy JG, Geddes JA, Black TA. 2017. Inverting the maximum carboxylation rate (Vcmax) from the sunlit leaf photosynthesis rate derived from

measured light response curves at tower flux sites. *Agricultural and Forest Meteorology* **236**: 48–66 DOI: 10.1016/j.agrformet.2017.01.008.

Zhang T, Barry RG, Knowles K, Heginbottom JA, Brown J. 1999. Statistics and characteristics of permafrost and ground–ice distribution in the Northern Hemisphere. *Polar Geography* **23** (2): 132–154 DOI: 10.1080/10889370802175895.

APPENDIX A: Modelling tools

To address all the fundamental processes that contribute to terrestrial biosphere, the model framework should be adequately robust. To accurately simulate water, energy and carbon fluxes, dynamic vegetation models need to be used. The potential models for this study are Canadian Land Surface Scheme (CLASS) and the coupled Canadian Land Surface Scheme and Canadian Terrestrial Ecosystem Model (CLASS–CTEM). CLASS–CTEM is one of the most cited and applied dynamic vegetation models used by academic researchers, and it is recommended by Environment and Climate Change Canada. In addition to considering its reputation as a valued tool, I chose both models because they display some of the deficiencies we intend to evaluate. These models can be applied to all the hypotheses and data. In the next section, the structures of the models are briefly explained.

A.1 Canadian Land Surface Scheme (CLASS)

The Canadian Land Surface Scheme (CLASS) can be run in coupled or uncoupled mode. In the coupled mode, CLASS integrates water and energy balances of the land surface from an initial point and run with an atmospheric model, which passed the simulated forcing data to CLASS at each time step. Afterward, CLASS simulates surface parameters such as turbulent fluxes, albedo and surface radiative, which are passed into the atmospheric model. In uncoupled mode, CLASS uses forcing data simulated from the atmospheric model or from field measurements.

In this research, the uncoupled mode of CLASS is used. CLASS simulates the water and energy balances of the soil, vegetation and snow, separately (Figure A–1). The variables including liquid and frozen moisture contents and temperatures of the soil layers, the albedo, density, temperature and mass of snow pack, the temperature and intercepted snow and rain on the vegetation, the depth of ponded water and temperature on the soil surface, and vegetation growth index should be

initialized. Values are associated with a set of soil parameters explaining the present state of vegetation and soil types should also be assigned.

CLASS considers four vegetation categories including needle leaf trees, broadleaf trees, crop and grass. CLASS aggregates the values of parameters including albedo, annual maximum and minimum plant area index, roughness length, rooting depth and so on, and consider diurnal and annual variation functions to determine the physiological characteristics of each vegetation category. Then, these characteristics are aggregated to model the bulk canopy characteristics. Four subareas including bare soil, snow over bare soil, vegetation over soil and vegetation over snow are considered in this model, and fluxes for four subareas are calculated.

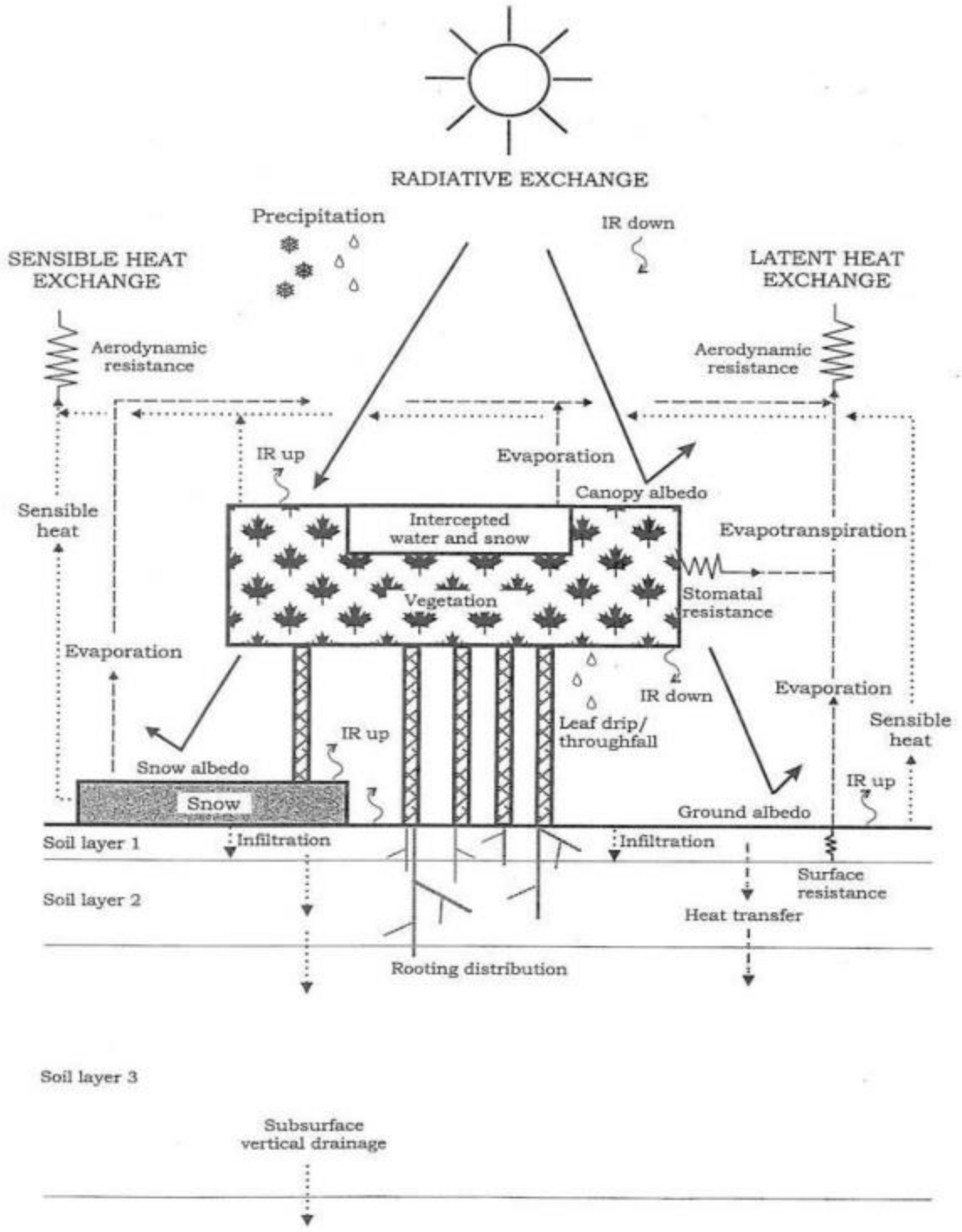

Figure A–1 The schematic diagram of water and energy balance for Canadian Land Surface Scheme (CLASS) (Verseghy, 2011).

A.2 Coupled Canadian Land Surface Scheme and Canadian Terrestrial Ecosystem Model (CLASS–CTEM)

The specific coupled CLASS–CTEM model proposed for this research is based on the Canadian Land Surface Scheme (CLASS) version 3.6.2 and Canadian Terrestrial Ecosystem Model (CTEM) version 1.2. The CLASS models exchange of water and energy fluxes between the atmosphere and the land surface including soil, snow and the vegetation canopy. This model includes three soil layers, with a total depth of 4.1 metres, and four plant functional types, namely needle leaf trees, broadleaf trees, crops and grasses. The land surface is divided into four subareas including bare soil, vegetation, snow over bare soil and snow with vegetation. The model calculates energy and water balances in half–hourly time steps. The model is run with prescribed physiological characteristics such as the maximum and minimum leaf area index (LAI), rooting depth, vegetation height and canopy mass. When CLASS is coupled with CTEM, the CTEM dynamically simulates these vegetation characteristics with a daily time step and then is passed to CLASS (Figure A–2).

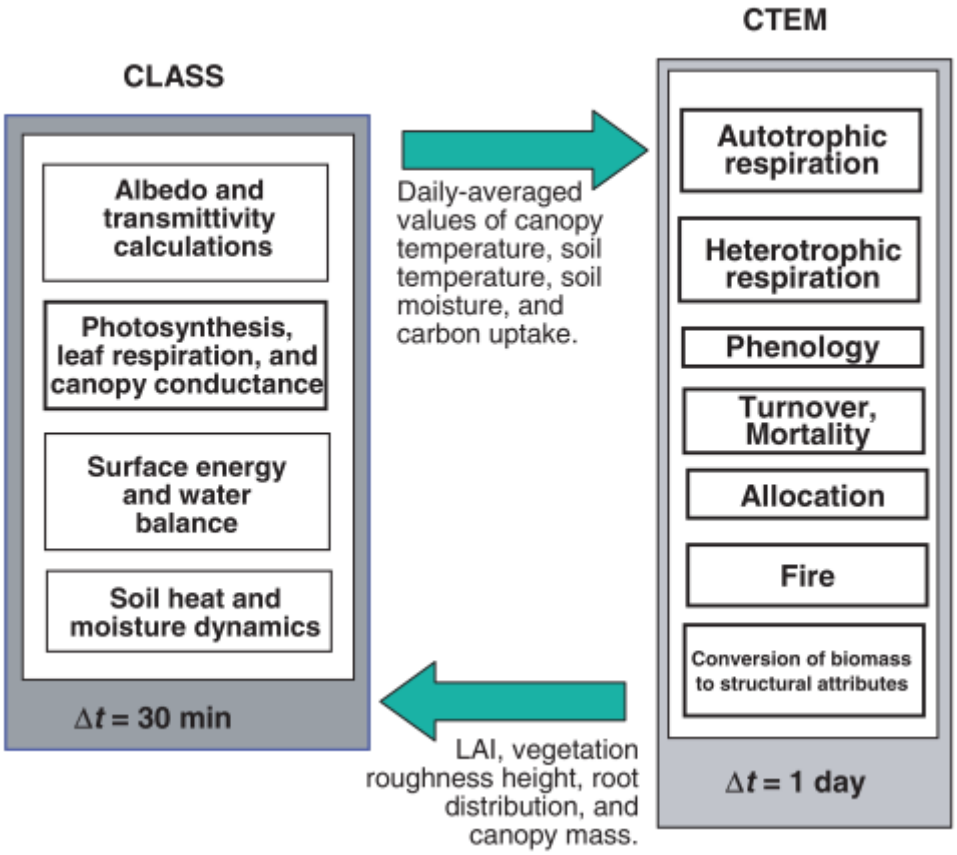

Figure A–2 Coupling of the Canadian Land Surface Scheme (CLASS) and the Canadian Terrestrial Ecosystem Model (CTEM) (Arora and Boer, 2005).

The CTEM is a terrestrial ecosystem model that simulates carbon fluxes between the atmosphere and the land surface (Figure A–3). This exchange of carbon balance occurs through the simulation of photosynthesis, phenology, ecosystem respiration, mortality, turnover, allocation and fire (Arora, 2003; Arora and Boer, 2005; Melton and Arora, 2016). The model is comprised of three vegetation pools, consisting of leaves, stems and roots, and two dead carbon pools, consisting of litter and soil organic matter. The terrestrial ecosystem model includes nine functional plant types: needle leaf evergreen, needle leaf deciduous, broadleaf evergreen, broadleaf cold deciduous, broadleaf drought or dry deciduous, crops (C_3 and C_4) and grasses (C_3 and C_4). Except for photosynthesis and leaf respiration simulated at half–hourly time steps, CTEM simulates all terrestrial ecosystem processes

at a daily time step. A comprehensive explanation of the model structure and its parametrizations are documented in Melton and Arora (2016), Arora (2014), Arora and Boer (2005) and Arora (2003).

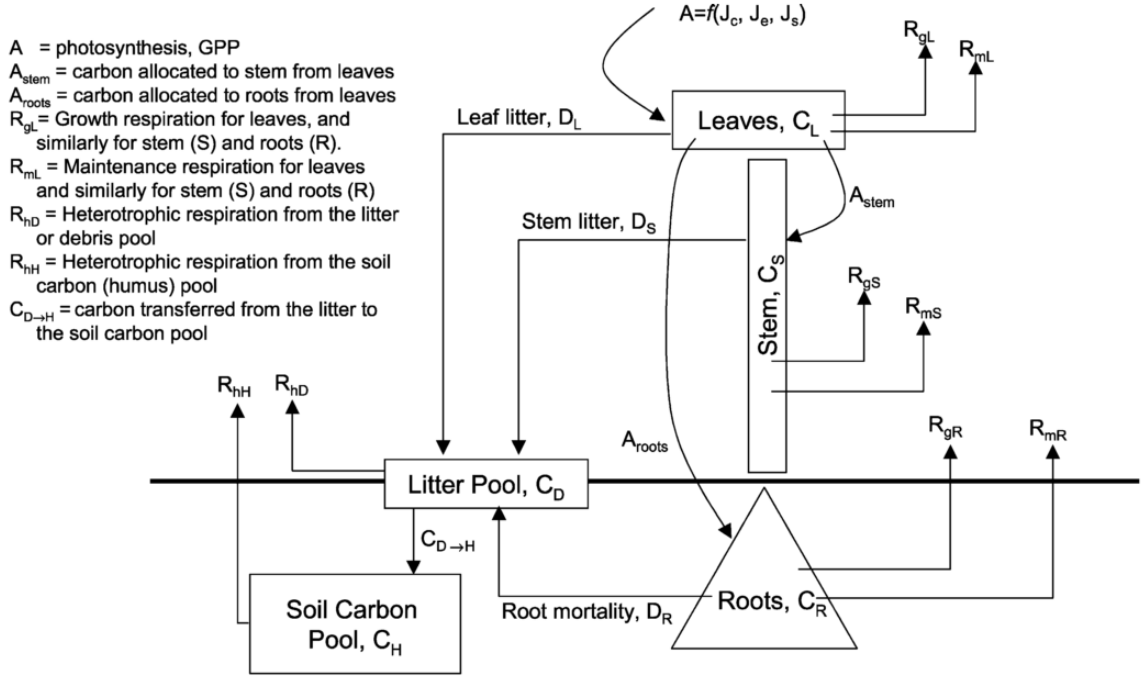

Figure A–3 The structure of the terrestrial ecosystem model and carbon equations in five pools (Arora, 2003).

APPENDIX B: Figures

In cold regions, snow and ice increasingly influence land surface processes (Luo *et al.*, 2003), and It is crucial to understand the partitioning of snowmelt between runoff over the frozen soils and infiltration into frozen soils for the prediction of water resource issues (Luo *et al.*, 2003; Appels *et al.*, 2018). In more northern latitudes, infiltration into frozen soil is the critical hydrological flux (Fang and Pomeroy, 2007; Ireson *et al.*, 2013). Most land surface and hydrological models inadequately represent the amount of snowmelt infiltration into frozen soils (Budhathoki, 2017). The need to improve the representation of snowmelt infiltration into frozen soils is vital. In the following, we present the partitioning of snowmelt between runoff and infiltration during the spring melt period using CLASS and CLASS–CTEM with dynamic and static vegetation for eleven years. The purpose of presenting all figures is to provide insights for the sake of modeling the partitioning of snowmelt into infiltration and runoff processes during the spring melt period in the future.

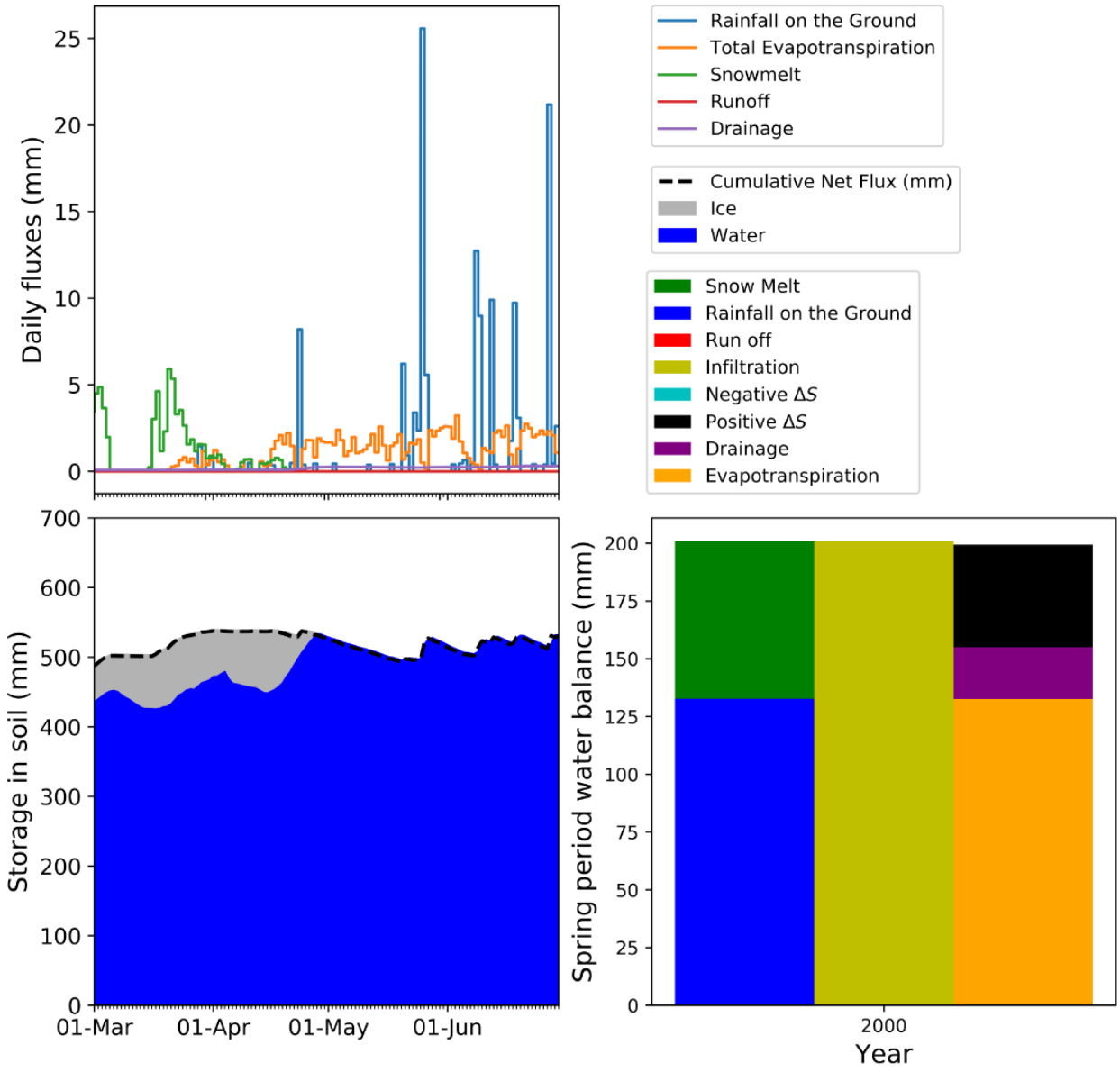

Figure B–1 Detailed water balance during the spring melt period using CLASS for the year 2000.

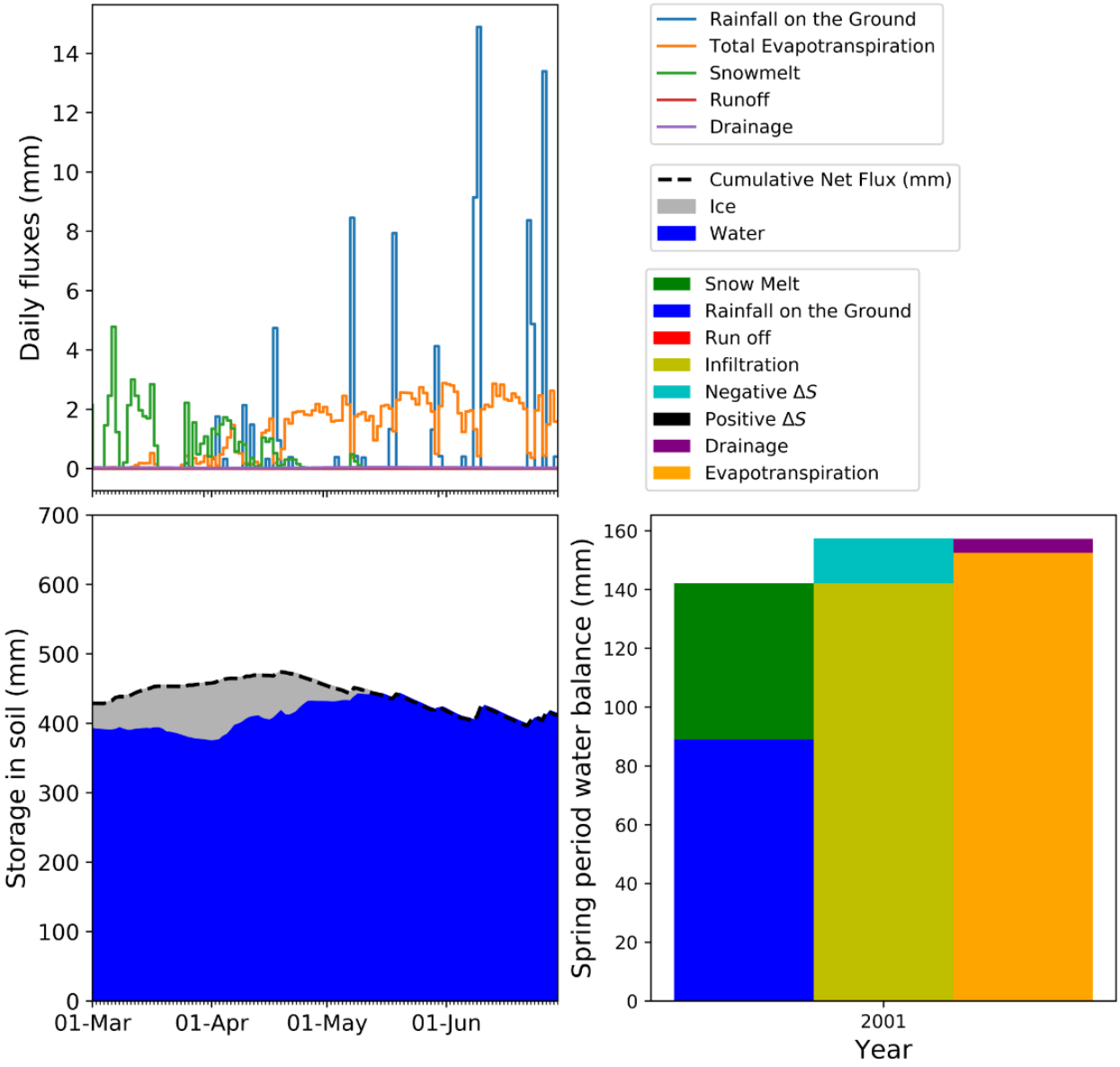

Figure B–2 Detailed water balance during the spring melt period using CLASS for the year 2001.

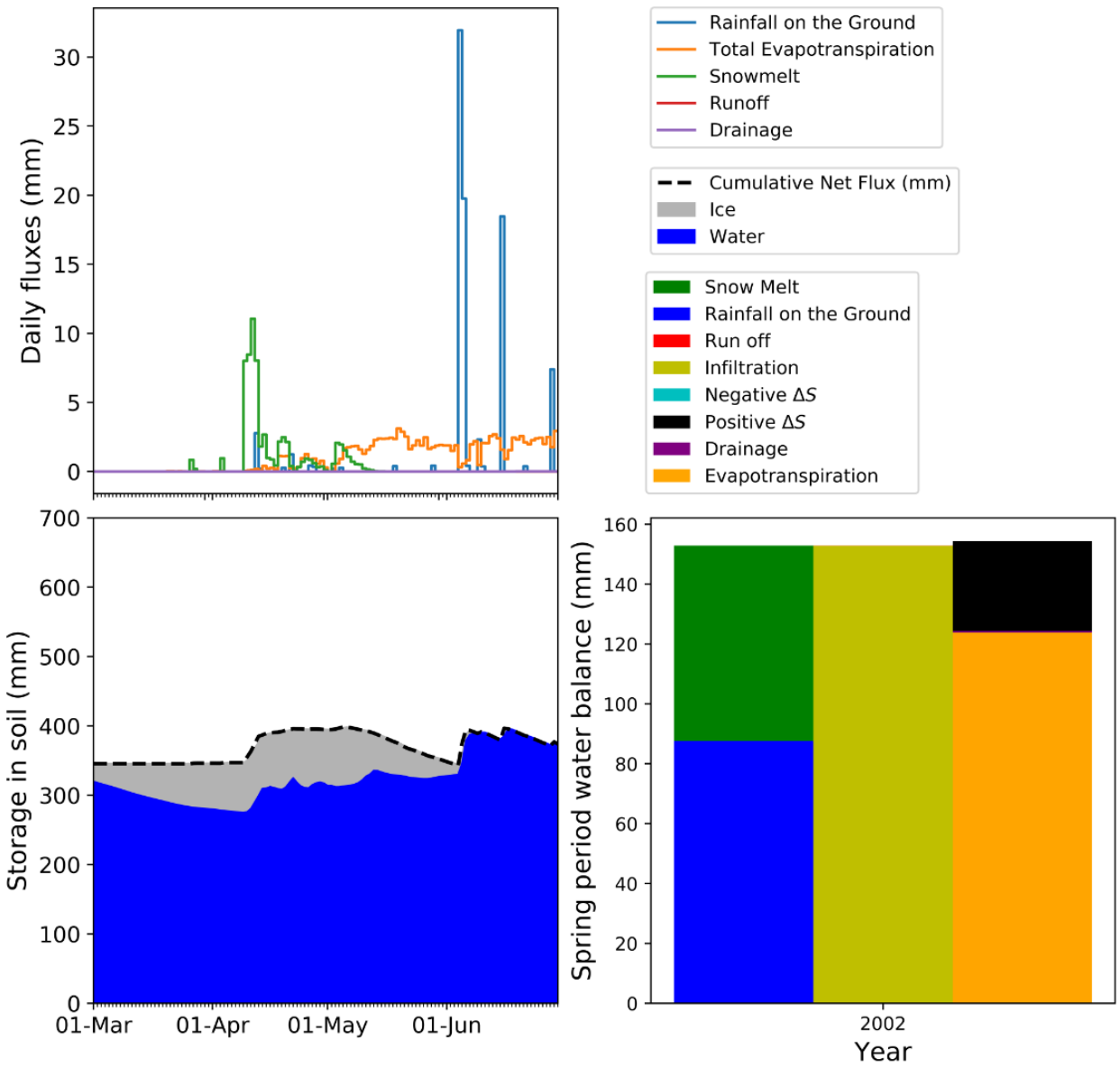

Figure B–3 Detailed water balance during the spring melt period using CLASS for the year 2002.

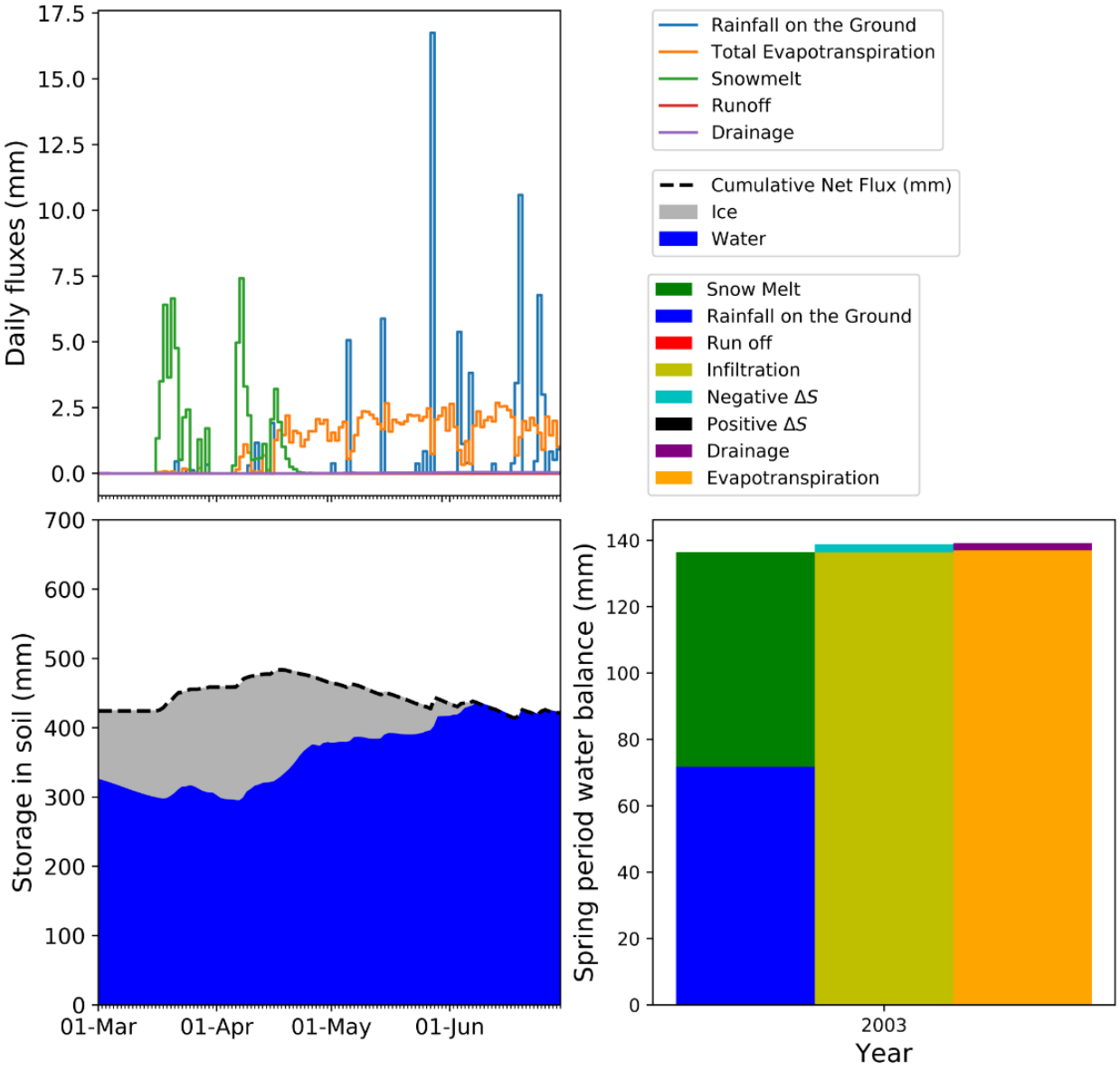

Figure B–4 Detailed water balance during the spring melt period using CLASS for the year 2003.

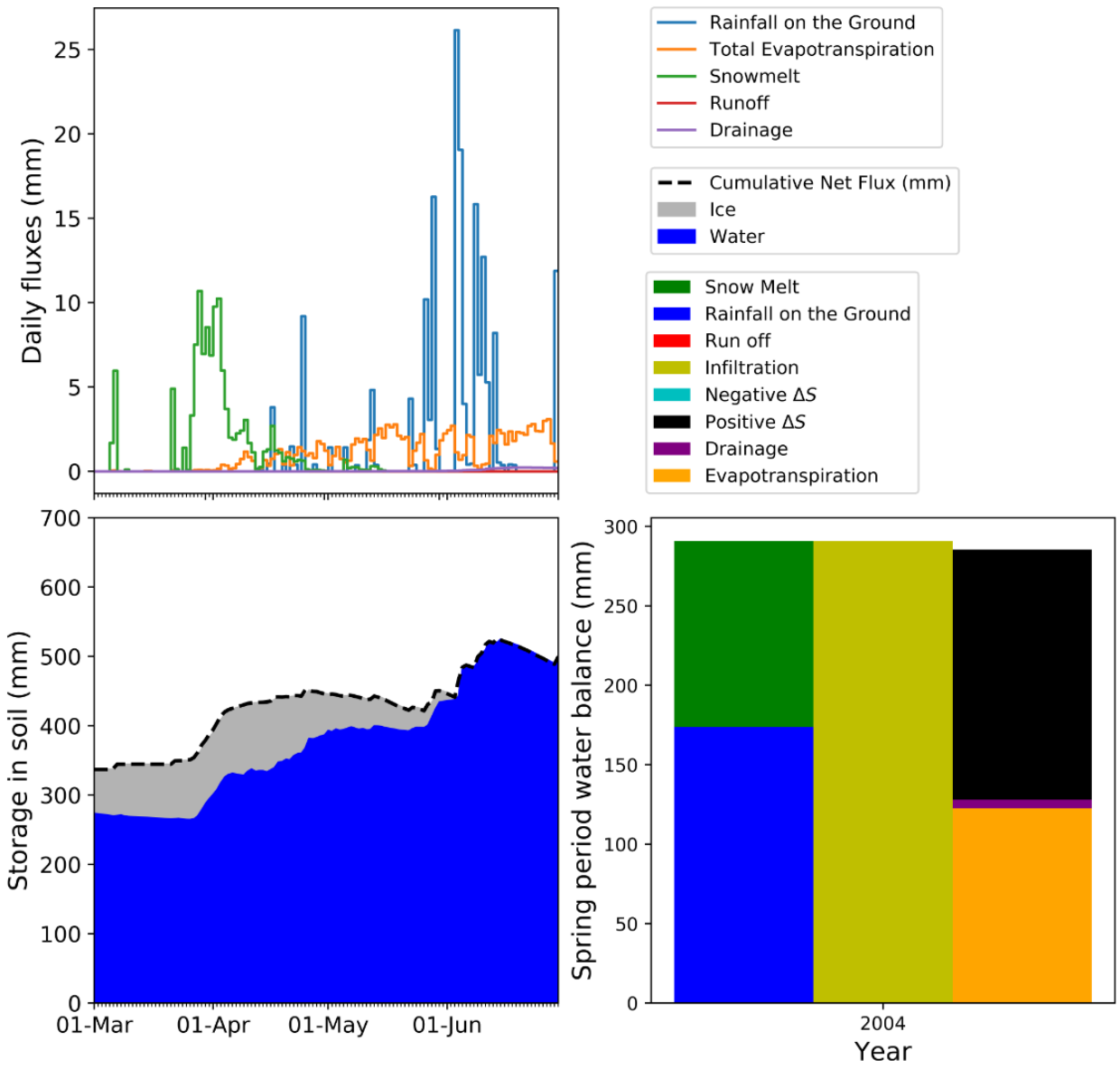

Figure B–5 Detailed water balance during the spring melt period using CLASS for the year 2004.

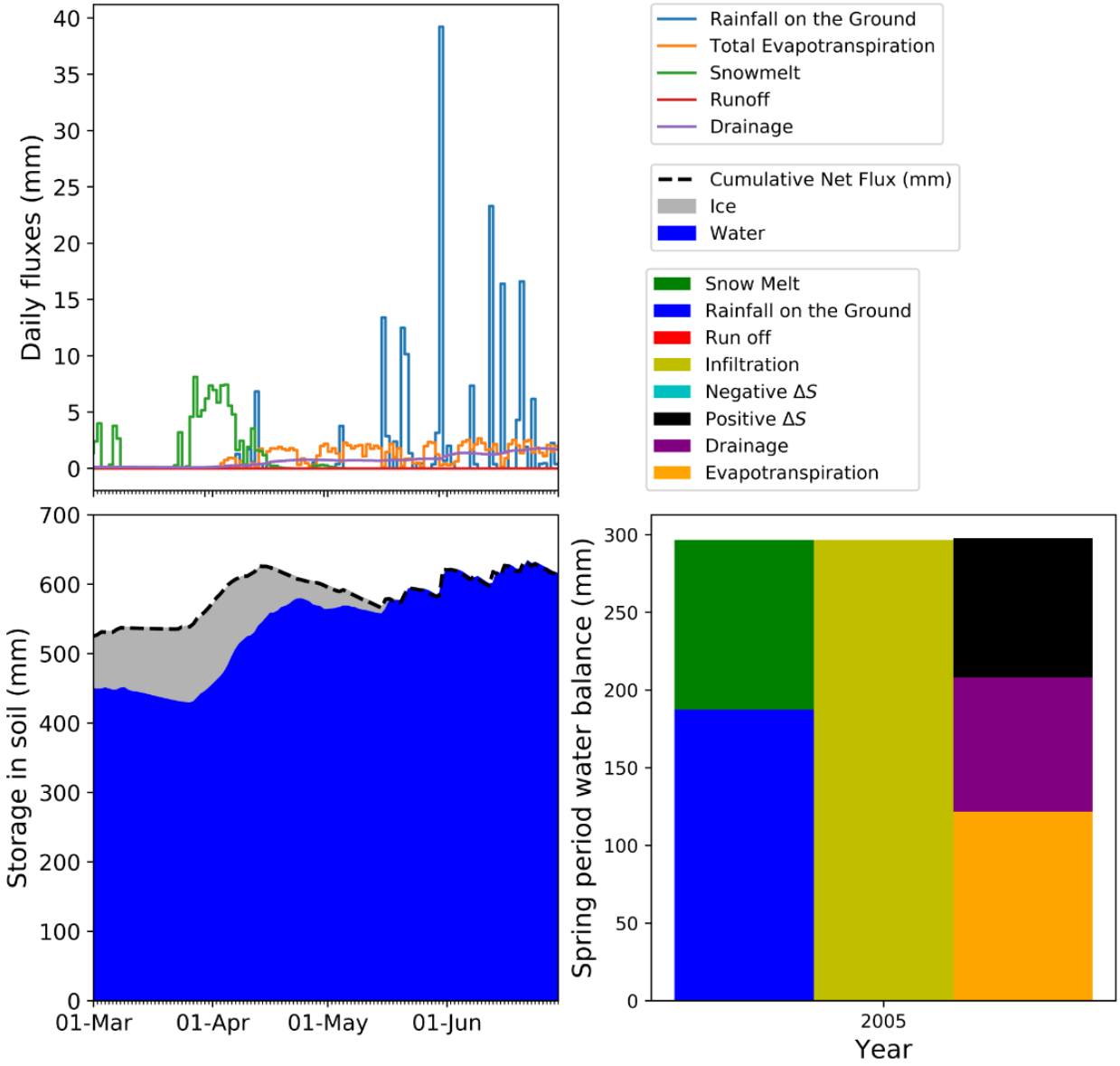

Figure B–6 Detailed water balance during the spring melt period using CLASS for the year 2005.

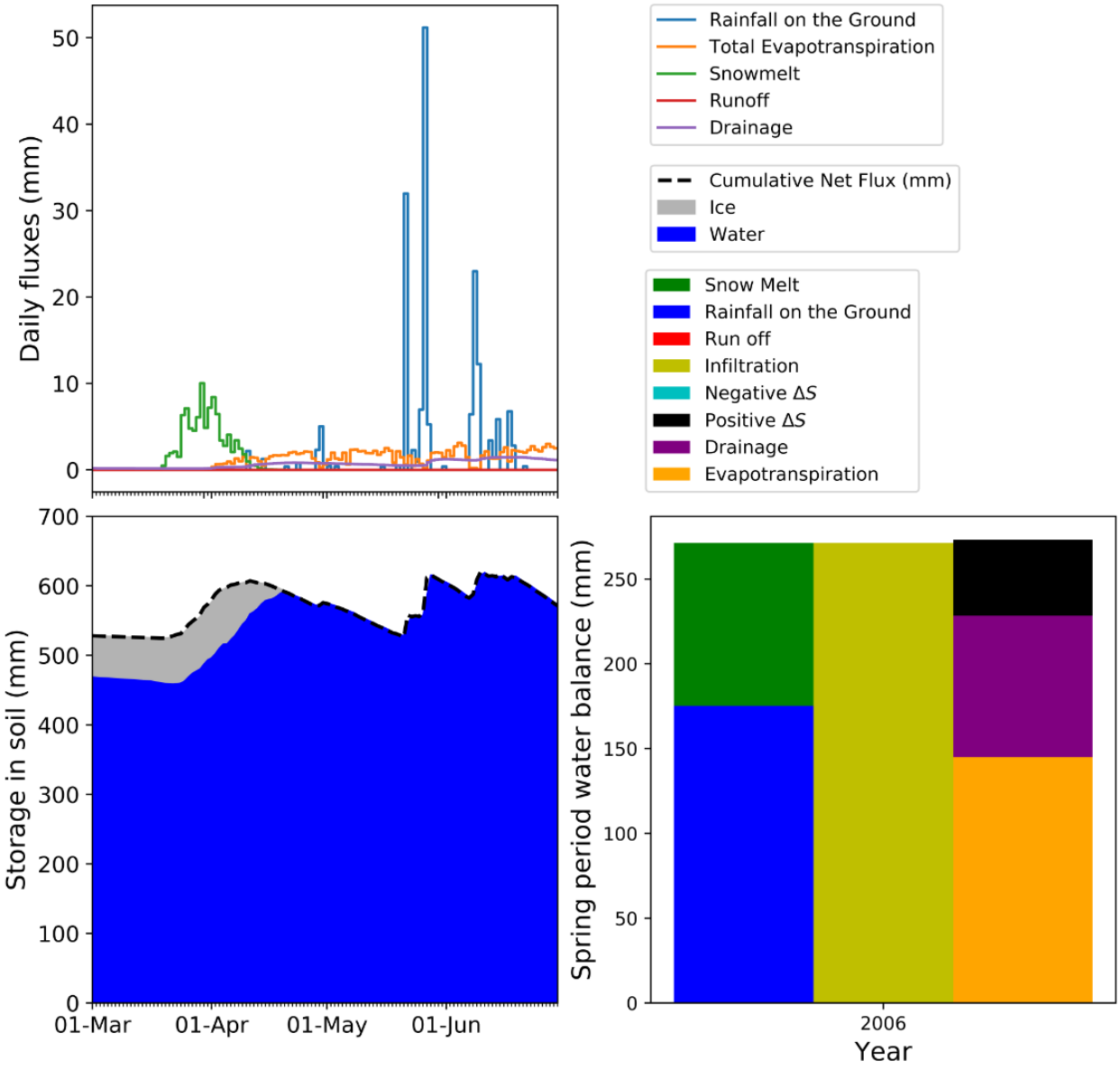

Figure B–7 Detailed water balance during the spring melt period using CLASS for the year 2006.

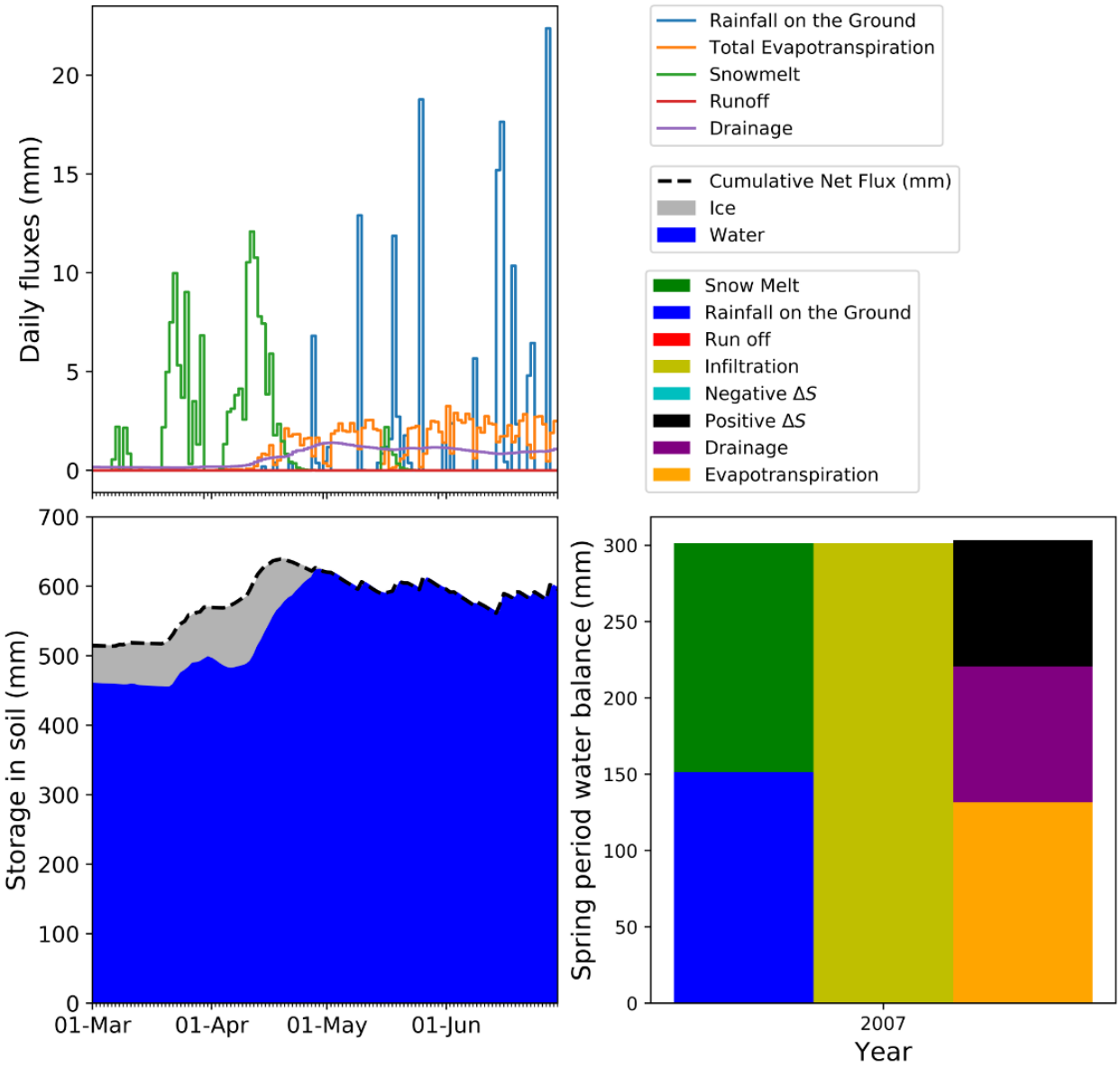

Figure B–8 Detailed water balance during the spring melt period using CLASS for the year 2007.

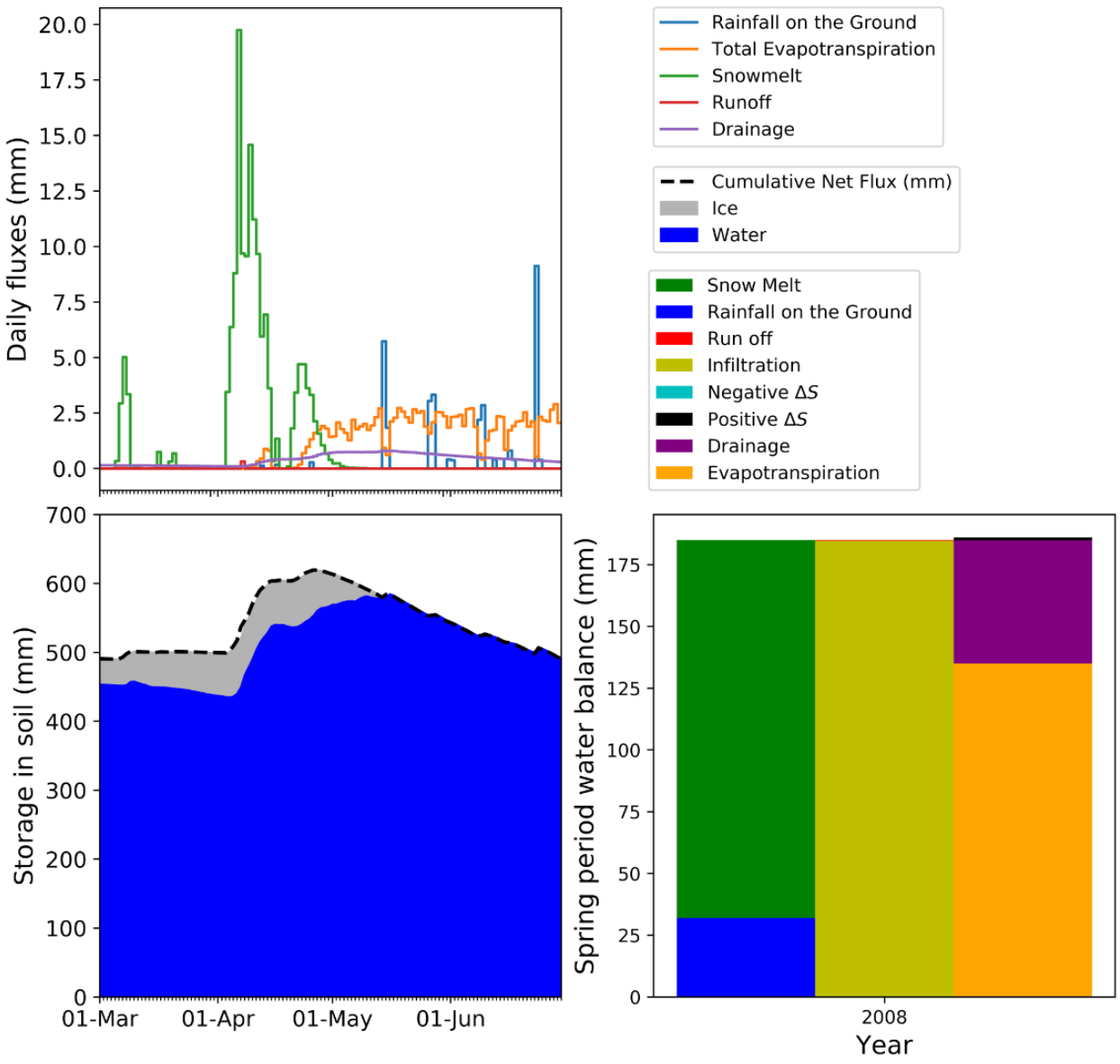

Figure B–9 Detailed water balance during the spring melt period using CLASS for the year 2008.

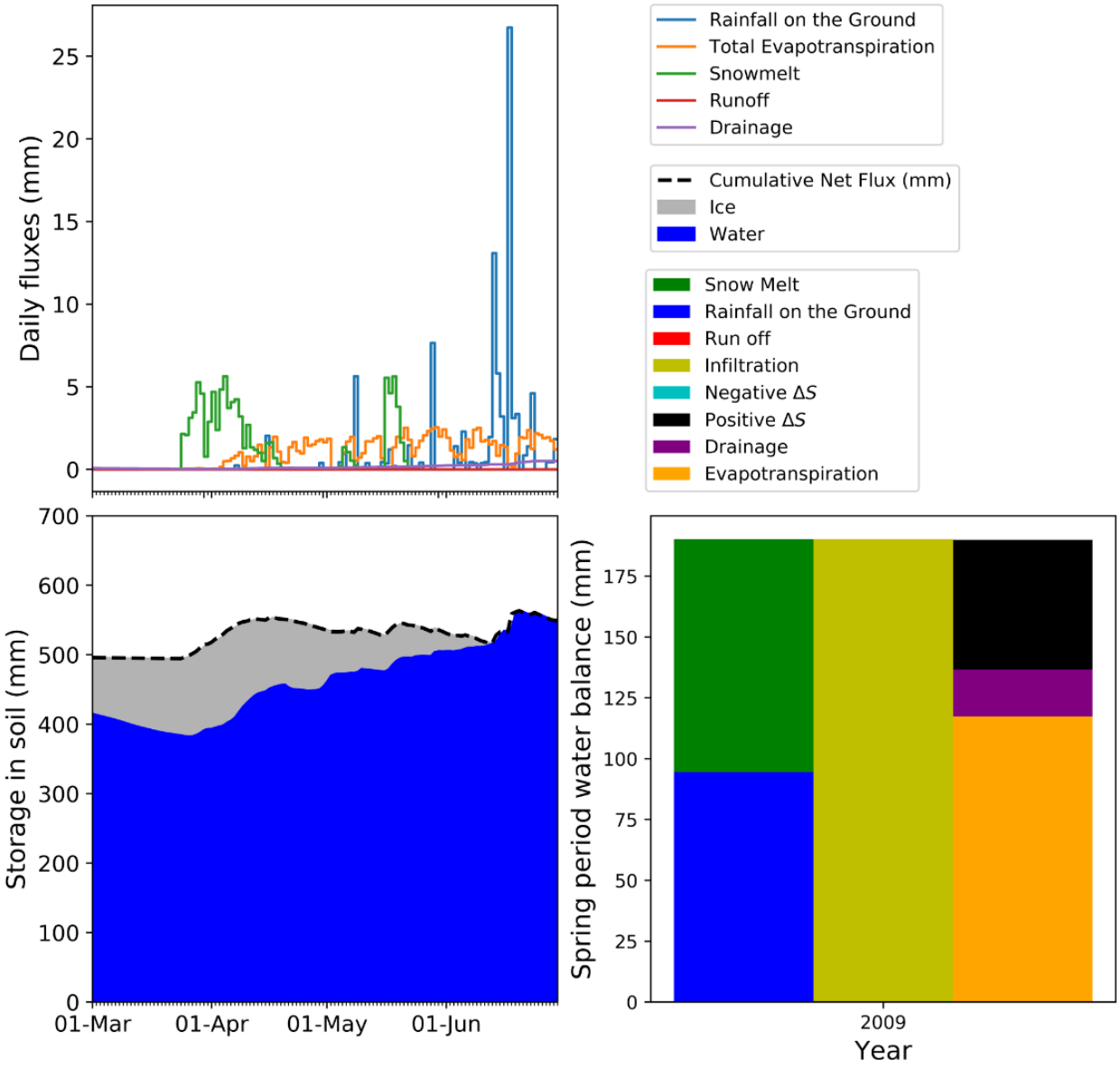

Figure B–10 Detailed water balance during the spring melt period using CLASS for the year 2009.

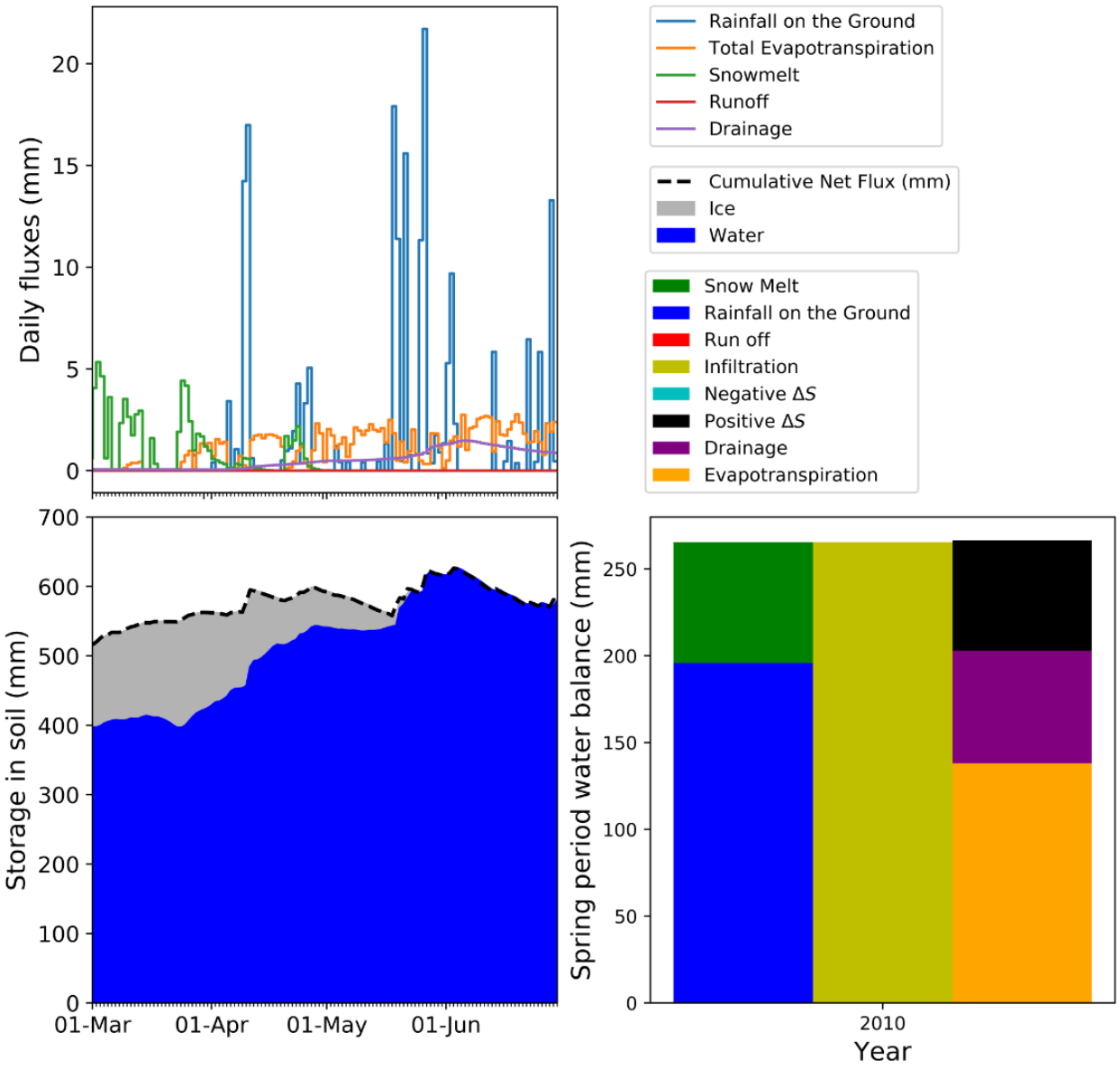

Figure B–11 Detailed water balance during the spring melt period using CLASS for the year 2010.

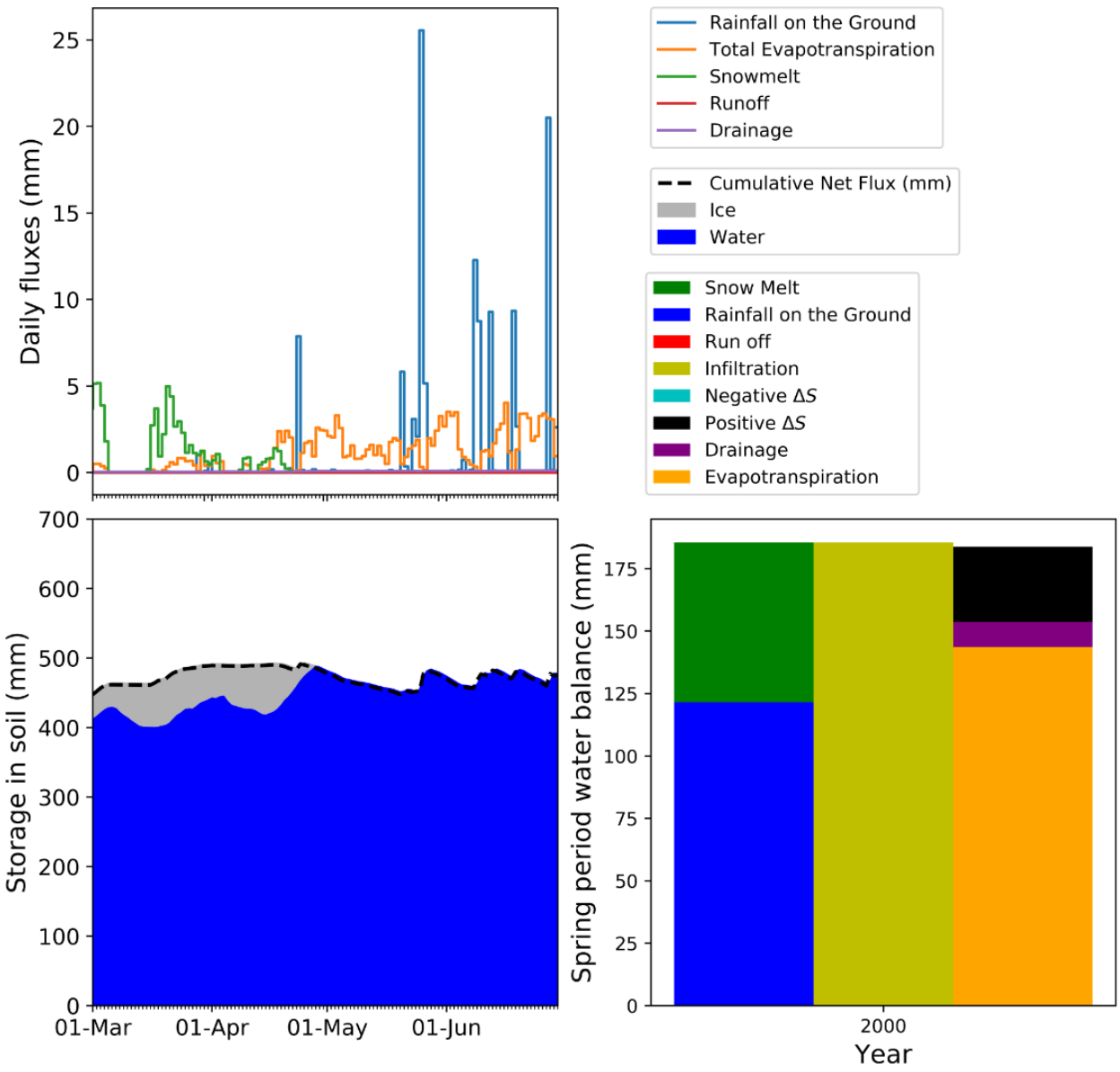

Figure B–12 Detailed water balance during the spring melt period using CLASS–CTEM with dynamic vegetation for the year 2000.

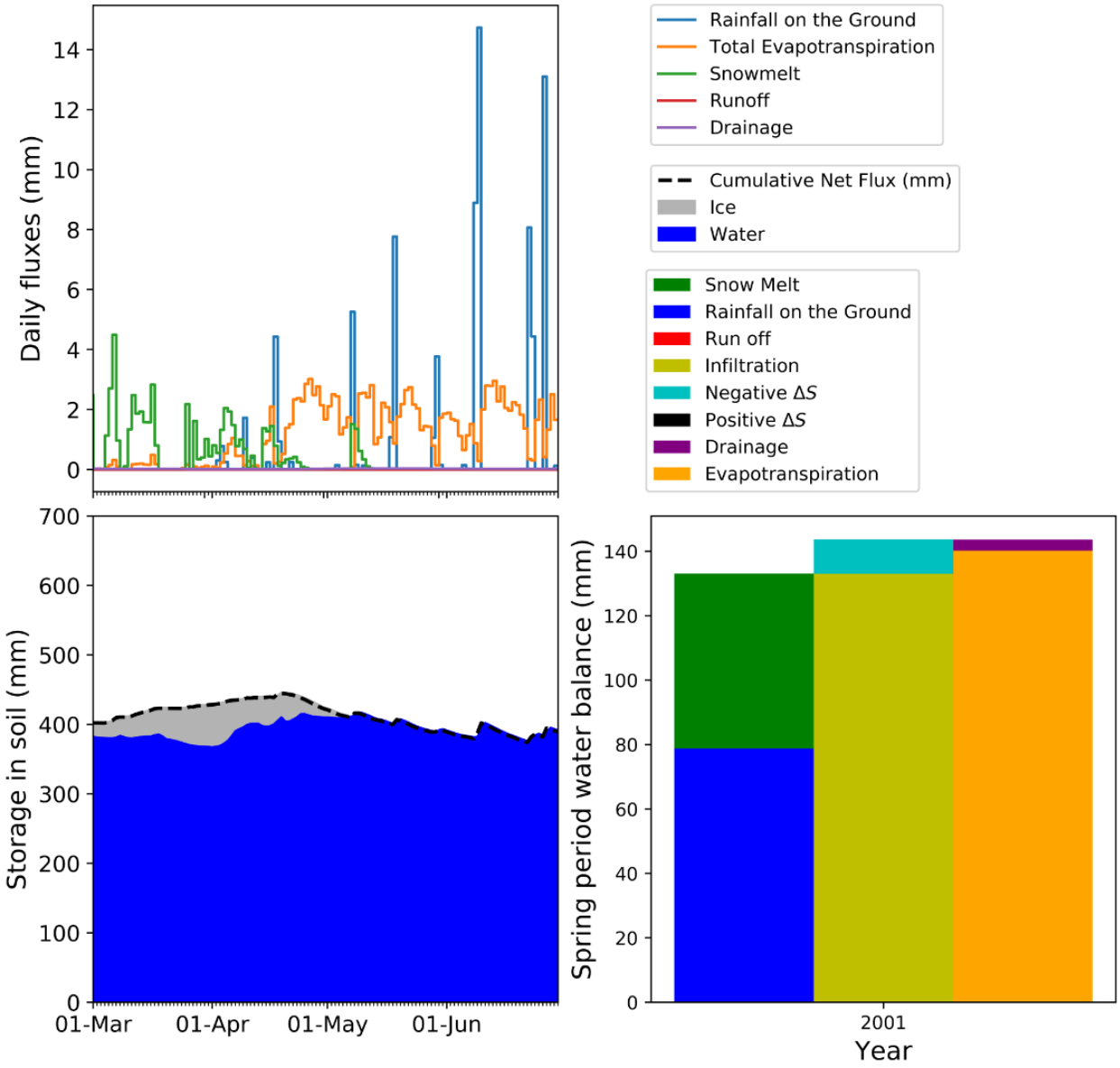

Figure B–13 Detailed water balance during the spring melt period using CLASS–CTEM with dynamic vegetation for the year 2001.

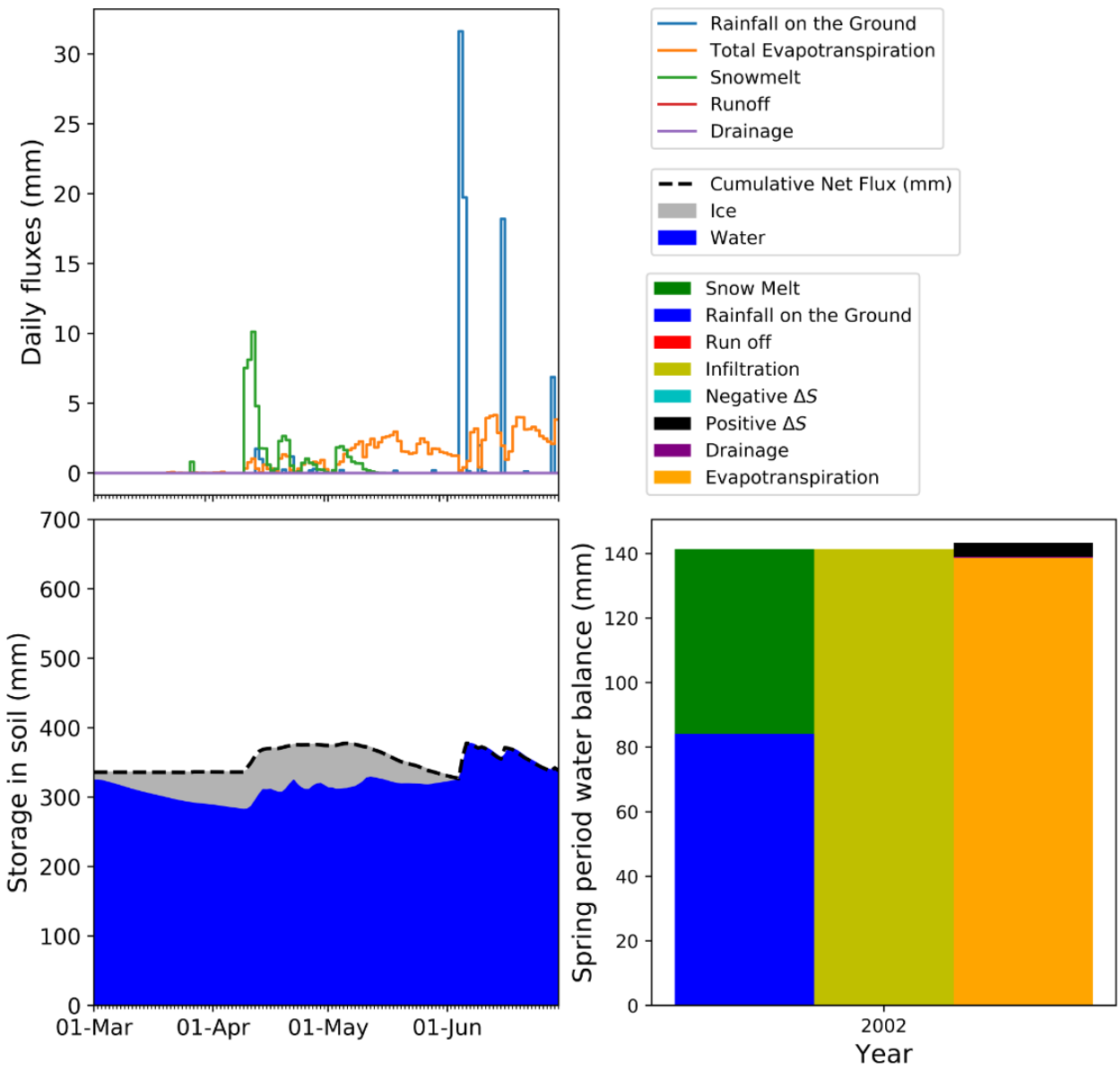

Figure B–14 Detailed water balance during the spring melt period using CLASS–CTEM with dynamic vegetation for the year 2002.

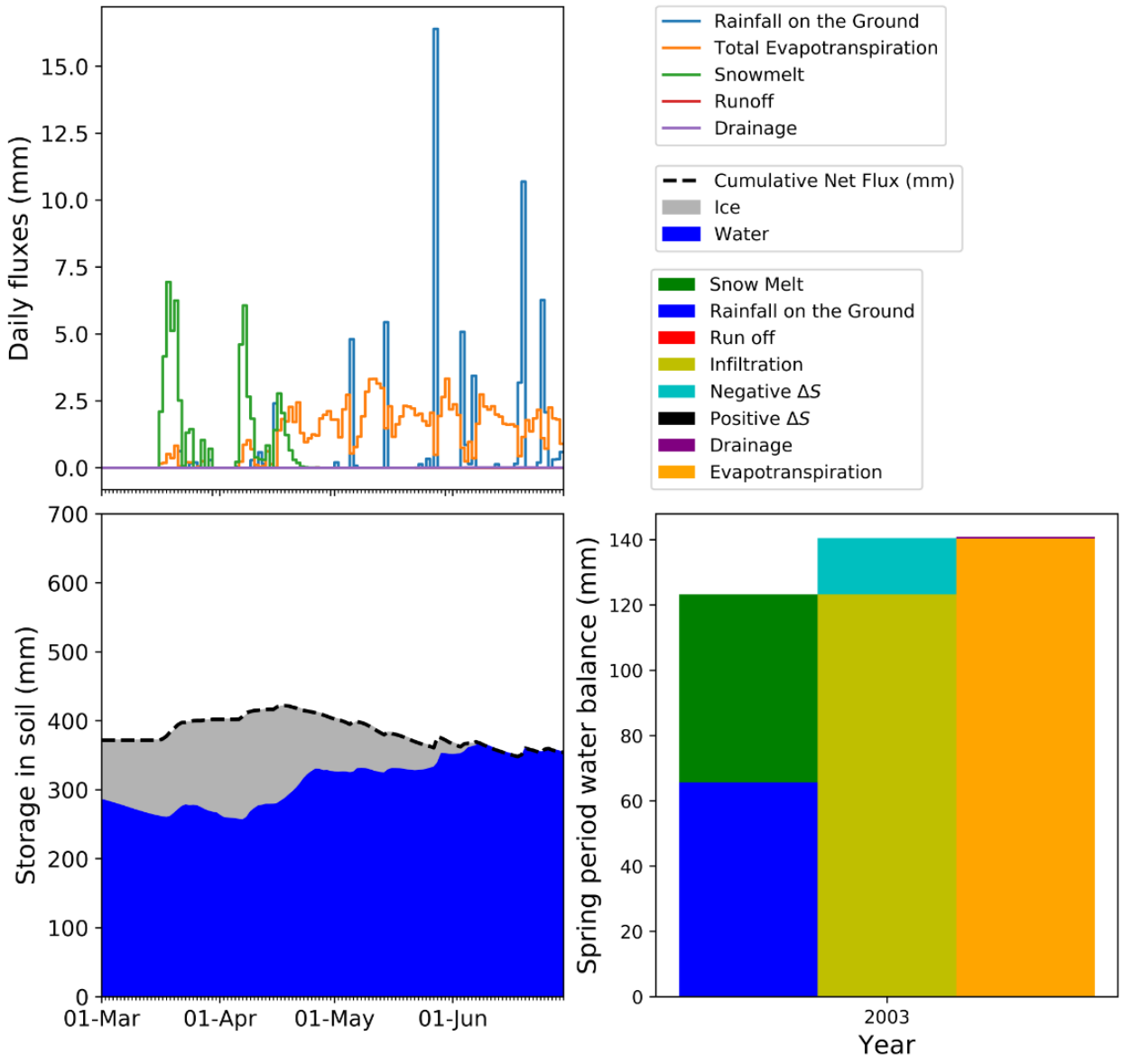

Figure B–15 Detailed water balance during the spring melt period using CLASS–CTEM with dynamic vegetation for the year 2003.

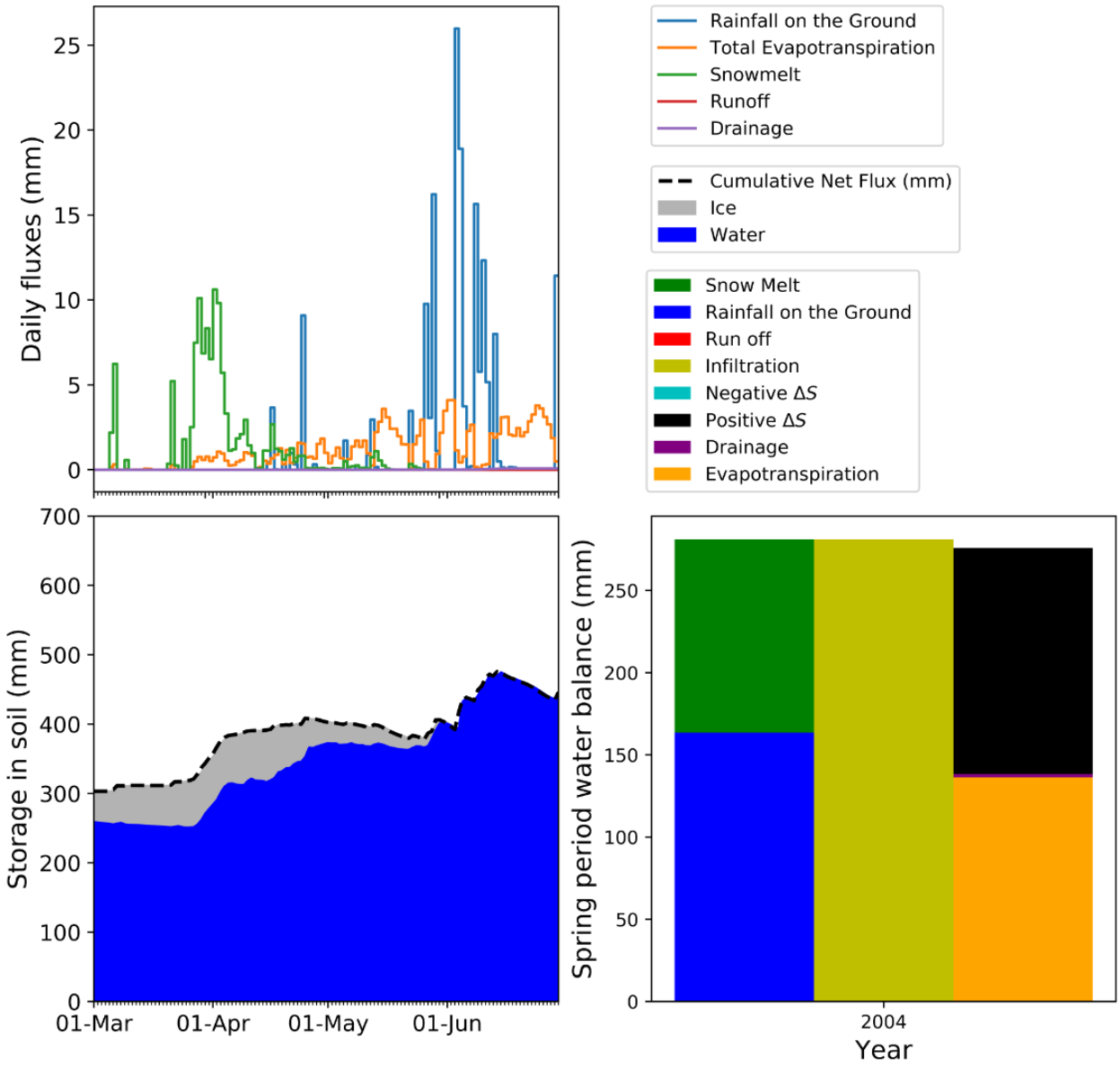

Figure B–16 Detailed water balance during the spring melt period using CLASS–CTEM with dynamic vegetation for the year 2004.

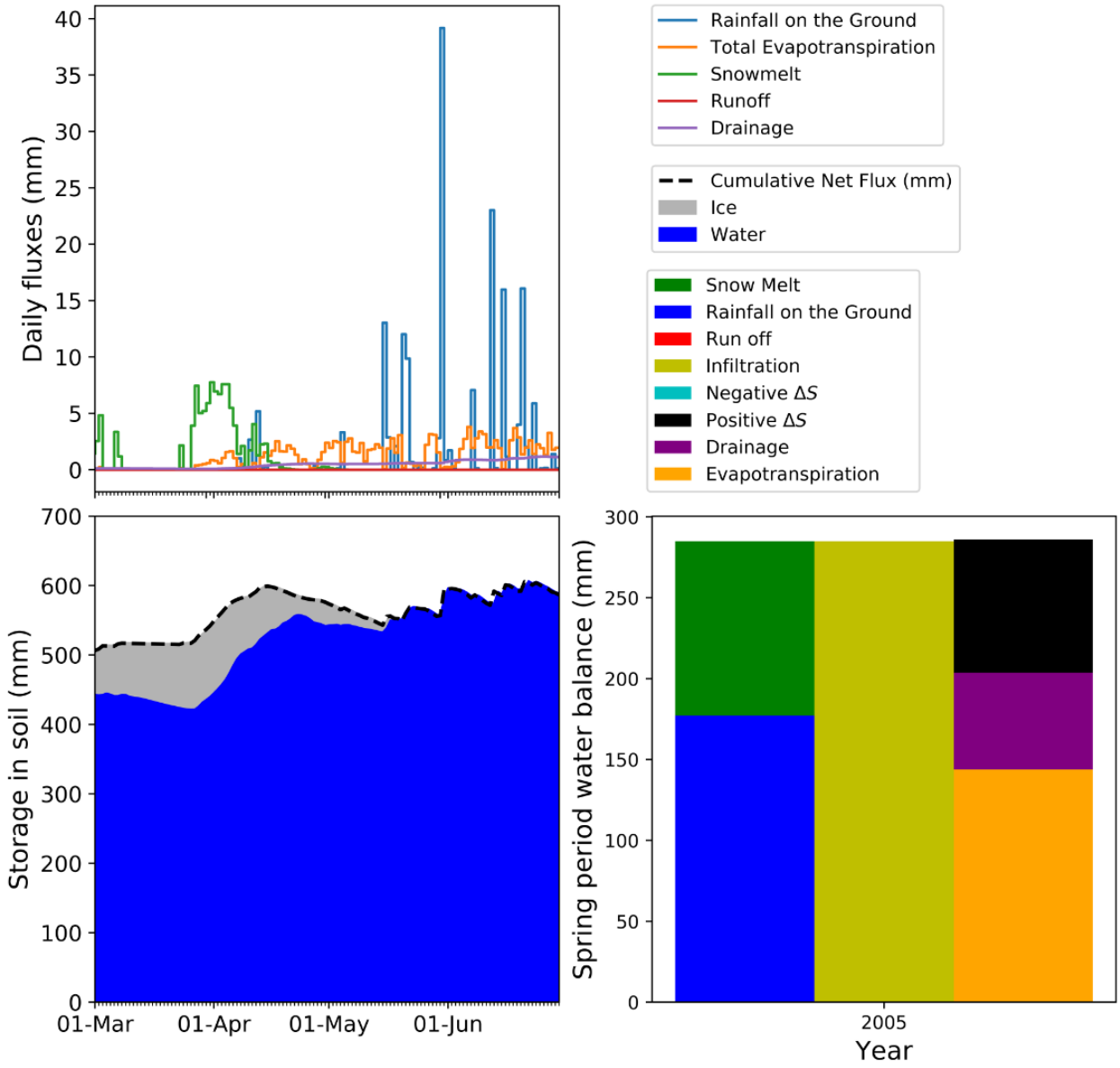

Figure B–17 Detailed water balance during the spring melt period using CLASS–CTEM with dynamic vegetation for the year 2005.

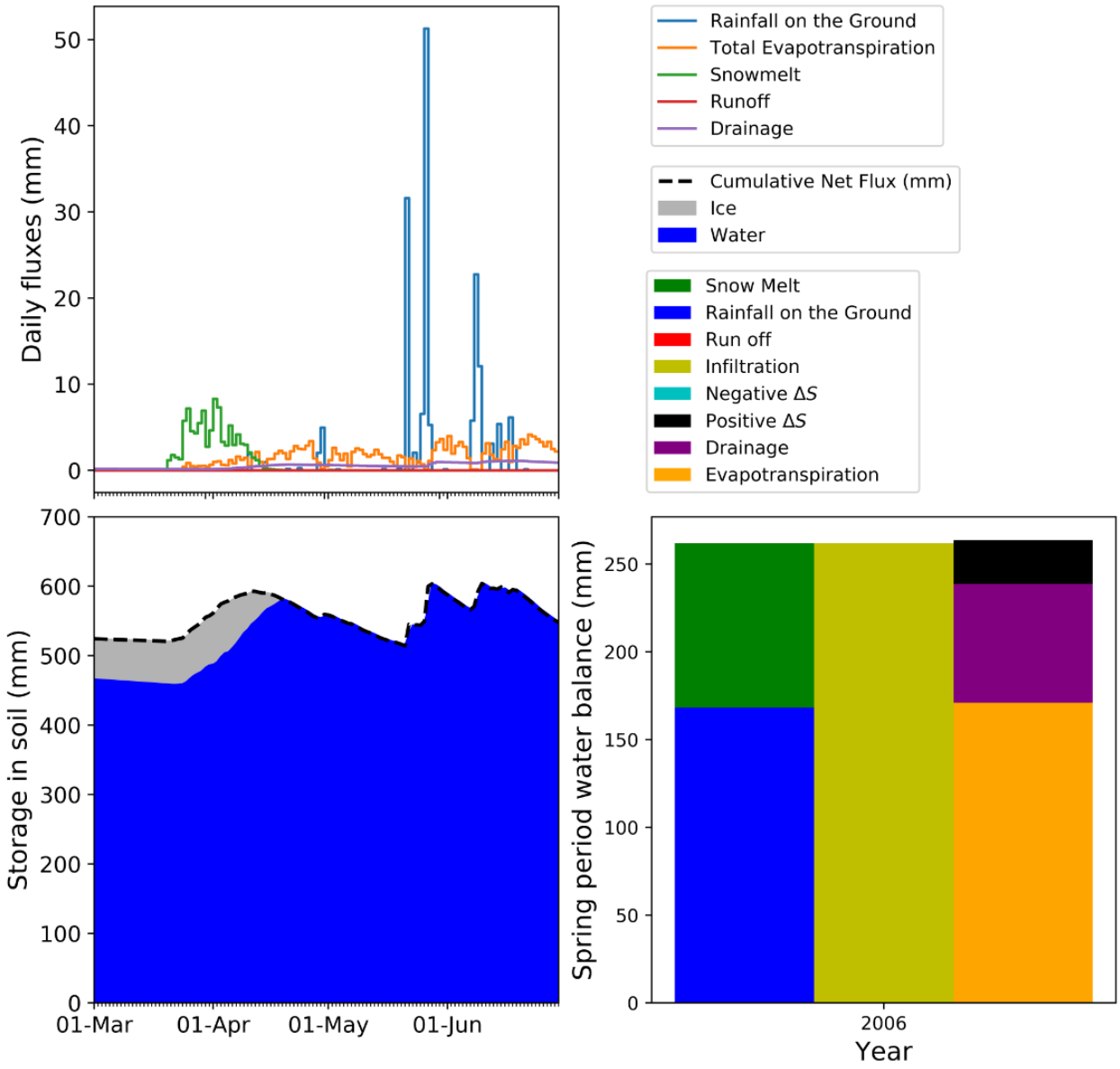

Figure B–18 Detailed water balance during the spring melt period using CLASS–CTEM with dynamic vegetation for the year 2006.

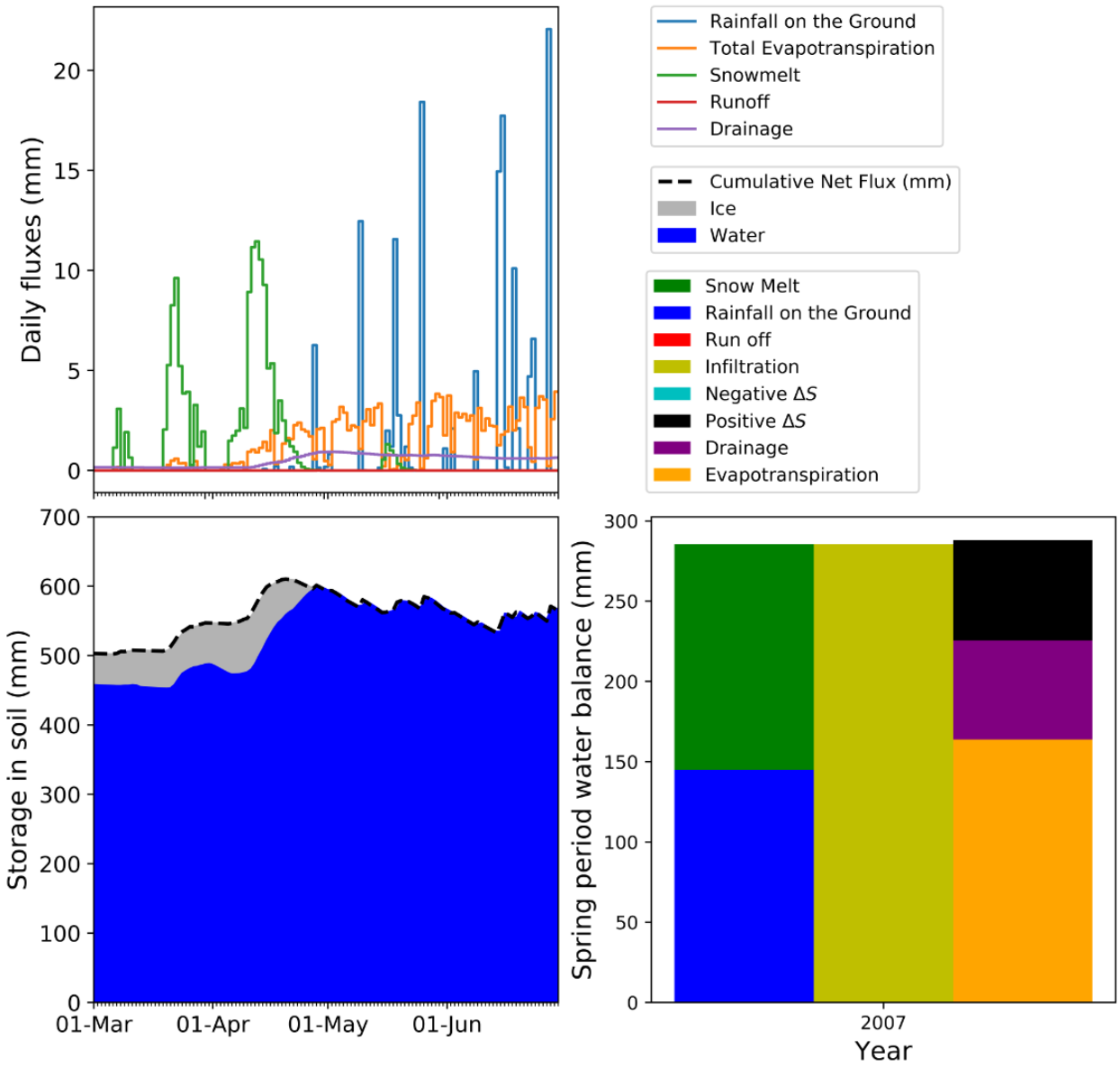

Figure B–19 Detailed water balance during the spring melt period using CLASS–CTEM with dynamic vegetation for the year 2007.

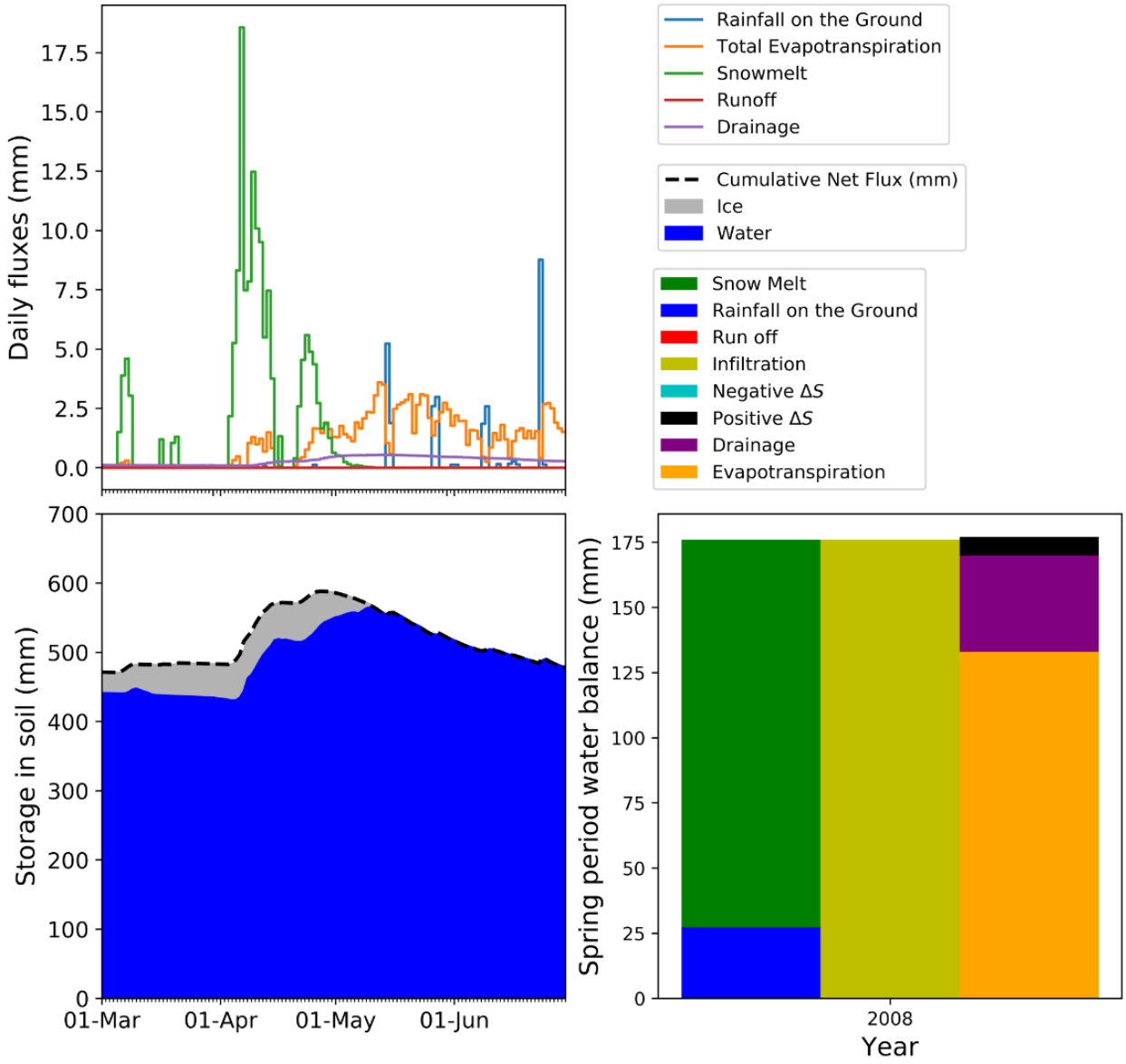

Figure B–20 Detailed water balance during the spring melt period using CLASS–CTEM with dynamic vegetation for the year 2008.

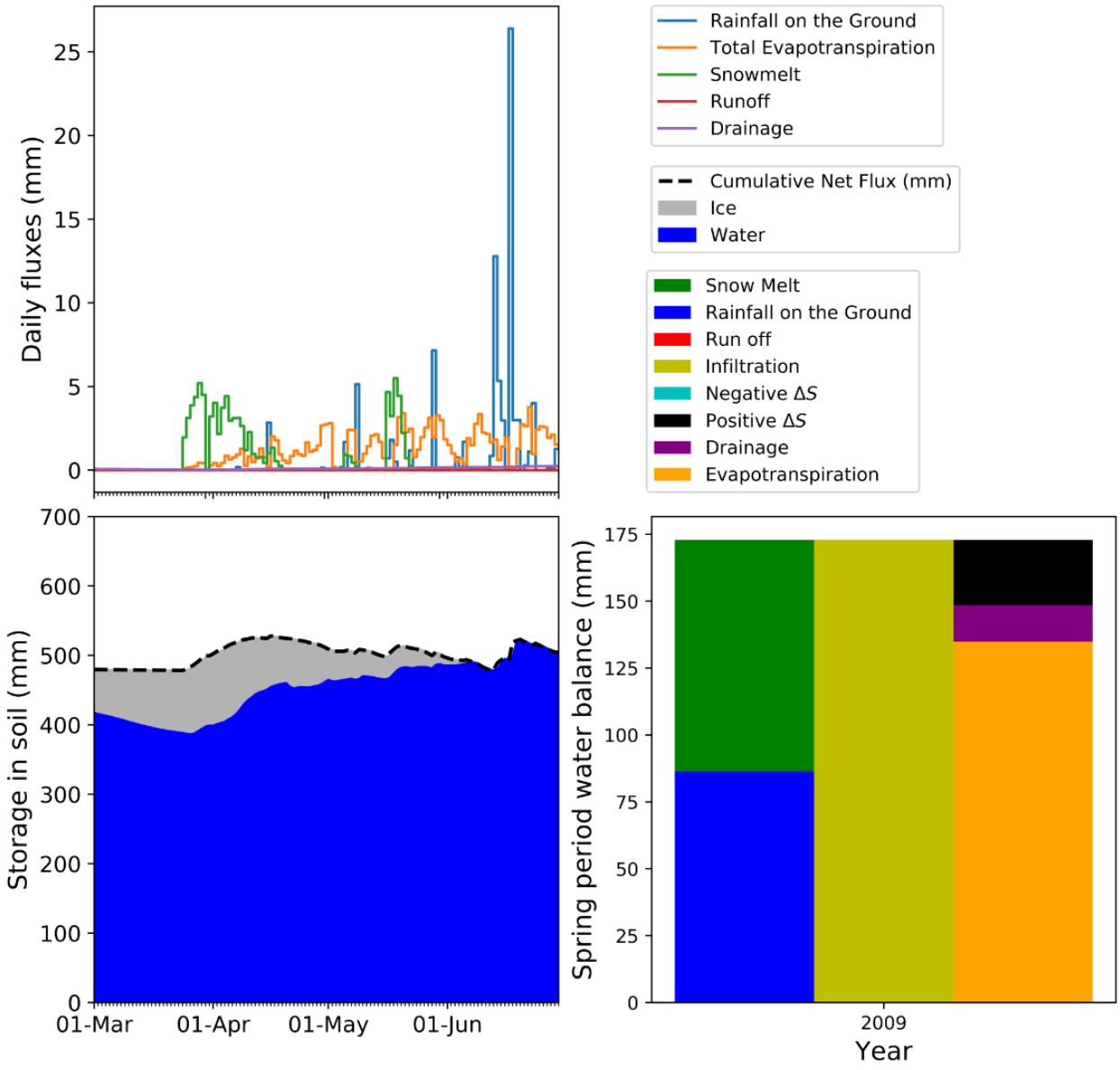

Figure B–21 Detailed water balance during the spring melt period using CLASS–CTEM with dynamic vegetation for the year 2009.

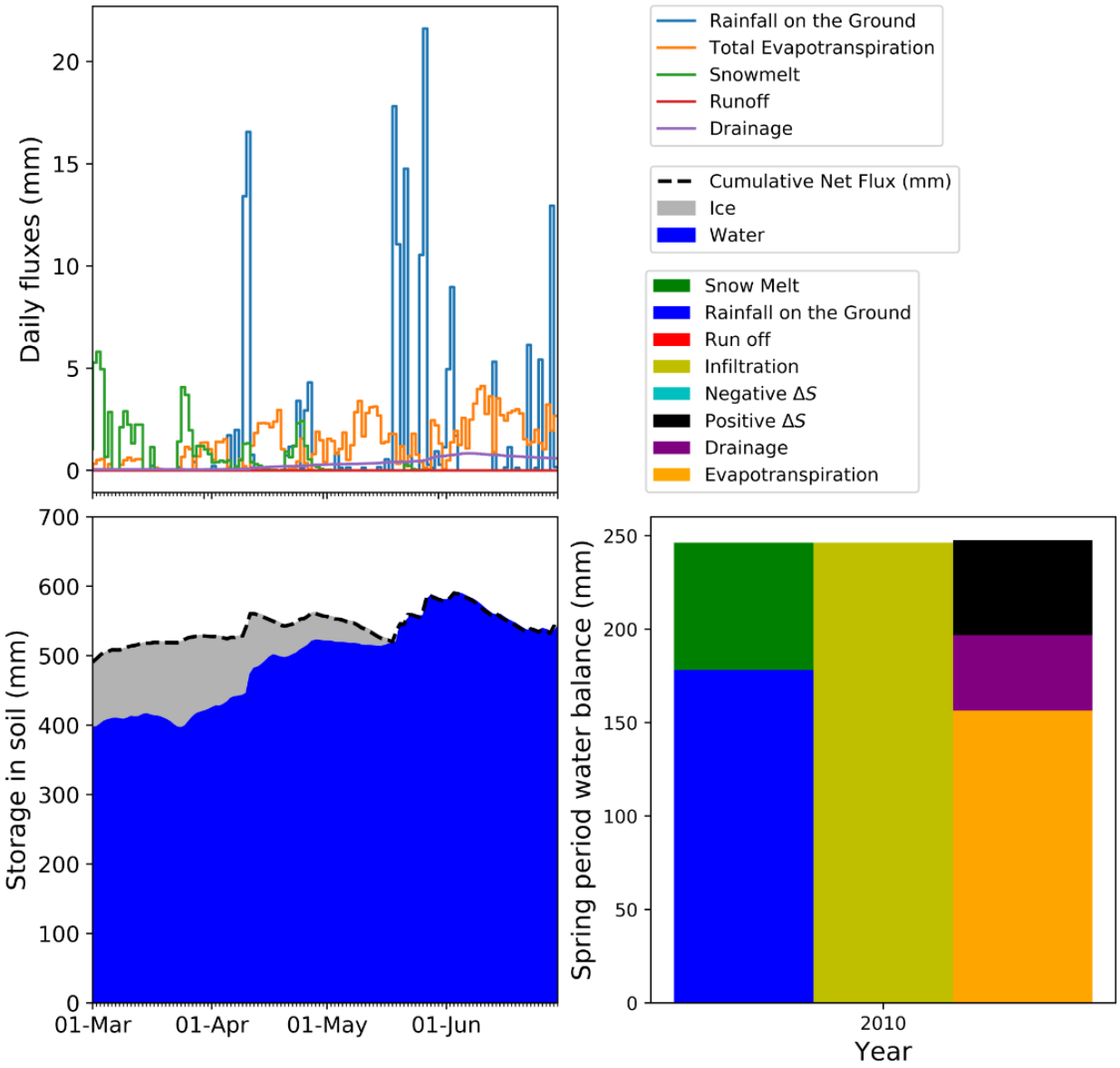

Figure B–22 Detailed water balance during the spring melt period using CLASS–CTEM with dynamic vegetation for the year 2010.

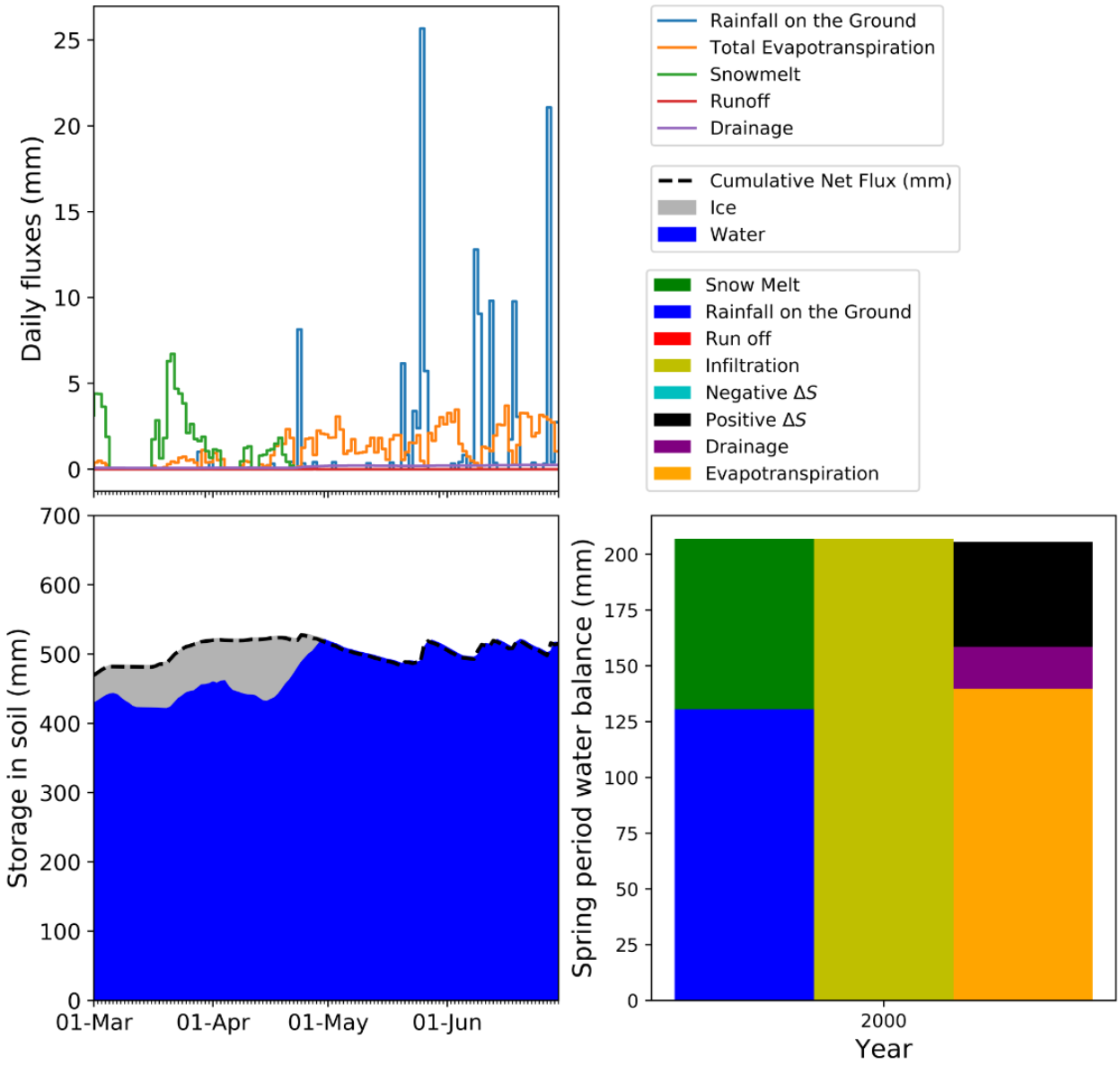

Figure B–23 Detailed water balance during the spring melt period using CLASS–CTEM with static vegetation for the year 2000.

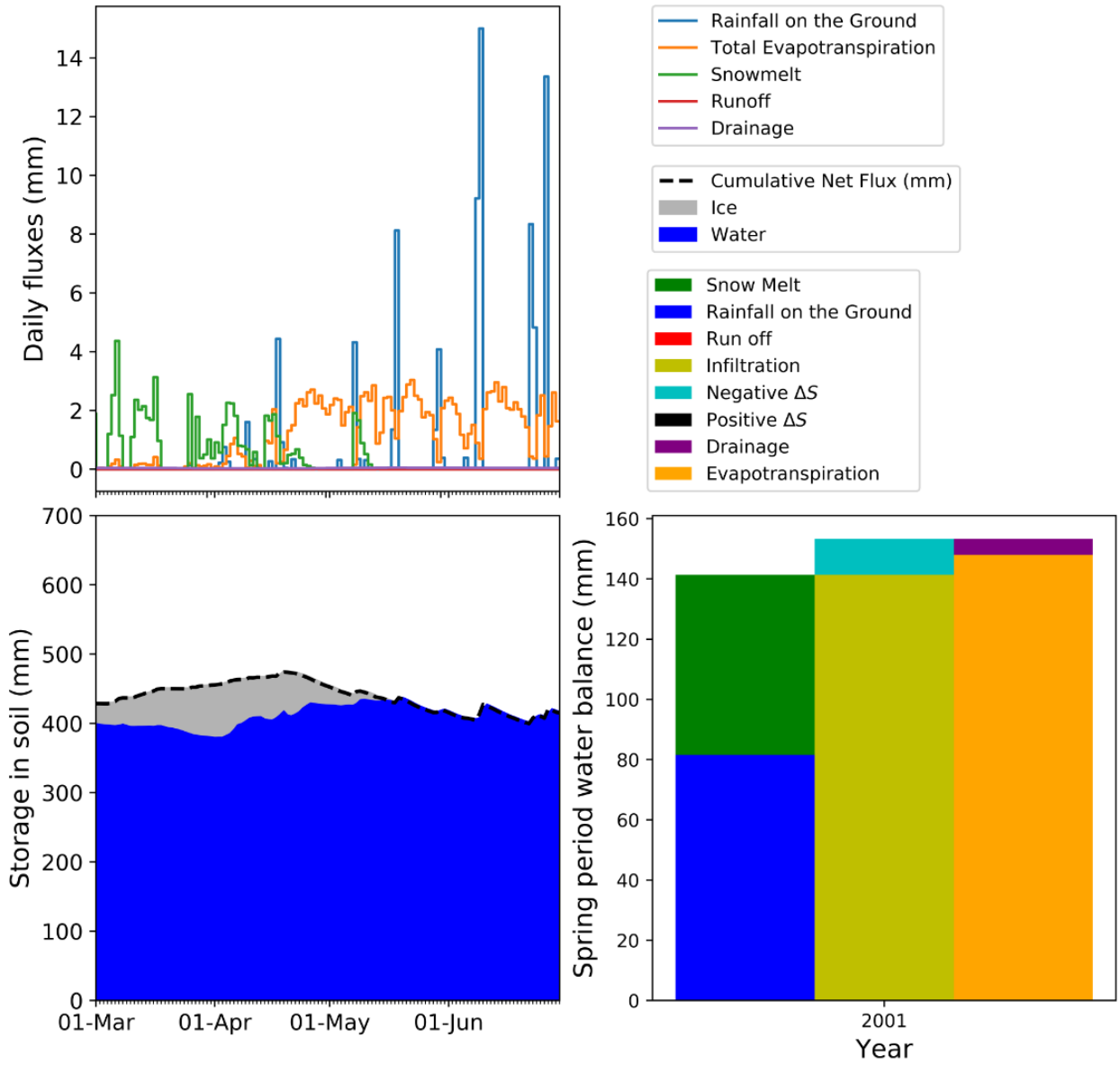

Figure B–24 Detailed water balance during the spring melt period using CLASS–CTEM with static vegetation for the year 2001.

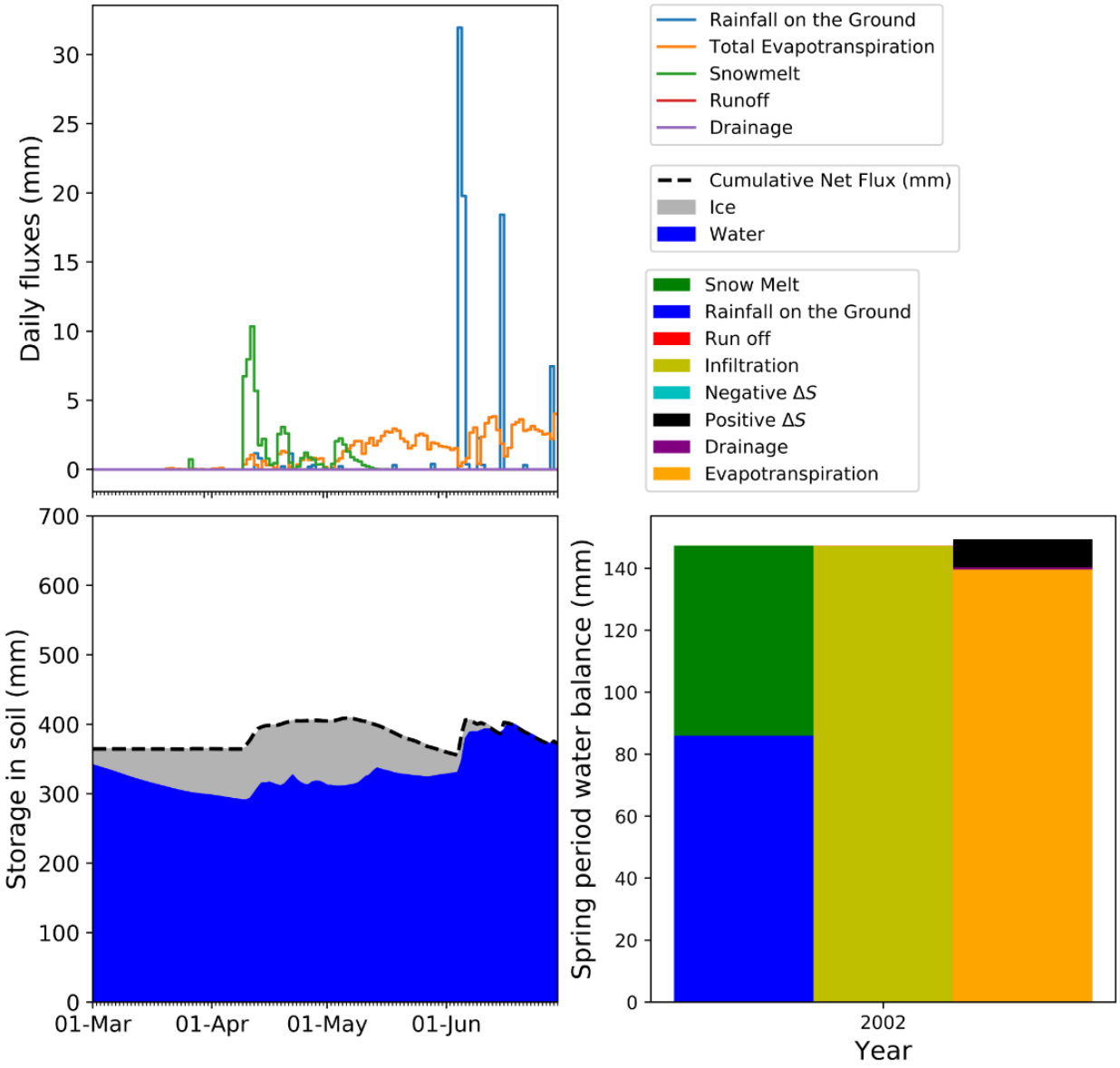

Figure B–25 Detailed water balance during the spring melt period using CLASS–CTEM with static vegetation for the year 2002.

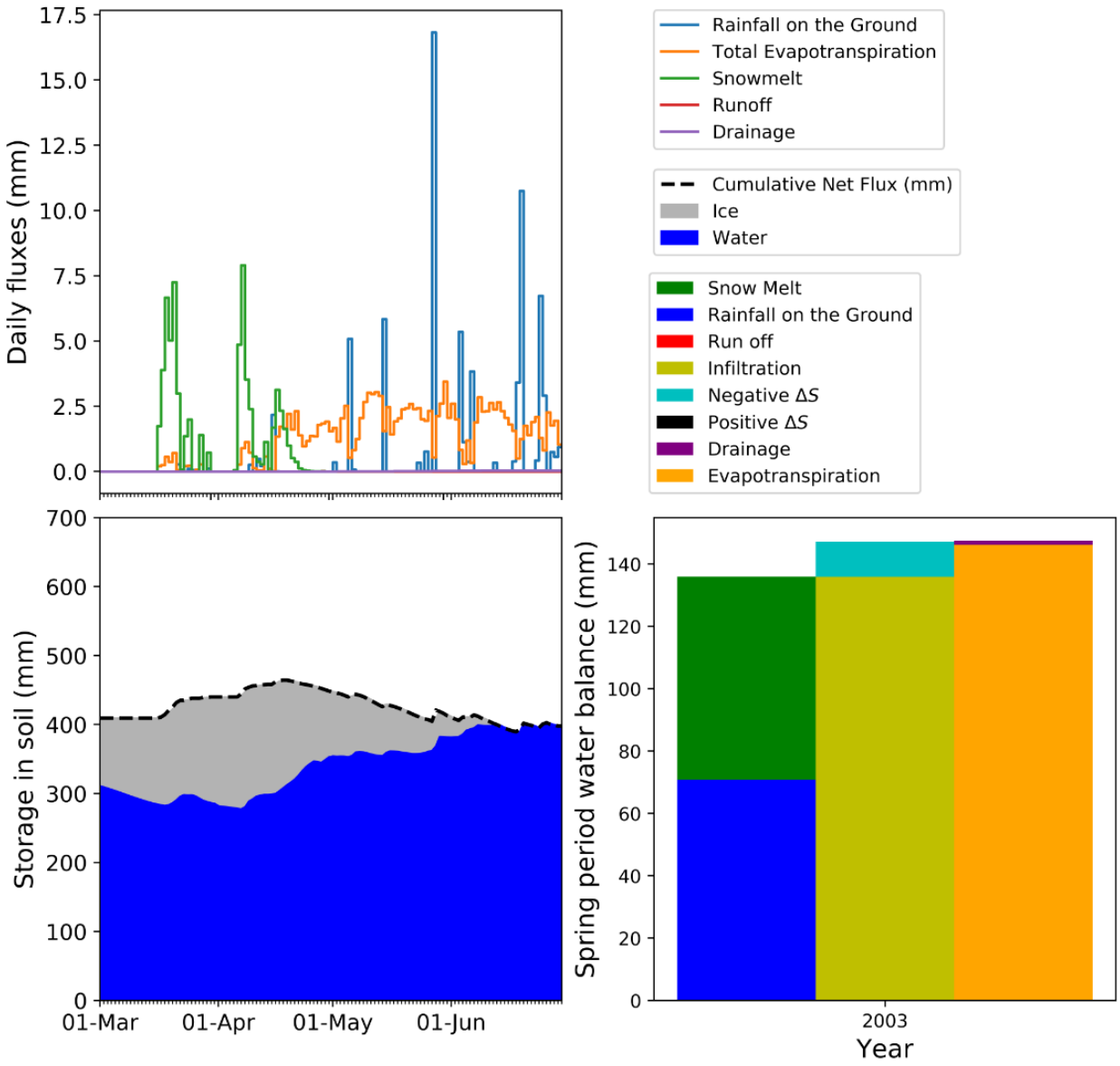

Figure B–26 Detailed water balance during the spring melt period using CLASS–CTEM with static vegetation for the year 2003.

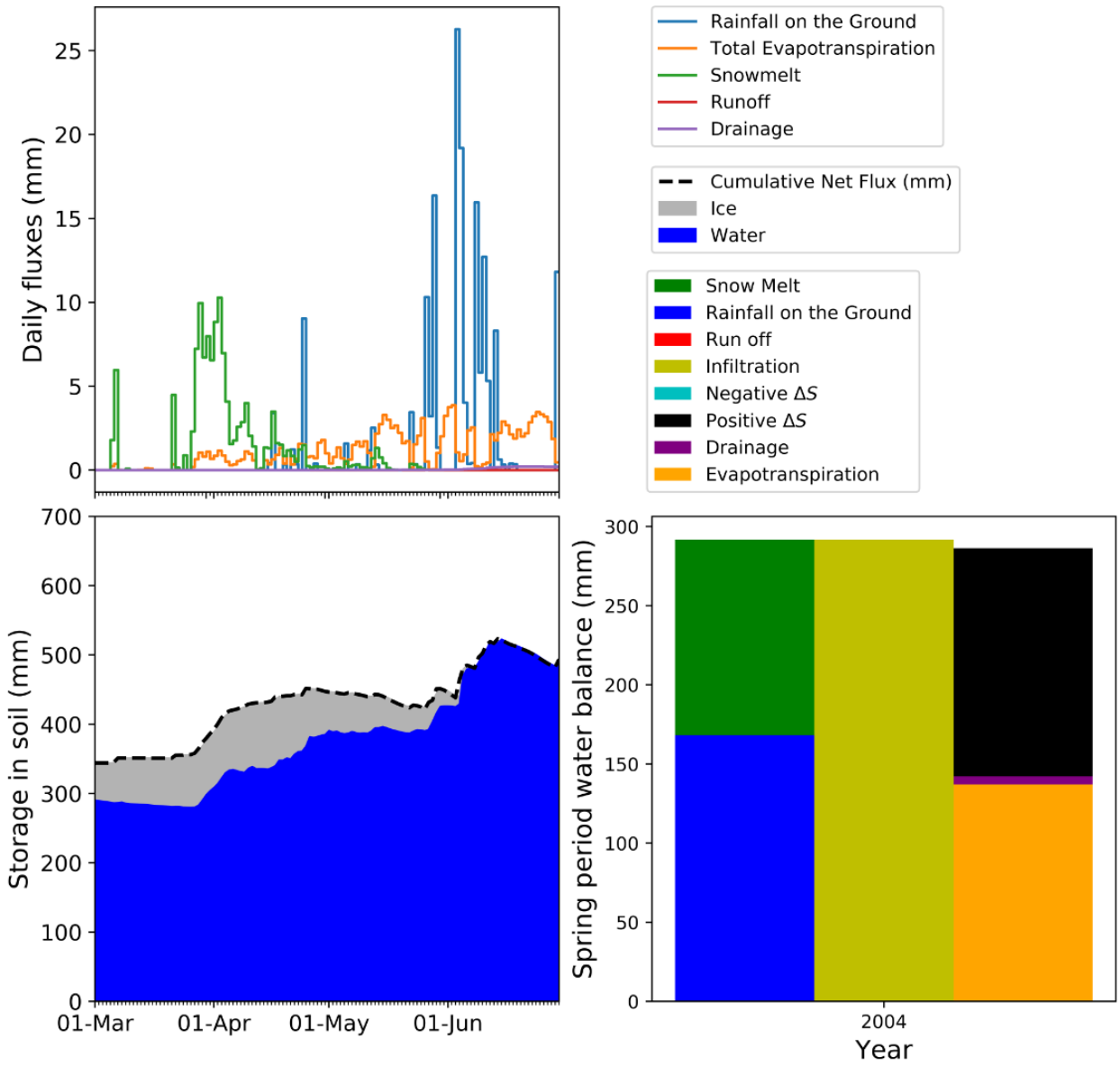

Figure B–27 Detailed water balance during the spring melt period using CLASS–CTEM with static vegetation for the year 2004.

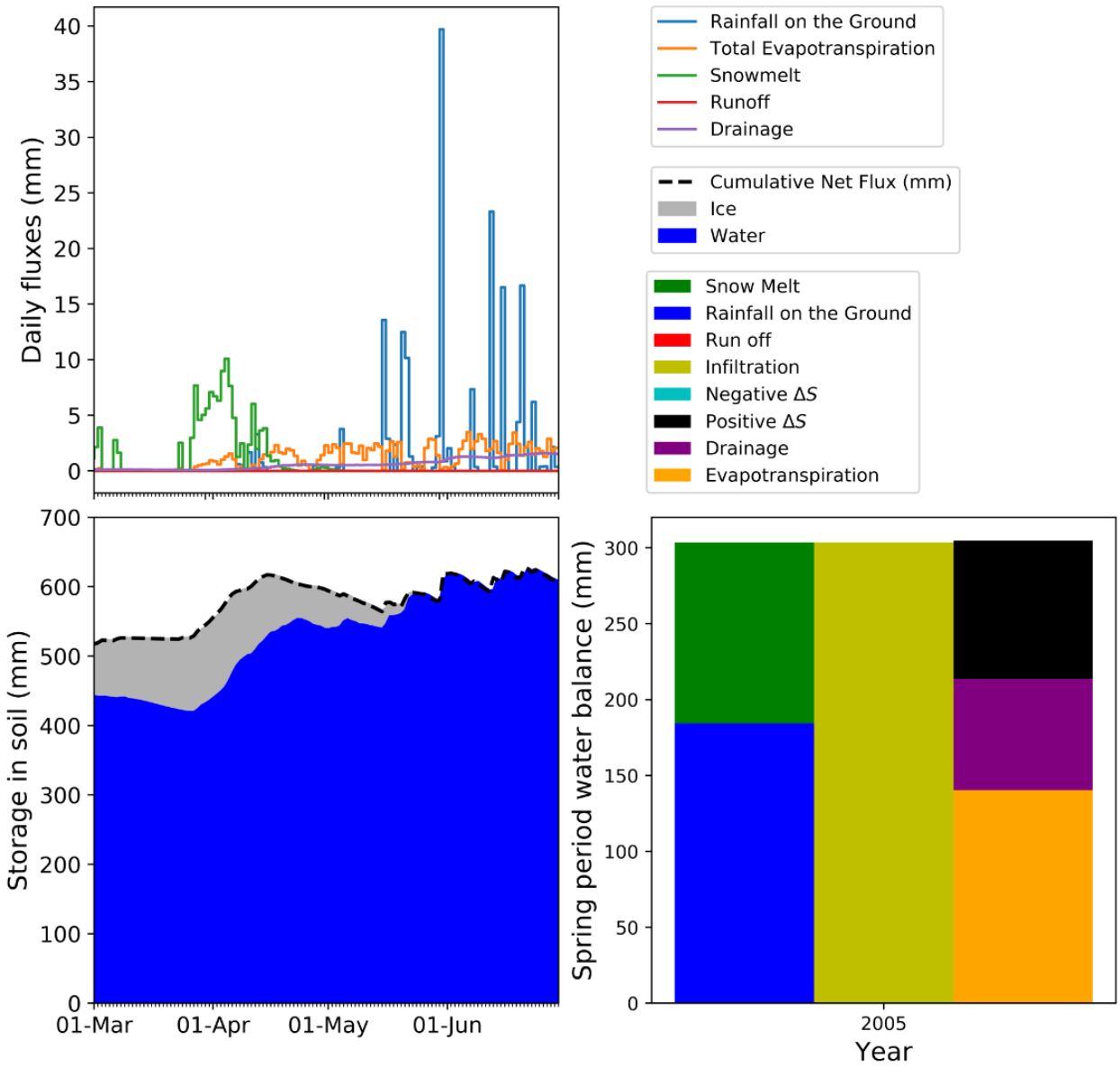

Figure B–28 Detailed water balance during the spring melt period using CLASS–CTEM with static vegetation for the year 2005.

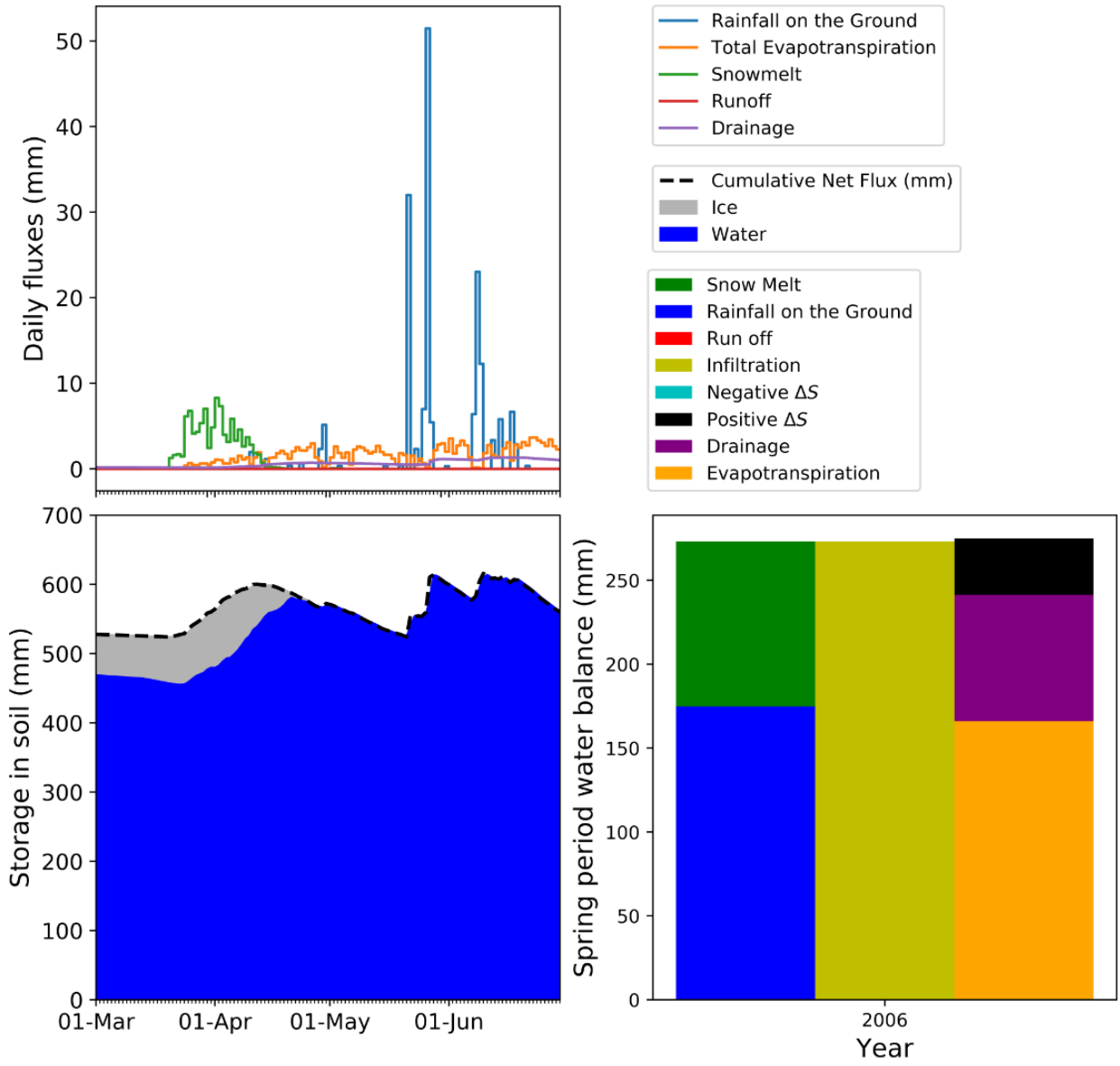

Figure B–29 Detailed water balance during the spring melt period using CLASS–CTEM with static vegetation for the year 2006.

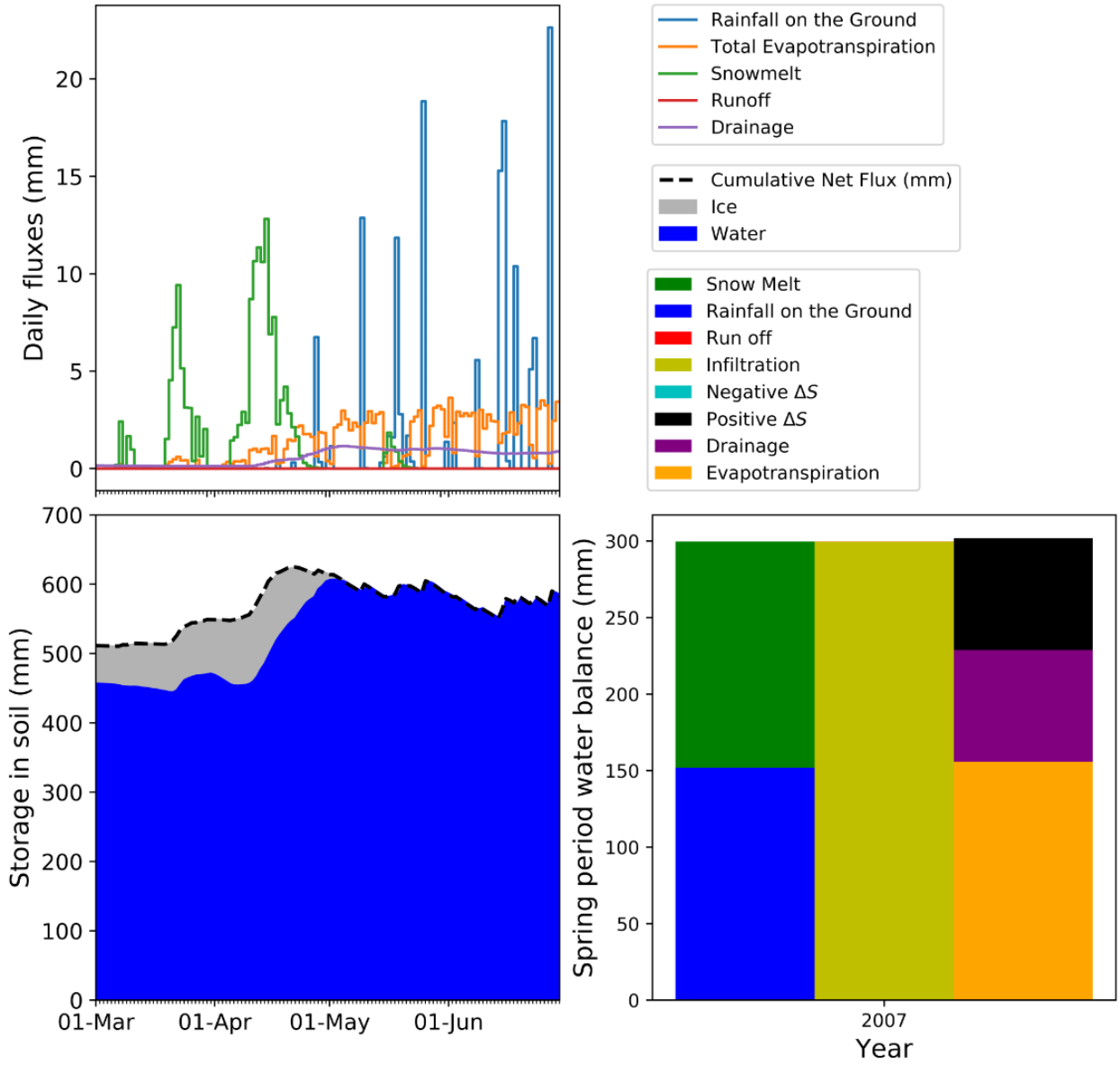

Figure B–30 Detailed water balance during the spring melt period using CLASS–CTEM with static vegetation for the year 2007.

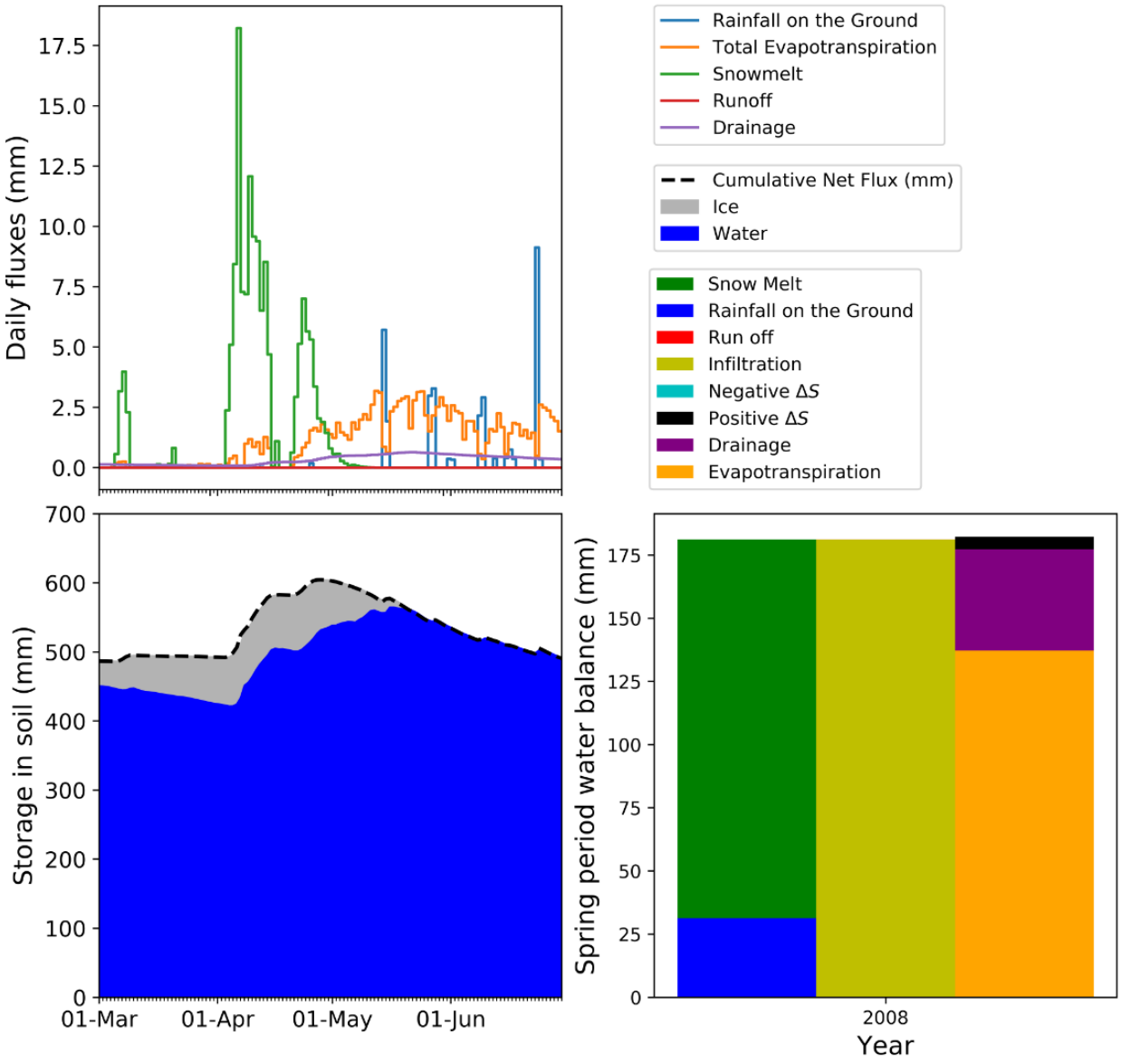

Figure B–31 Detailed water balance during the spring melt period using CLASS–CTEM with static vegetation for the year 2008.

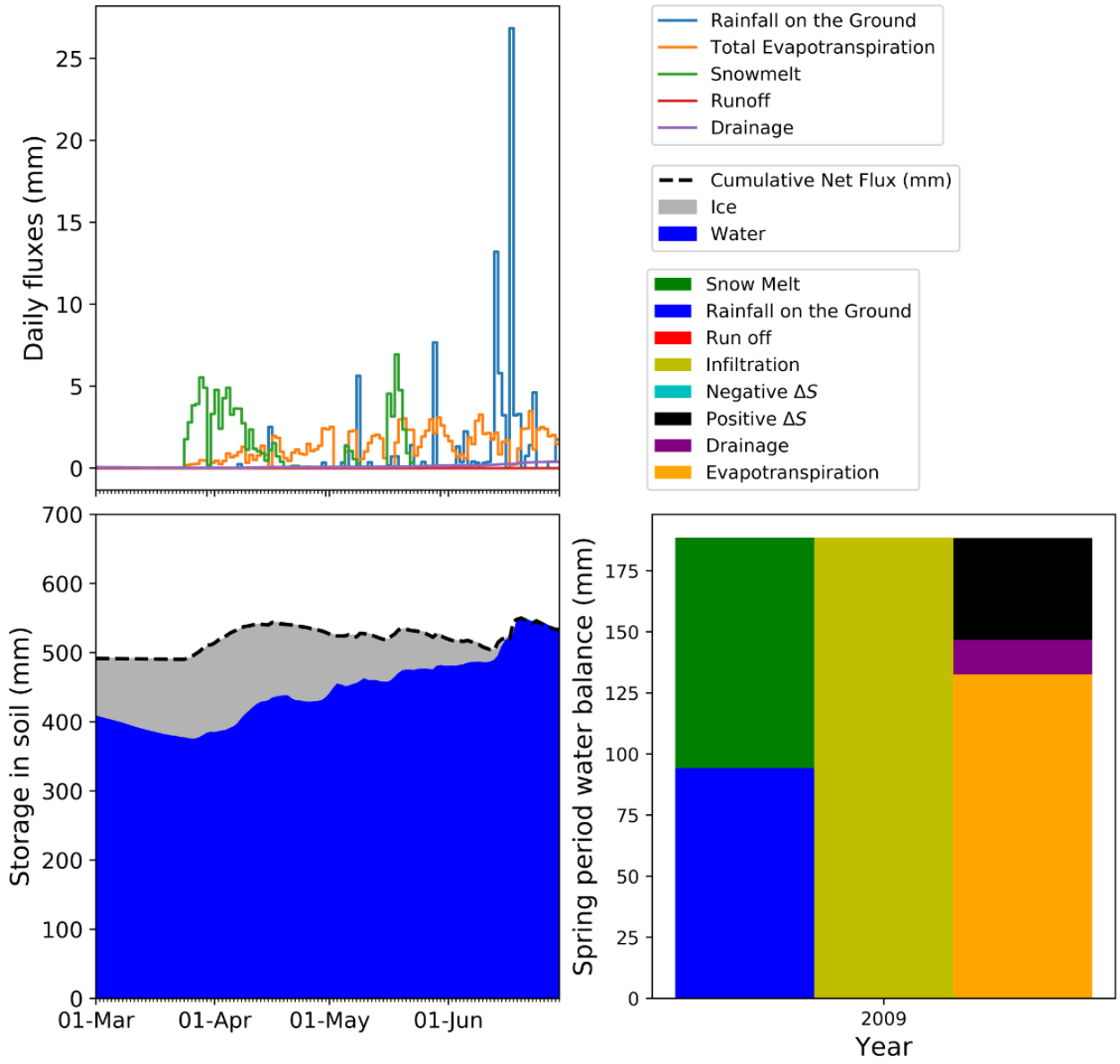

Figure B–32 Detailed water balance during the spring melt period using CLASS–CTEM with static vegetation for the year 2009.

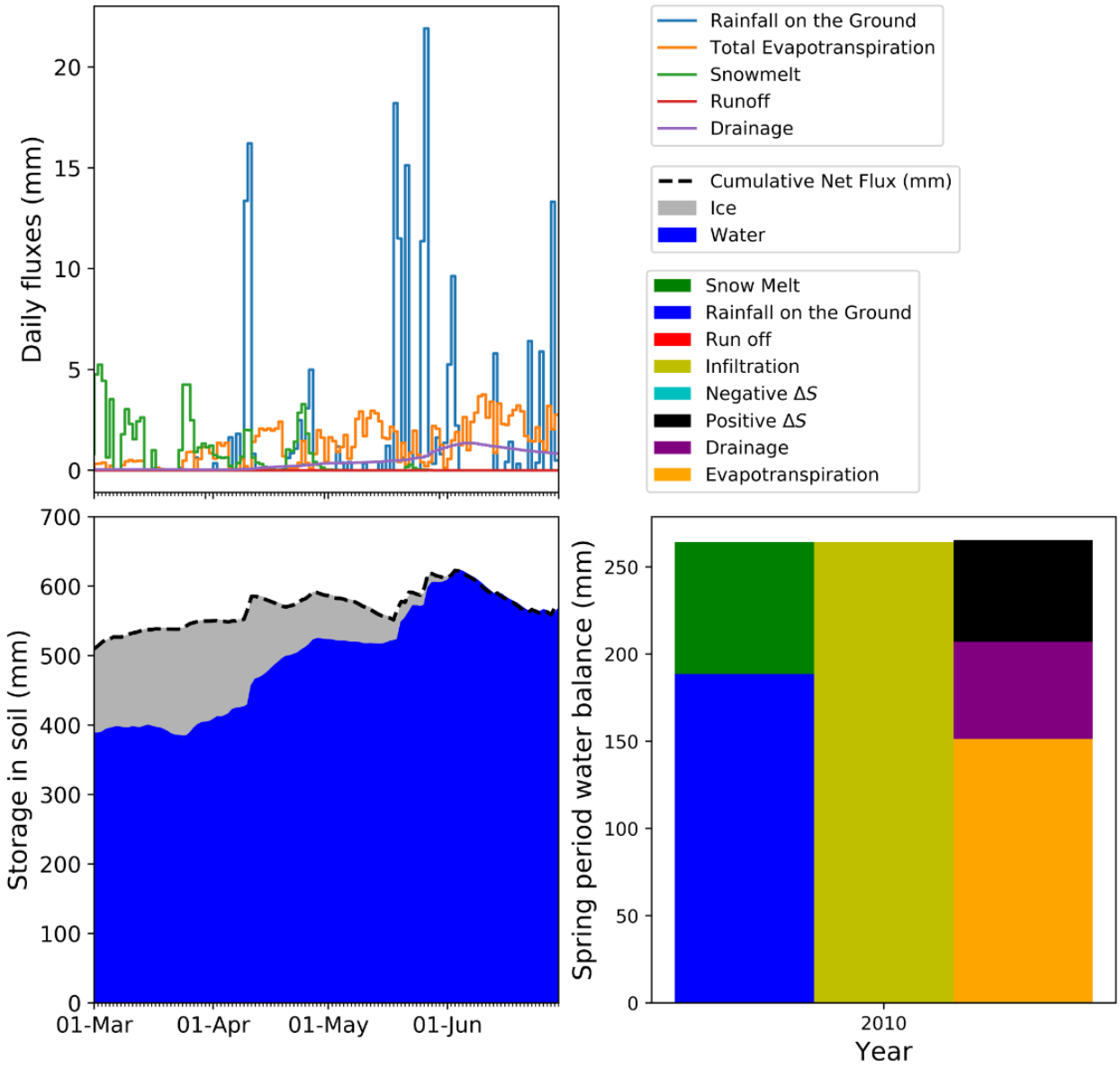

Figure B–33 Detailed water balance during the spring melt period using CLASS–CTEM with static vegetation for the year 2010.